

https://dspace.org/

Comparing the silencing efficacy of dicer-independent and dependent shRNAs

Nhlabatsi, Neliswa

2015-04-22
http://hdl.handle.net/10539/17510

Downloaded from a DSpace repository. https://dspace.org/

COMPARING THE SILENCING EFFICACY OF DICER-INDEPENDENT AND DEPENDENT shRNAS

Neliswa Nhlabatsi

A dissertation submitted to the Faculty of Science, University of the Witwatersrand, Johannesburg, in fulfilment of the requirements for the degree of Master of Science.

Johannesburg, 2014.

Declaration

I, Neliswa Nhlabatsi, declare that this dissertation is my own work. It is being submitted for the degree of Master of Science in Medicine in the University of the Witwatersrand, Johannesburg. It has not been submitted before, for any degree or examination at this or any other university.

.....

.....day of August, 2014

Dedication

To my ever supportive family and friends

and the gods of science that toyed with me.

Publications and presentations

1. Nhlabatsi N, Arbuthnot P, Weinberg M. Comparing the silencing efficacy of Dicer-independent and –dependent shRNAs. Molecular Biosciences Research Thrust Postgraduate Research Day oral presentation; 4 Dec 2013; Johannesburg.
2. Nhlabatsi N, Arbuthnot P, Weinberg M. Determining the silencing efficacy of anti-HIV Dicer-independent short hairpin RNAs. Molecular Biosciences Research Thrust Postgraduate Research Day poster presentation; 5 Dec 2012; Johannesburg.
3. Nhlabatsi N, Arbuthnot P, Weinberg M. Determining the silencing efficacy of anti-HIV Dicer-independent short hairpin RNAs. WITS Cross-faculty Symposium poster presentation; 19 & 22 Oct 2012; Johannesburg.
4. Nhlabatsi N, Arbuthnot P, Weinberg M. Determining the silencing efficacy of anti-HIV Dicer-independent short hairpin RNAs. WITS Faculty of Health Sciences Research Day poster presentation; 19 Sept 2012; Johannesburg.
5. Nhlabatsi N, Arbuthnot P, Weinberg M. Determining the silencing efficacy of anti-HIV Dicer-independent short hairpin RNAs. Proceedings of the 23rd Congress of the SASBMB poster presentation; Jan 29-Feb 1 2012; Drakensburg.
6. Nhlabatsi N, Arbuthnot P, Weinberg M. Determining the silencing efficacy of anti-HIV Dicer-independent short hairpin RNAs. Molecular Biosciences Research Thrust Postgraduate Research Day poster presentation; 7 Dec 2011; Johannesburg.

Acknowledgements

I would like to extend my immense gratitude to my supervisor Prof. Marco Weinberg. I never would have guessed that an accidental meeting would have led to such a great opportunity. You forced me to expect better of myself and for that, I'm incredibly grateful.

To my co-supervisor, Prof. Patrick Arbuthnot, I'd like to thank you for allowing me the privilege of being a part of the Antiviral Gene Therapy Research Unit. I appreciate your support and patience but most of all, your optimism when I needed it most.

To all of my Yoda's (you know who you are) I could never have done this without you. Thank you for your guidance and never-ending willingness to help a noob out.

To my lab mates, thank you for the good times and kind words during the bad times. I'm willing to ignore the fact that you were all willing to sacrifice me in a hypothetical zombie apocalypse because we've been through enough together to ignore such.

I'd like to thank The Antiviral Gene Therapy Research Unit, The National Research Fund, and The Poliomyelitis Research Fund for the financial support that I received personally.

Abstract

RNA interference (RNAi) is a highly conserved gene regulatory mechanism triggered by the presence of double-stranded RNAs and results in post-transcriptional and transcriptional gene silencing. RNAi has been demonstrated to have therapeutic potential to treat chronic viral infections including HIV-1. Due to the side effects of and eventual drug resistance to highly active antiretroviral therapy, a novel anti-HIV-1 therapy is required. The most suitable exogenous RNAi triggers to use in anti-HIV-1 RNAi-based therapy are expressed short hairpin RNAs (shRNAs). Despite being highly developed, shRNA systems still pose safety concerns. Highly expressed shRNAs are at risk of over-saturating the endogenous RNAi pathway, inducing an innate immune response or silencing off-target mRNA. The purpose of this study was to minimise shRNA-associated off-target effects and simultaneously maximise the potency and specificity of expressed shRNAs for potential therapeutic application. ShRNAs shorter than 19 base pairs are not recognised by the endonuclease Dicer, which is an important component of the RNAi pathway, but miR-451 is Dicer-independent. Smaller shRNAs that retain their potency would be easier to deliver into a disease model. For this study, 25mers and miR-451-mimicking 19mers were generated. The shRNA pairs exhibited significant knockdown of their respective targets in dual-luciferase assays. The 19mers are more specific gene silencers compared to the 25mers. A 19mer that is more potent than its 25mer counterpart was identified. None of the hairpins induced an innate immune response, caused cytotoxic effects or saturated the endogenous RNAi pathway. This study concludes that the 19mers were processed in a manner similar to miR-451 resulting in a single ~30 nt mature RNA product. We dubbed these miR-451-mimicking 19mers, guide shRNAs. The single RNA strand of mature guide shRNAs abolishes the risk sense strand-associated off-targeting thus improving shRNA specificity. These revolutionary guide shRNAs can be developed into highly potent activators of the RNAi pathway in a therapeutic setting.

Table of Contents

Declaration ii

Dedication iii

Publications and presentations iv

Acknowledgements v

List of Figures xi

List of Tables xiii

Abbreviations xvi

Chapter 1: Introduction 1

1.1 RNA interference 1

1.1.2 Transcriptional gene silencing 1

1.1.1 The canonical RNAi pathway 2

1.1.3 RNAi effectors 5

1.2 Alternative approaches to express shRNAs 8

1.2.1 tRNA-shRNA 8

1.1.2 Trans-kingdom RNAs 8

1.2 Limitations of RNAi-based therapy 9

1.3 shRNAs and RNAi efficacy 11

1.3.1 Features of functional siRNAs 11

1.3.2 Strand orientation and shRNA efficacy 12

1.3.3 Strand bias 12

1.4 The distinct biogenesis of miR-451 13

1.5 Dicer and Ago2 15

1.5.1 Dicer 15

1.5.2 Ago2 16

1.6 Mimicking miR-451 to improve shRNA specificity and potency 19

Chapter 2: Materials and Methods 23

2.1 Plasmids generated prior to this study 23

2.1.1 The H1 promoter 23

2.3.2 The H1 Mock vector 24

2.3.4 The GFP reporter plasmid 25

2.4 Molecular cloning 25

2.4.1 Generation of the PTZ-H1shRNA expression cassettes 25

2.4.2 Generation of target reporter plasmids 29

2.5 Mammalian tissue culture 33

2.6 Dual-luciferase assay 34

2.6.1 Dual-luciferase knockdown assay 35

2.6.2 Dose response assay 35

2.7 Interfering with the RNAi pathway 37

2.7.1 Interferon response assay 37

2.7.2 MTT assay 39

2.7.3 Saturation assay 40

2.8 Processing of the shRNA constructs 41

2.8.1 RNA extraction for northern blot analysis 41

2.8.2 Radio-labelling Decade marker 41

2.8.3 Radio-labelling the probes 41

2.8.4 Northern blot analysis to visualise processed shRNA products 42

Chapter 3: Results 45

3.1 Hairpin sequence selection 45

3.2 Design of shRNAs 47

3.3 Molecular cloning of the H1-driven shRNAs 50

3.5 Generation of reporter plasmids with target sequence inserts 53

3.6 The 19mer shRNA RNAi products are larger than that of the 25mers 55

3.7 Knockdown comparison of the 5' and 3' arms 60

3.8 The H1-driven shRNA expression cassettes inhibit expressed targets in a dose-dependent manner 65

3.9 The PTZ-H1shRNAs do not compete with other exogenous RNAi effectors 69

3.10 The 19mers and 25mers induce a negligible interferon response compared to poly I:C 72

3.11 The shRNAs do not negatively affect cell viability 74

Chapter 4: Discussion 76

4.1 shRNA potency and stem length 76

4.2 The 19mers have guaranteed strand bias with a single RNA strand 78

4.3 The guide shRNAs reduce off-targeting and maximise potency 80

4.4 Insignificant interferon response 82

4.5 Negligible interference of the endogenous RNAi pathway 83

4.7 Potential antiviral combinatorial therapy 85

4.8 Future work 85

Chapter 5: Conclusion 87

References 88

Appendix A – Experimental protocols 105

A.1 MinElute Gel extraction 105

A.2 Chemically competent *E.coli* cells 105

A.3 Blue/white screening 106

A.4 Small scale plasmid isolation (mini prep) 107

A.5 Phenol chloroform extraction 108

A.6 Medium scale plasmid (midi-prep) preparation 109

A.7 Cell seeding calculation 110

A.8 Mammalian tissue culture 111

A.9 Northern blot hybridisation 111

A.10 Radioactive labelling of the probes 112

Appendix B - Supplementary Data 113

List of Figures

Figure 1.1: Endogenous miRNA biogenesis. 4

Figure 1.2: RNAi effectors interacting with the endogenous miRNA pathway. 6

Figure 1.3: The unconventional structure of the miR-451 hairpin. 13

Figure 1. 4: Schematic of the Dicer and Ago2 domains. 17

Figure 1.5: Relocating the seed region. 21

Figure 2.1: One-step PCR approach. 26

Figure 3.1: Relocation of the antisense strand to the 5' arm of the hairpin. 48

Figure 3.2: Design of the PTZ-H1shRNA cassettes.... 49

Figure 3.3: An example of a PCR gradient conducted for an shLTR25 amplicon. 51

Figure 3.4: Chromatogram of the sequenced positive shE25 clone. 52

Figure 3.5: Example of EcoRV-screening of the psi-target clones. 54

Figure 3.6: Chromatogram of sequence-verified LTR target plasmid, psi-LTR-AS.... 54

Figure 3.7: Processing of the shRNAs detected by northern blot analysis.... 56

Figure 3.8: Northern blot analysis with radio-labelled LNA-modified oligonucleotide probes.... 59

Figure 3.9: Dual-luciferase reporter assay.... 61

Figure 3.10: Knockdown efficacy of the guide (Gag/Env/LTR target) and passenger strands respectively. 64

Figure 3.11: *Gag* dose response assay. 66

Figure 3.12: *Env* dose response. 67

Figure 3. 13: Dose response of LTR target. 67

Figure 3.14: Explanation of the saturation assay. 70

Figure 3.15: Assessment of the repressing effect of shRNAs on an exogenous HBV-expressing cassette. 71

Figure 3.16: The induction of the interferon response in shRNA-transfected cells measured by real-time RT-qPCR. 73

Figure 3.17: Cytotoxicity assessment. 75

Figure B.1: An example of the shRNA clone screening process. 113

Figure B.2: *SacI* and *BamHI* digest of confirmed positive pTZ-shRNA clones. 114

Figure B.3: Example of GFP expression. 115

Figure B.4: The induction of the interferon response in shRNA-transfected cells measured by real-time qPCR. 116

List of Tables

Table 2.1: Primers used to generate shRNA-expressing constructs. 27

Table 2.2: Guide strand target sequences. 30

Table 2.3: Target sequences of the passenger strand of each hairpin. 31

Table 2.4: Layout of the dose response assay. 36

Table 2.5: The primers used for the qRT-PCR to assess the induction of an interferon response. 39

Table 2.6: A list of the probe sequences used to detect RNA in the Northern blots. 44

Table 3.1: The HIV-1 target sequences used in this study. 46

Abbreviations

2-5-OAS	-	2’,5’-oligoadenylate synthase
3’ OH	-	3’ hydroxyl
3’ UTR	-	3’ untranslated region
5’ P	-	5’ monophosphate
Ago2	-	Argonaute 2
DDH	-	Aspartate-aspartate-glutamate [HIS/]
DGCR8	-	DiGeorge critical region 8
DMSO	-	Dimethyl sulfoxide
dsRBD	-	Double-stranded RNA binding domain
DUF283	-	Domain of unknown function
EC	-	Effective concentration
eGFP	-	Enhanced green fluorescent protein
FCS	-	Fetal calf serum
GAPDH	-	Glyceraldehyde-3-phosphate dehydrogenase
HAART	-	Highly active antiretroviral therapy
HEK293	-	Human embryonic kidney 293
HIV-1	-	Human Immunodeficiency Virus type I
Huh7	-	Human hepatoma 7

IFN-β	-	Interferon-β
IPTG	-	Isopropyl thiogalactoside
LAR II	-	Luciferase activity agent II
LNA	-	Locked nucleic acid
LTR	-	Long terminal repeat
mRNA	-	Messenger RNA
miRNA	-	MicroRNA
MTT	-	Thiazolyl blue tetrazolium bromide
nt	-	Nucleotide
PACT	-	Protein activator of PKR
PNK	-	Polynucleotide kinase
pre-miRNA	-	Precursor microRNA
pre-miR-451	-	Precursor miR-451
pri-miRNA	-	Primary microRNA
pri-miR-451	-	Primary miR-451
PKR	-	Protein kinase R
PVC	-	Polyvinyl chloride
RIG-I	-	Retinoic acid inducible gene I
RISC	-	RNAi-induced silencing complex
RITS	-	RNA-induced transcriptional silencing

RNAi	-	RNA interference
RNA Pol	-	RNA polymerase
RNP	-	Ribonucleoprotein
SDS	-	Sodium dodecyl sulphate
shRNA	-	Short hairpin RNA
siRNA	-	Short inhibitory RNA
snoRNA	-	Small nucleolar RNA
TGS	-	Transcriptional gene silencing
TRBP	-	TAR RNA binding protein
tRNA	-	Transfer RNA
tk-RNA	-	Trans-kingdom RNA
TLR	-	Toll-like receptor
X-gal	-	5-bromo-4-chloro-3-indolyl-beta-D-galactopyranoside

Chapter 1: Introduction

1.1 RNA interference

RNA interference (RNAi) is an evolutionarily conserved mechanism that is triggered by double-stranded RNA (dsRNA) resulting in the transcriptional and post-transcriptional regulation of gene expression (Fire *et al*, 1998; Bernstein *et al*, 2001b). RNAi interferes with protein synthesis by blocking the conversion of messenger RNA (mRNA) into protein (Heo and Kim, 2007). Interest and research into the process of RNAi has increased at a rapid rate since its discovery in *C. elegans* resulting in numerous topics including gene function analysis, exploring clinical testing and therapeutic applications (Fire *et al*, 1998; Grimm and Kay, 2007).

1.1.1 Transcriptional gene silencing

Epigenetics refers to the study of altered and heritable gene expression in a genome caused by external influences that do not affect DNA sequence (Wolffe & Matzke, 1999). Transcriptional gene silencing (TGS) otherwise known as RNA-induced transcriptional silencing (RITS), like post-transcriptional RNAi, is a signalling pathway highly-conserved in mammals but the process occurs prior to transcription (Morris *et al*, 2004). DNA coils around histone proteins and together (known as the nucleosome), the two aggregate into chromatin which forms into chromosomes (Kornberg and Klug, 1981). The way that histone proteins interact with DNA affects how small RNAs can access eukaryotic genetic material (Allfrey *et al*, 1964).

Small RNAs, such as small interfering RNAs (see Section 1.1.3), cause TGS by interacting with and remodelling chromatin (Noma *et al*, 2004). This interaction causes epigenetic changes via histone modifications including the addition of a methyl group (methylation) (Rea *et al*, 2000). The altered histone proteins act by binding to a genomic region that will force the modified chromatin to be formed (now known as heterochromatin) (Noma *et al*, 2004). The complex that facilitates small

RNA-histone binding is known as the RITS complex (Verdel *et al*, 2004). The RITS complex plays a key role in heterochromatin silencing (Noma *et al*, 2004).

1.1.2 The canonical RNAi pathway

There are numerous natural endogenous small non-coding dsRNAs that exist in the RNAi pathway including microRNAs (miRNAs) (Cai *et al*, 2004). Primary miRNAs (pri-miRNAs) are transcribed from the exons, introns and intergenic regions of genomic DNA (Figure 1.1) (Kim and Nam, 2009). Pri-miRNAs are long polyadenylated RNA polymerase II (RNA Pol II) transcripts that have stem-loop structures containing mismatched nucleotides and bulges (Lagos-Quintana *et al*, 2001; Zeng and Cullen, 2005). After being processed by the RNase III enzyme, Drosha, and its double-stranded RNA binding domain (dsRBD)-containing chaperone protein DGCR8 (DiGeorge critical region 8) /Pasha, the hairpins are cut down to precursor miRNAs (pre-miRNAs) and are 70-80 nucleotides (nt) in length (Lee *et al*, 2003). These pre-miRNAs have a 5' monophosphate (5'P) and a 2-nucleotide (dinucleotide) overhang with a 3' hydroxyl (3'OH) end (Lee *et al*, 2003). RNA Pol III generates transcripts with distinct 5' and 3' ends this trait allows for proficient nuclear export, therefore short hairpins RNAs (shRNAs) that mimic pre-miRNAs circumvent Drosha processing (Figure 1.2 b) all together (Paddison *et al*, 2002; Yi *et al*, 2003). Exportin-5, when in the presence of Ran-GTP, recognises the Drosha-characteristic dinucleotide 3' overhang of pre-miRNAs (and most shRNAs), binds to and transports the hairpins into the cytoplasm (Bohnsack *et al*, 2004; Castanotto *et al*, 2007). After nuclear expulsion, the RNase III endonuclease Dicer and its companions, protein activator of PKR (PACT) and the dsRBD protein, TAR RNA binding protein (TRBP), cleave the pre-miRNAs and shRNAs (Lee *et al.*, 2013). The resultant double-stranded short inhibitory RNA (siRNA) duplex has 2-nucleotide overhangs at the 3' ends characteristic of Dicer-processing (Hammond *et al.*, 2001). The Dicer-processed duplex binds to the ribonucleoprotein complex (RNP) known as the RNAi-induced silencing complex (RISC) (Meister and Tuschl, 2004).

Argonaute 2 is the catalytic centre of RISC. The Ago2 component of RISC cleaves and degrades the sense (passenger) strand and uses the antisense (guide) strand of the dsRNA to identify and target homologous mRNA (Martinez *et al*, 2002). Guide strand selection hinges on factors that include thermodynamic stability (Schwarz *et al*, 2003; Khvorova *et al*, 2003). The stability of the final base pair at the 5' end of either siRNA strand is a major determinant in selection- the lower the free energy; the more stable the strand is (Khvorova *et al*., 2003). The introduction of mismatched base pairs in the same position can induce thermodynamic instability and thus improve a strand's guide strand eligibility (Sano *et al*., 2008).

RISC (bound to the guide strand) is activated when it interacts with additional components including the protein Ago2. The activated RISC induces gene silencing either by targeting messenger RNA (mRNA) for cleavage (in the event of high sequence homology between the dsRNA and mRNA) or translational inhibition (due to partial homology between the miRNA and mRNA) (Doench and Sharp, 2004; Chu and Rana, 2006). Normally, RISC binds the 5'-end of the mature miRNA or shRNA duplex within a 2-7 nucleotide "seed region" to the 3' untranslated region (3'UTR) of the target mRNA (Lewis *et al.*, 2003). Gene silencing is achieved either by perfect Watson-Crick pairing between RISC and the guide strand leading to target mRNA cleavage, or by translational repression due to imperfect complementarity (Figure 1.1) (Han *et al.*, 2006).

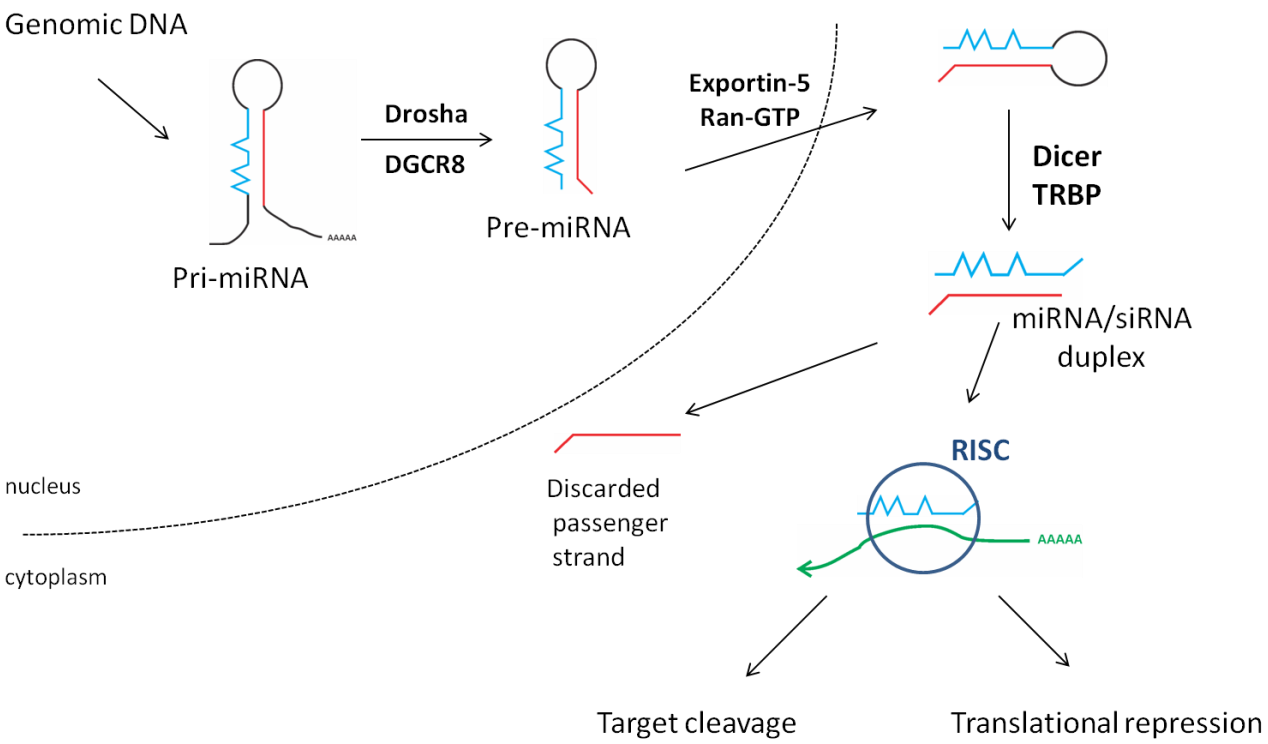


Figure 1.1: Endogenous miRNA biogenesis.

A long polyadenylated stem-loop structure (pri-miRNA) is transcribed in the nucleus. The ribonuclease Drosha and its partner protein DGCR8 cleave the ends of the pri-miRNA, resulting in pre-miRNA. Pre-miRNA is transported to the nucleus by Exportin-5. Pre-miRNA is processed by Dicer, yielding mature miRNA. The guide strand (blue) is incorporated into RISC and the passenger strand (red) is discarded. The miRNA/RISC complex is partially complementary to corresponding target mRNA therefore translational repression occurs.

1.1.3 RNAi effectors

An RNAi effector is a small RNA mimic that exploits the endogenous miRNA biogenesis pathway for post-transcriptional gene silencing. Hairpin transcription is controlled by either an RNA polymerase II (RNA Pol II) or RNA polymerase III (RNA Pol III) promoter. An RNA Pol II promoter, in nature, usually transcribes miRNA-containing precursors but some miRNAs are expressed under the control of an RNA Pol III promoter (Lee *et al.*, 2004; Zeng & Cullen, 2005). RNA Pol III transcripts are normally ubiquitously expressed at a more potent degree in comparison to RNA Pol II-driven expression (Dickins *et al.*, 2007). The turnover of transcripts derived from RNA Pol II promoters is generally controlled by the additional step (compared to RNA Pol III transcripts) of Drosha-processing thus resulting in comparably lower levels of transcripts (McBride *et al.*, 2008; Boudreau *et al.*, 2009). Exogenous RNAi effectors can be introduced into the endogenous pathway to trigger sequence-specific targeting for gene function studies and research for development of novel therapies. RNAi effectors are designed to mimic miRNA at various stages of processing.

1.1.3.1 miRNA constructs

In mammalian RNAi, the most characterised endogenous small RNAs that guide sequence-specific gene silencing are the miRNAs (Bartel, 2004; He *et al*, 2005). ShRNAs or siRNAs can be incorporated into an endogenous miRNA construct to mimic a natural primary miRNA transcript therefore allowing for stable and controlled RNA Pol II-transcribed expression (Figure 1.2 a) (Boden *et al*, 2004; Silva *et al*, 2005; Stegmeier *et al*, 2005). These shRNA/siRNA-based miRNA constructs offer a safer alternative to RNA Pol III-transcribed shRNAs. The constituitive expression of RNA Pol III-driven shRNAs can be controlled with a change in promoter. Embedding potent shRNAs into a miRNA construct has been shown to reduce RNA Pol III shRNA-associated toxicities (Castanotto *et al*, 2007; McBride *et al*, 2008). The tissue-specific and temporal expression of shRNA/siRNA-based miRNA expression is promising but it has been speculated that because these constructs require Drosha-DGCR8-processing, which traditional shRNAs do not need, the extra processing step may introduce a new potential step for small RNAs to compete over (Giering *et al*, 2008).

1.1.3.2 siRNAs

Synthetic RNAi effectors that mimic a Dicer-processed miRNA duplex are known as siRNAs. These RNA duplexes with full complementarity mimic Dicer products and are therefore incorporated into RISC (Figure 1.2 c) (Schwarz *et al*, 2002). siRNAs can be introduced into the cytoplasm of cultured cells via transfection but siRNAs transfect poorly into many cell types (Elbashir *et al*, 2001a). These RNAi effectors can be potent but the suppressive effects are not long-lasting *in vitro* (Fellman *et al*, 2011).

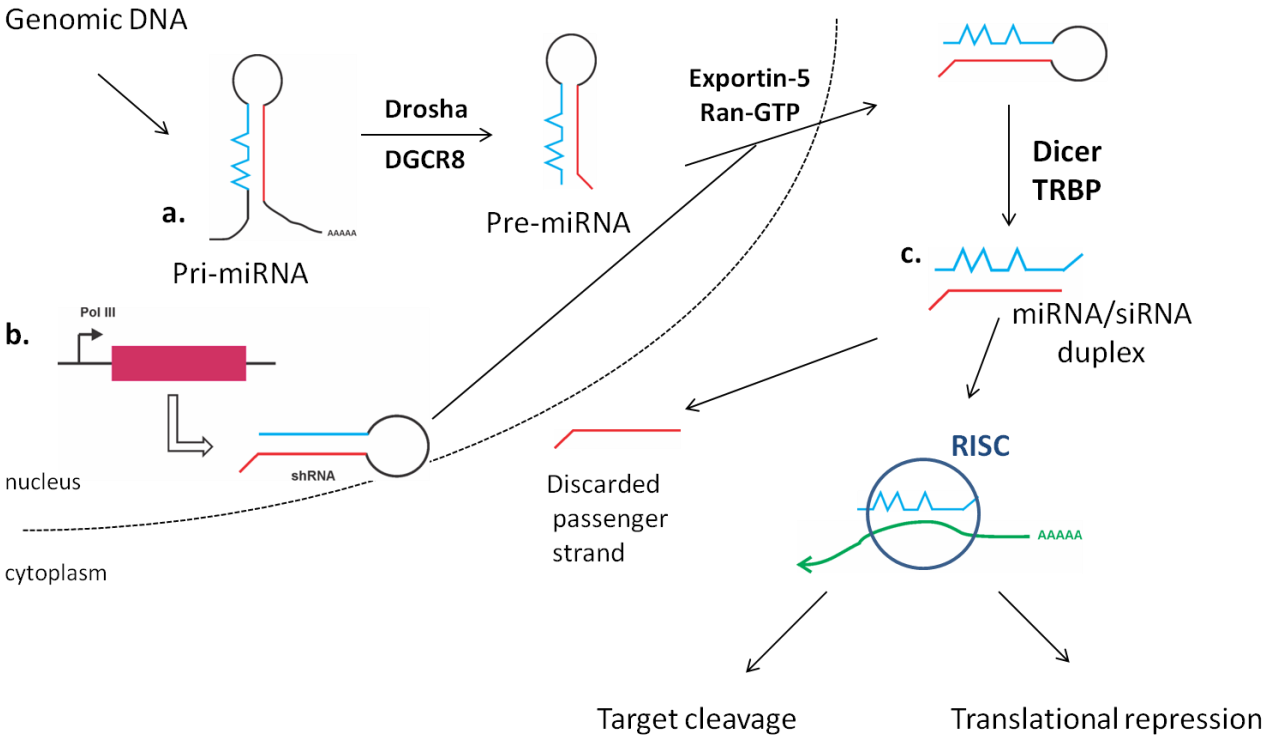


Figure 1.2: RNAi effectors interacting with the endogenous miRNA pathway.

RNAi effectors are introduced into the RNAi pathway in one of three forms: a. a pri-mRNA mimic that will be processed by all of endogenous RNAi machinery, b. a pre-miRNA otherwise known as a shRNA. Expressed shRNAs are generally transcribed by a Pol III promoter and c. Synthetic siRNAs that are transfected into the cell.

1.1.3.3 shRNAs

Alternatively to miRNAs and siRNAs, short hairpin RNAs (shRNAs) can be used to induce post-transcriptional gene silencing (Paddison *et al*, 2002). Using shRNAs rather than siRNAs in RNAi studies is cheaper, grants easier delivery and the silencing effects last longer (McIntyre and Fanning, 2006). These stem-loop structures that resemble Drosha-processed pre-miRNAs can induce stable and continuous gene expression knockdown from one cell division to the next (Brummelkamp *et al*, 2002; Paddison *et al*, 2002). shRNAs are transcribed in the nucleus and processed into an siRNA duplex by the host RNAi machinery (Figure 1.2 b).

The majority of expressed shRNA systems use a RNA Pol III promoter because these promoters yield transcripts with defined ends (Figure 1.2 b) (Brummelkamp *et al*, 2002; Paddison *et al*, 2002; Stegmeier *et al*, 2005). Due to the constituitive active nature of these promoters in all cell types, cell toxicity becomes a problem (Stegmeier *et al*, 2005; Grimm *et al*, 2010). The selection of a weak RNA Pol III promoter (e.g. H1), or a grouped set of polycistronic shRNAs (shRNAs expressed in tandem) transcribed by a single promoter, or combinatorial therapy including non-RNAi therapies are all viable options (Li *et al*, 2005; Zhang and Rossi, 2010).

1.2 Alternative approaches to express shRNAs

Multiple tools have been devised to mimic endogenous RNAi effectors and manipulate the RNAi signalling pathway. The traditional shRNA RNAi effector mimics pre-miRNA after Drosha processing. The use of vector-based shRNAs has its disadvantages. These limitations have forced researchers to develop different shRNA designs in order to overcome the hurdles of using expressed shRNAs.

1.2.1 tRNA-shRNA

The issue of over-expression of shRNAs has been linked to promoter selection. RNA Pol III promoters (e.g. U6 and H1) are constitutively active which can lead to the ectopic RNA out-competing endogenous RNAi machinery. The U6 and H1 promoters are classified as type III. An alternative to highly expressed and potentially cytotoxic H1 or U6-driven shRNAs are the tRNA-shRNAs. The tRNA promoter is a type II Pol III promoter which is structurally more complicated than U6 and H1 with its distinct cloverleaf secondary structure (Sibley, 2010; Boden *et al*, 2003a). This promoter allows the shRNA to circumvent Exportin-5 transport, relying on the Exportin-t instead (Sibley *et al*, 2010). The use of an alternate nuclear export route contributes to a reduction in Exportin-5-linked saturation and cytotoxicity.

1.2.2 Trans-kingdom RNAs

Trans-kingdom (tk) RNAs utilise an elaborate method to avoid Exportin-5 toxicities. Xiang *et al* (2006) engineered *Escherichia coli* that could be delivered into mammalian cell systems and transcribe shRNAs using T7, a promoter derived from bacteriophage T7. The shRNAs bypass the mammalian endogenous miRNA pathway but remain active RNAi triggers in the host mammalian cells thus preventing potential saturation (Xiang *et al*, 2006). One concern associated with this system is that T7-transcribed siRNAs have been reported to induce a strong interferon response

(due to the presence a 5' triphosphate), which is a major safety concern in gene therapy (Kim and Rossi, 2004).

1.3 Limitations of RNAi-based therapy

As promising as the RNAi technology is, the field has hurdles to overcome before fully realising its therapeutic potential. The delivery problems associated with gene therapy also apply to RNAi; safety is another issue. RNAi effectors can have cytotoxic effects either due to overwhelming the endogenous RNAi pathway, stimulating an innate immune response or inadvertently silencing unintended targets due to sequence similarity (Aagaard and Rossi, 2007).

RNAi effectors generally use the same RNAi machinery as endogenous miRNAs, therefore some pathway components are at risk of oversaturation if a high dose of RNAi triggers is used (Grimm *et al*, 2006; Aagaard and Rossi, 2007). ShRNAs with dinucleotide 3' overhangs mimicking Drosha-processing, like endogenous miRNAs, rely on Exportin-5-mediated nuclear export (Yi *et al*, 2005). This observation suggests that strong and constitutive shRNA-guided target mRNA knockdown can potentially saturate the endogenous microRNA biogenesis pathway leading to cell toxicity (Grimm *et al*, 2010 and Castanotto *et al*, 2007). The nuclear exporter Exportin-5 may be at risk of oversaturation as it transports both endogenous pre-miRNAs and most exogenous RNAi effectors (with the exception of tRNAs which rely on Exportin-t and RanGTP for nuclear export) from the nucleus to the cytoplasm (Grimm *et al*, 2006; Kutay *et al*, 1998). At high dosages, exogenous RNAi effectors can potentially out-compete endogenous miRNAs for Exportin-5-mediated nuclear export and negatively affect cell function. Endogenous miRNAs serve functions that range from tumour suppression to mammalian development (Chan *et al*, 2005; Papapetrou *et al*, 2010). Recent literature has identified active Ago2 in the nucleus which introduces a new aspect to consider in limiting exogenous RNAi trigger-induced saturation of the endogenous miRNA biogenesis. Ago2 is

a major component of the RNAi pathway suggesting that Ago2, rather than Exportin-5, is at the most risk of oversaturation (Börner *et al*, 2013).

Target specificity is important with RNAi effector design. To minimise unwanted targeting, the target mRNA sequence should not be similar to non-target mRNAs. This is a difficult task because a mere 6-7 nucleotide target match to the siRNA "seed region" can cause unwanted translation inhibition (Lin *et al*, 2005; Jackson *et al*, 2006b; Ui-Tei *et al*, 2008a). RNAi effector thus will have unwanted targeting. Off-targeting may affect genes that are essential for normal cell function hence shRNAs have potentially lethal cytotoxic effects due to off-target gene regulation (Jackson *et al*, 2003; Grimm *et al*, 2006). Off-targeting remains a major concern for RNAi-based therapeutic applications (Aagaard and Rossi, 2007). Identifying highly effective RNAi effectors that function at low doses would abate any off-targeting concerns (Liu *et al*, 2013).

The degree at which double-stranded RNA can induce an immune response is influenced by duplex length and cell type (Reynolds *et al*, 2006). RNA duplexes longer than 30 nt can rapidly induce cytotoxic effects in mammalian cells by activating the innate immune system via Toll-like receptors (TLRs), protein kinase (PKR) that is activated by double-stranded RNA and retinoic acid inducible gene I (RIG-I) and activating interferon-stimulated genes including 2',5'-oligoadenylate synthases (2-5-OAS); all of which are conserved mechanisms to protect a host against pathogen invasion (Reynolds *et al*, 2006; Garcia-Sastre and Biron, 2006; Aagaard and Rossi, 2007). RNAi effectors are generally designed to yield siRNAs with a <30 nt duplex to minimise the chance of immunostimulation.

1.4 shRNAs and RNAi efficacy

Since the discovery and manipulation of this highly conserved pathway, methods have been developed to enhance the potency of RNAi triggers. Successful application of RNAi as a therapeutic requires the use of potent RNAi triggers at low concentrations, specificity to reduce off-targeting and minimal immunostimulation (Uprichard *et al*, 2005; Castanotto, 2011). The design of expressed shRNAs has varied throughout the years.

1.4.1 Features of functional siRNAs

A set of rules have been established to ensure the design of an effective siRNA and these same rules have been applied to shRNA design (Amarzguioui *et al*, 2005; Ding *et al*, 2008). Algorithms have been developed to identify highly functional siRNA favouring the following features: (i) duplex asymmetry to ensure guide strand incorporation into RISC, (ii) low GC content (32-50%), (iii) have a minimum of 3 A/U pairings at positions 15-19, (iv) accessibility of the target mRNA (v) a U at position 10, (vi) no internal repeats with a melting temperature (T_m) less than 20°C and (vii) A or U at position 19 (Holen *et al*, 2002; Reynolds *et al*, 2004; Heale *et al*, 2005). These guidelines are helpful but are not discriminative enough to filter out false positives (non-functional siRNAs) (Yiu *et al*, 2005). Additionally, it has been suggested that not all functional siRNA design rules apply to shRNAs but most rules do (Matveeva *et al*, 2007; Zhou and Zeng, 2009). Additional sequence factors that have been shown to positively influence shRNA efficacy are: A/U at positions 2, 10, 13 and 14, a guide strand with a U-rich 5' end, the target sequence adjacent to where the guide strand binds must be taken into account (e.g. ~8 nt of the sequence flanking the binding site must be A-rich) (Tan *et al*, 2012). Functional shRNAs have been shown to be most potent if both terminal ends have a high free energy state (Zhou and Zeng, 2009). ShRNAs with a Dicer cleavage site positioned 2 nt from the loop exhibit greater potency and reduced off-targeting (Gu et al, 2012). Gu *et al* developed this "loop-counting rule" to improve Dicer-cleavage accuracy. Potent shRNAs are rare and are difficult to predict using algorithms which leads to either large-scale empirical testing or more creative shRNA designs to ensure efficacy (Fellman *et al*, 2011). Li *et al* (2007) were able to

create an accurate computer algorithm to screen for functional shRNAs, the small data set reduces its validity and studies have identified highly functional shRNAs that weren't predicted by algorithms (Fellman *et al*, 2011).

1.4.2 Strand orientation and shRNA efficacy

Other factors must be considered for efficient shRNA design. There is a correlation between RNAi activity and shRNA structure (Zhou and Zeng, 2009; Ge *et al*, 2010). Early RNAi studies identified 5'-arm guide strand shRNAs more potent than their 3'-arm guide strand (typical shRNA design) counterparts (McManus *et al*, 2002; Harborth *et al*, 2003). This class of shRNA can be potent at a very low picomolar range which is ideal for therapeutic applications (Ge *et al*, 2010). Despite these observations, the standardised shRNA design used in most studies has a 3'-arm guide strand (Ilves *et al*, 2006; Vlassov *et al*, 2007; Wang *et al*, 2013).

1.4.3 Strand bias

Ensuring that only the guide strand of a shRNA is incorporated into RISC is an important design feature for maximising shRNA silencing efficacy and specificity (Ding *et al*, 2008). The stability of the 5'-arm terminal base pair of a functional duplex determines strand bias (Khvorova *et al*, 2003; Schwarz *et al*, 2003). RNAi studies observed that the less thermodynamically stable strand is incorporated into RISC; the same strand bias exists in mammalian RNAi (Schwarz *et al*, 2003). A nucleotide residue mismatch within the 5'-arm terminal base pair introduces thermodynamic asymmetry in a RNA duplex resulting in the strand with a 5' end that is less tightly bound to be loaded into RISC (Schwarz *et al*, 2003). shRNAs are designed to include siRNA functional asymmetry for biased guide strand selection (Schwarz *et al*, 2003; Ding *et al*, 2008). shRNA potency is affected by the accuracy of strand bias (Fellman et al, 2011), which highlights the importance of guide strand bias. Evidently there are many ways to positively affect the potency of

functional shRNAs. It would be preferable to simplify shRNA design without compromising RNAi efficacy.

1.5 The distinct biogenesis of miR-451

Separate research groups simultaneously discovered an endogenous miRNA that defies the generally accepted hypothesis that Dicer is the unifying enzyme in the RNAi pathway (Siolas *et al*, 2005; Cheloufi *et al*, 2010; Cifuentes *et al*, 2010). The microRNA in question is miR-451, which plays a major role in erythropoiesis (Cheloufi *et al*, 2010).The maturation process of this particular miRNA is Dicer-independent but miR-451 is still incorporated into RISC and thus requires Ago2-processing (Cheloufi *et al*, 2010; Cifuentes *et al*, 2010). This miRNA is also non-canonical due to its structure (Cifuentes *et al*, 2010). The conserved precursor miR-451 (pre-miR-451) is a 42 nt hairpin with a 17 nt-long stem; this is an uncharacteristically short stem due to Dicer only processing hairpins with a ≥ 19 nt stem (Cheloufi *et al*, 2010; Cifuentes *et al*, 2010). Mature miR-451 varies in length from 20 to 30 nt; six nucleotides of the terminal end follow the length of the loop region to double-back into the complementary strand of pre-miR-451 (Figure 1.3), which is an insufficient Dicer substrate (Siolas *et al*, 2005; Cheloufi *et al*, 2010). The 3' end is intermediate in length with an unpaired uridine tail (Cifuentes *et al*, 2010; Cheloufi *et al*, 2010).

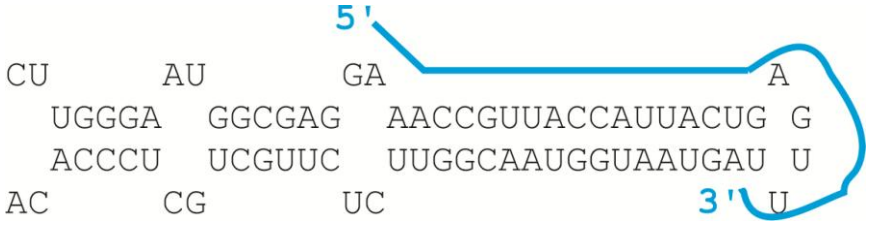


Figure 1.3: The unconventional structure of the miR-451 hairpin.

The mature miR-451 extends over the loop (depicted in blue).

Primary miR-451 (pri-miR-451) exists in a miRNA cluster with miR-144 upstream of miR-451 (Cheloufi *et al*, 2010). Drosha excises pre-miR-451 from the primary miRNA transcript as per canonical miRNA biogenesis (Cheloufi *et al*, 2010). After Drosha cleavage, pre-miR-451 interacts directly with the core component of RISC, Ago2 (Cheloufi *et al*, 2010; Cifuentes *et al*, 2010). The miR-451 Ago2 product is an intermediate hairpin (with a uridine tail of inconsistent length) that is further trimmed (Cifuentes *et al*, 2010). The slicer activity that mammalian Ago2 retains is essential for pre-miR-451 cleavage and maturation (Yang *et al*, 2010). A study discovered that pri-miR-451 can be reprogrammed to serve as a vector that yields active miRNA and retain Dicer independence rescues miRNA maturation and function (Yang *et al*, 2010). These pri-miR-451 mimic vectors can be used in Dicer-null environments but may also have therapeutic potential. Prior to this discovery, only Drosha-independent non-canonical miRNAs had been identified such as small nucleolar RNA (snoRNA), tRNAs and miRtrons (Berezikov *et al*, 2007; Babiarz *et al*, 2008). The canonical RNAi pathway depicts Dicer as the central enzyme required for dsRNA processing (Yang *et al*, 2010). miR-451 is processed by Drosha but bypasses Dicer to be loaded directly onto Ago2 (Cheloufi *et al*, 2010).

Due to identifying the Dicer-independent nature of miR-451, a link has been found between the conserved slicer activity that Ago2 retains and miRNA maturation (Cheloufi *et al*, 2010). Ago2 binds to and processes miR-451 (Cifuentes *et al*, 2010). The discovery of a Dicer-independent RNAi pathway disputes the generally accepted hypotheses that Dicer-processing and RISC-loading only function in tandem and that Dicer-processing determines small RNA silencing efficacy (Siolas *et al*, 2005; Chendrimada *et al*, 2005; Wang *et al*, 2009). The discovery of miR-451 has expanded our understanding of the RNAi pathway and offers an alternative pathway with potential therapeutic applications.

1.6 Dicer and Ago2

The major miRNA-processing steps in mammalian RNAi involve the following enzymes: Drosha, Dicer and Ago2. Due to shRNAs bypassing interaction with Drosha, I shall focus on Dicer and Ago2. With the discovery of miR-451 and its alternate Dicer-independent but Ago2-dependent processing route, it is worth briefly describing the structural differences and similarities of Ago2 and Dicer.

1.6.1 Dicer

Bernstein *et al* (2001a) identified Dicer as the enzyme that yields 21-27 nt sequences that guide gene silencing. Dicer is a member of the RNase III nuclease family that process dsRNAs (pre-miRNAs, shRNAs and long dsRNAs) into duplexes (siRNAs and mature miRNAs) with a 2 nt hydroxyl 3'overhang and 5' monophosphate (Bernstein *et al*, 2001a; Czech and Czech and Hannon, 2011). Mammalian genomes encode a single Dicer protein that consists of the following domains: a PAZ domain, two highly conserved RNase III domains (RNase IIIa and b), dsRNA-binding domain (dsRBD), domain of unknown function (DUF283) and an ATPase/DExD helicase (Figure 1.3 a) (Song *et al*, 2003; Carmell and Hannon, 2004; Park *et al*, 2011).

The dsRBD binds Dicer to dsRNAs, aiding in anchoring the enzyme. It has been suggested that the DUF283 acts as a dsRNA binding domain (Dlakic, 2006). The helicase domain plays a part in the unwinding and "dicing" of dsRNAs (Bernstein *et al*, 2001a; Welker *et al*, 2011). The RNase III domains work in tandem (RNase IIIa cleaves the 3'-arm and IIIb, the 5'-arm), allowing Dicer to process dsRNAs as a monomer (Paddison, 2008). Dicer acts as a molecular ruler for determining cleavage sites, typically ~22 nt in length. The distance between the PAZ and RNase III domains matches the length of the resultant processed RNA duplex. In mammals, the positively-charged Dicer PAZ domain binds to both the 5' and 3' ends of pre-miRNAs, binding Dicer to the dsRNA and measures a pre-determined distance from the 5' end to cut the pre-miRNA (Carmell and Hannon, 2004; Park *et al*, 2011).

1.6.2 Ago2

A small double-stranded RNA species needs to interact with a member of the Argonaute family in order to perform its effector function. The human Argonaute subfamily consists of Ago1, Ago2, Ago3 and Ago4. All four Argonaute proteins are ubiquitously expressed and associate with miRNAs and siRNAs.

This highly conserved family of proteins can be divided into three subclasses according to sequence homology: Ago (similar to *Arabidopsis* Ago1), the worm-specific WAGO clade and PIWI (resembles the *Drosophila* PIWI protein) (Tolia and Joshua-Tor, 2006; Hutvagner and Simard, 2008). These protein types generally bind to the guide strands of small RNAs that share the following characteristics: a 5' monophosphate, are ~20-35 nt long and have a 2-nt overhang with a 3' hydroxyl terminus which can be modified (Czech and Hannon, 2011).

An Argonaute protein bound to a small RNA guide strand makes up the mature RISC (Filipowicz, 2005). Before the passenger strand of a small RNA duplex is cleaved and discarded by Ago2, the complex is known as pre-RISC (Grimm *et al*, 2010). The mature RISC must be assembled correctly (with the correct guide strand) to facilitate target recognition and repression (Filipowicz, 2005; Matranga *et al*, 2005; Rand *et al*, 2005). The Argonaute protein is the catalytic core of RISC but other proteins may be complexed with RISC to either enhance Argonaute function or direct the complex to target specific sites (Meister *et al*, 2004). Argonautes serve to cleave its RNA target at a single phosphodiester bond, between the tenth and eleventh nucleotides of the target (Elbashir *et al*, 2001).

The exact three-dimensional structure of any eukaryotic Argonaute protein has yet to be determined but due to studies of bacterial and archaeal Argonaute proteins and individual eukaryotic components, broadly-applying principles have been observed. Both AGO and PIWI proteins consist of the following key domains: 1) PIWI, 2) middle (Mid) and 3) Piwi-Argonaute-Zwille (PAZ) (Figure 1.3 b).

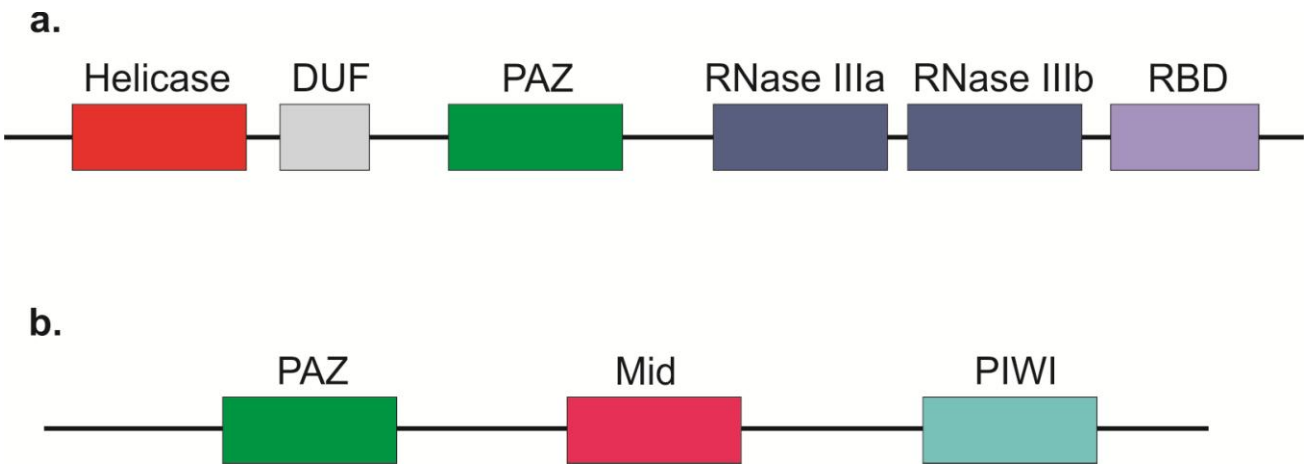


Figure 1. 4: Schematic of the Dicer and Ago2 domains.

a. Mammalian Dicer has a helicase and domain of unknown function (DUF283) at its N terminus. There is a PAZ domain. The two RNase III domains and dsRNA-binding domain (RBD) are located at the C terminal end. b. Ago2 has a PAZ, Mid and PIWI domain.

The PAZ domain has a 3'-OH binding site where it anchors the 3'-end of the small single-stranded RNA (Song *et al*, 2003b; Jinek and Doudna, 2009). The carboxy-terminal PIWI domain structure contains the Argonaute endonuclease and resembles RNAse H due to a motif that consists of three negatively charged amino acids, DDH (aspartate-aspartate-glutamate [HIS/]) (Song *et al*, 2004; Czech and Hannon, 2011). The DDH motif determines whether an argonaute has the catalytic activity known as slicing (Czech and Hannon, 2011). Thus PIWI is the endonucleolytic cleaving

domain of eligible AGO proteins. Despite the great homology between the Ago proteins, Ago2 alone has endonuclease or “slicer” activity (Tolia and Joshua-Tor, 2007). Ago2’s ability to slice depends on the level of complementarity between the guide strand and its target mRNA. In the event of a perfect match, RISC cuts the mRNA at position 10 (10 nt from the site where the 5’ end of the RNAi effector is bound to the target mRNA) (Elbashir *et al*, 2001). If the guide strand and target mRNA do not complement each other perfectly (generally the case with miRNAs) then translational repression occurs (forms of translational control reviewed by Valencia-Sanchez *et al*, 2006). The Mid domain acts as a binding site for the 5’ phosphate of the terminal of the RNAi effector (Frank *et al*, 2010). Human Ago2 is able to sort through small RNAs due to its Mid domain which selects for 5’ terminal adenosine or uridine (Figure 1.3 a) (Frank *et al*, 2010).

1.7 Mimicking miR-451 to improve shRNA specificity and potency

During the infancy of RNAi-based studies, systems were developed to manipulate the gene silencing mechanism in transfected mammalian cells (Brummelkamp *et al*, 2002; Paddison *et al*, 2002; Zeng *et al*, 2002). ShRNAs can be exogenously introduced into cells (as chemically synthesised shRNA or in DNA vectors) or transcribed *in vivo* to stably suppress gene expression in a heritable manner in continuous cell lines (Paddison *et al*, 2002; Sui *et al*, 2002; Siolas *et al*, 2005). Most developed shRNAs are DNA vector-based rather than synthetic (Ge *et al*, 2010; Terasawa *et al*, 2011). Expressed RNAi effectors (including shRNAs) offer longer lasting target suppression compared to their synthetic counterparts and, contrary to synthetic RNAi triggers, are compatible with viral vectors which is a preferable trait for therapeutic application (Ter Brake *et al*, 2006; Knoepfel *et al*, 2012). shRNA expression systems can be altered in various ways to enhance RNAi efficacy.

The most commonly used shRNA design consists of a 21 bp stem and 5 nt loop but for the purposes of this study, three sets of short (19 bp stem) and long (25 bp stem) shRNAs were designed with each 19mer/25mer pair targeting the same sequence (Brummelkamp *et al*, 2002; Bernards *et al*, 2006; Ter Brake *et al*, 2006 and 2008; Huang *et al*, 2008; Asparuhova *et al*, 2008). The siRNA core of the long shRNAs was positioned at the terminus of the hairpin and the sequence extended to the base of the loop. This design ensured that the position of the siRNA core was the same between the short and long shRNAs and maximised silencing efficacy of each class of shRNA (McIntyre *et al*, 2011).

Short hairpin RNA stems are typically 19-29bp long because the shorter shRNAs (≤ 19bp) are not Dicer substrates and are thus not considered potent without Dicer processing (Siolas *et al.*, 2005). Additionally, a comparative study of 19bp and 29bp shRNAs, in a 4nt loop context, the 29bp shRNAs were more potent than their shorter counterparts and increasing the loop length (to 9nt)

improved efficacy in both 19mers and 29mers compared to their 4nt versions (Li *et al*, 2007). The Dicer-independent nature miR-451 suggests that a short shRNA design (< 19 bp stem) has the potential to be highly functional regardless of Dicer-processing (Cheloufi *et al*, 2010; Cifuentes *et al*, 2010).

Manipulating the guide strand orientation affects the gene silencing efficacy of shRNAs (McManus *et al*, 2002; Ge *et al*, 2010). ShRNAs typically have the guide strand located at the 3'-arm even though studies have shown that the reverse orientation (5'-arm guide strand) can yield stronger shRNA inhibitory capability (Harborth *et al.*, 2003; Li *et al*, 2007; Vlassov *et al*, 2007; Ge *et al* 2010; Liu *et al*, 2013). Relocating the guide strand to the 5'arm of shRNAs creates a defined starting point for transcription thus granting more accurate prediction. This alteration will provide a level playing field (between the 19mers and 25mers) in determining how Dicer-independent hairpin processing affects downstream gene silencing. Moving the guide strand to the 5'-arm also places the seed region at the 5' terminal of the base of the shRNA which secures the seed region from possible Dicer cleavage as a precautionary measure (Figure 1.4).

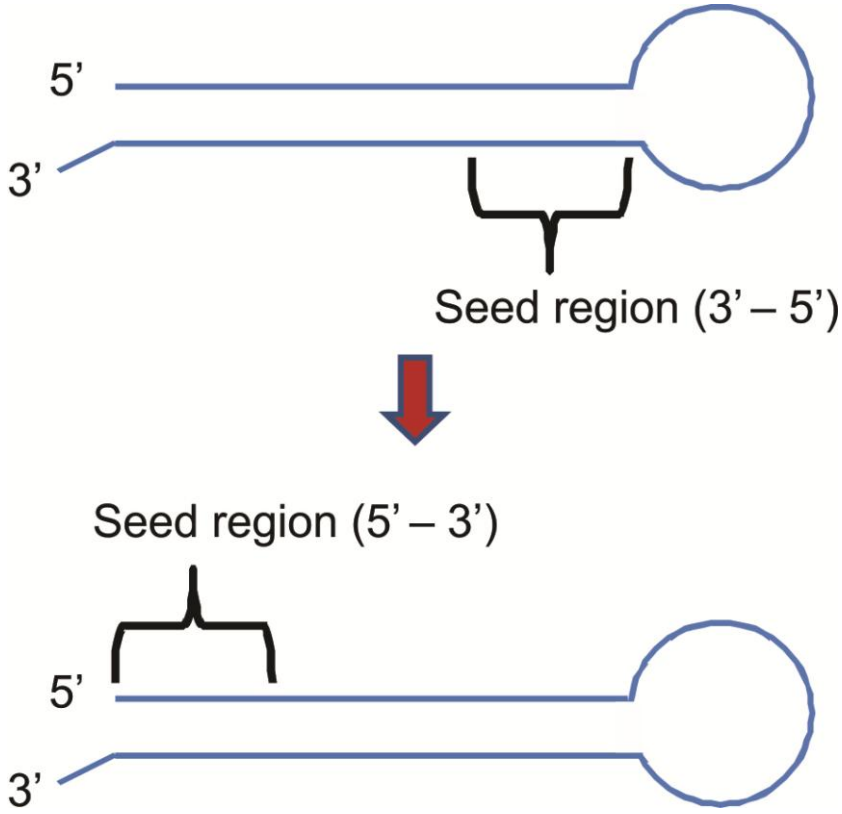


Figure 1.5: Relocating the seed region.

The guide strand being relocated to the 5’-arm results in a seed region at position 2 to 7 of the 3’-arm to be repositioned to the 5’ terminal end at the base of the hairpin.

Introducing exogenous RNAi effectors can potentially cause unwanted off-target effects (Reynolds *et al*, 2006). A miR-451-based shRNA design may alleviate the negative side effects associated with RNAi effectors. The use of smaller hairpins in therapeutic applications is ideal due to increased ease and safety of delivering the therapy into a subject (Huang *et al*, 2008; Asparuhova *et al*, 2008).

1.8 Aims and objectives

The main aim of this study was to determine whether the RNAi efficacy and potency of expressed shRNAs could be improved using a design that mimics Dicer-independent miR-451. The study objectives included:

1) Pairs of 19mer and 25mer shRNAs that targeted the same sequence were constructed.
2) Assessed how repositioning the seed region affected the RNAi efficacy of the shRNAs.
    a) The silencing efficacy and potency of the shRNAs (19mer versus 25mer) were compared.
3) Determined whether the shRNAs induced unwanted off-target effects.
    a) Assessed the interferon response, cell function and saturation of the RNAi pathway.
4) Investigated how the 19mer shRNAs were processed by the RNAi machinery.
    a) Did the 19mers mimic miR-451 processing?

Chapter 2: Materials and Methods

2.1 Plasmids generated prior to this study

2.1.1 The H1 promoter

Each of the shRNAs generated for this study are expressed from an H1 promoter that was first characterised by Chen *et al* (2005, PNAS, A universal library encoding all permutations of siRNA). Dyer *et al* (2010) cloned the entire H1 promoter. The H1 forward (5'-GAT C*GA ATT C****AC*** **TAG T**GA ACG CTG ACG TCA TCA A-3') and reverse (5'-GGA TCC GTG GTC TCA TAC AGA ACT TAT AAG ATT CCC AAA TC-3') primers were synthesised by Integrated DNA Technologies (IDT, USA). The H1 forward primer was designed to include including *EcoRI* (underlined) and *SpeI* (in bold) restriction sites. A resuspended 100 µM stock solution was prepared for each H1 primer oligonucleotide and from each, a 15 µM working solution. PCR was used to amplify the H1 promoter in a reaction with the final volume of 25 µl consisting of the following: 15 pmol H1 forward primer, 15 pmol H1 reverse primer, 100 ng H1 genomic DNA, 2.5 mM dNTP mix (Thermo Scientific, USA), 0.25 U TripleM™ Taq polymerase in 1x High Fidelity buffer from the High Fidelity PCR kit (Roche, Germany). The H1 promoter was amplified using the following PCR protocol: 1) denaturation at 94°C for 5 minutes and ten rounds of touchdown PCR (94°C for 10 seconds of denaturation, 67°C for 10 seconds of annealing and an elongation step of 72°C for 10 seconds; the annealing temperature was decreased by 1 degree centigrade each cycle); 2) the touchdown PCR was followed by 14 cycles of denaturation at 94°C for 20 seconds, 57°C for 20 seconds of annealing and 72°C for 45 seconds of elongation and 3) a final step at 72°C for two minutes and thirty seconds of elongation (Eppendorf Mastercycle Gradient, Germany). The amplicon (PCR product) was resolved on an agarose gel for electrophoresis to confirm the DNA fragment size and excised from the gel and purified using the MinElute™ Gel Extraction Kit (Qiagen, Germany) (Appendix A.1). The purified H1 promoter DNA will be referred to as H1 promoter template DNA.

2.1.2 The H1 Mock vector

Dyer *et al* (2010) produced an H1-transcribed empty plasmid (referred to as H1 mock) using an H1 mock reverse primer (5'-GAT CAA AAA ACG GAT CCG AGT GGT-3') with a *BamHI* (underlined) restriction site and the termination signal. The H1 mock reverse primer was synthesised by Inqaba Biotec (Pretoria, RSA) and prepared as described in section 2.3.1. The PCR had a final volume of 20 µl consisting of 15 pmol H1 forward primer, 15 pmol H1 mock reverse primer, 500 ng H1 promoter template DNA and 2.5 µl MasterMix™ (Thermo Scientific, USA). The PCR protocol was run as described (section 2.3.1) and the amplicon size was determined via agarose gel electrophoresis. The amplified DNA was excised from the agarose gel and purified using the MinElute™ Gel Extraction Kit (Qiagen, Germany) (Appendix A.1). The H1 mock amplicon was inserted into the pTZ57R/T cloning vector (Thermo Scientific, USA). The ligation reaction had a final volume of 20 µl and contained the following: 0.165 µg pTZ57R/T, 7.5 U T4 DNA ligase, 300 ng H1 mock amplicon; all diluted in 1x ligation buffer (Thermo Scientific, USA). The ligation reaction was incubated overnight at room temperature and used to transform competent *E.coli* DH5-α cells (Appendix A.2). The transformed DH5-α cells were plated on a X-gal/IPTG (40 µl5-bromo-4-chloro-3-indolyl-beta-D-galactopyranoside (X-gal, Sigma, USA) and 8 µl of isopropyl thiogalactoside (IPTG, Roche, Germany) Luria-Bertani (LB) agar plate (Appendix A.3). The plate was incubated overnight at 37°C. Blue/white screening was used to pick the successfully transformed bacteria (Appendix A.3). Five clones transformed with the H1 mock plasmid were selected to each inoculate 4 ml LB and left to incubate overnight at 37°C in a shaking incubator. On the following day, the H1 mock plasmid DNA was purified using the High Pure Plasmid Isolation Kit (Roche, Germany) (Appendix A.4).

2.1.3 The GFP reporter plasmid

Passman *et al* (2000) cloned enhanced green fluorescent protein (*eGFP*) into the mammalian expression vector pCI-neo (Promega, USA). The EGFP-encoding sequence was PCR-amplified from the pBI-EGFP vector (Clonetech, USA). The amplicon was digested with *XhoI* and *XbaI* and cloned into complementary sites in the multiple cloning site of pCI-neo. The resultant reporter plasmid is known as pCI-eGFP. This vector served as the reporter plasmid in all mammalian culture work. The supplementary Figure B.3 is an example of GFP expression under fluorescence microscopy.

2.2 Molecular cloning

2.2.1 Generation of the PTZ-H1shRNA expression cassettes

A one-step PCR approach was used to generate the shRNA-expressing cassettes (depicted in Figure 2.1). The H1 mock (pTZ H1+1) plasmid serves as the template DNA; it is complementary to both the 3'-end of the reverse primer and the 3'-end of the forward primer. A single reverse primer complementary to the whole hairpin was synthesized for each hairpin based on the selected target sequences as described in section 2.1 (Table 2.1). The primer contains the sense strand, loop, antisense strand and termination sequence. The shRNA primer oligonucleotides (Table 2.2) were prepared by Integrated DNA Technologies (IDT, Germany). The H1 forward primer (5'-GAT CGA ATT CAC TAG TGA ACG CTG ACG TCA TCA A-3') is complementary to the 5' end of the human H1 promoter in pTZ H1+1 (Dyer *et al*, 2010). Dyer *et al* (2010) inserted *EcoRI* and *SpeI* restriction sites at the 5' end of the H1 primer. The H1 forward and hairpin 3' reverse primers were used to generate a shRNA expression cassette (Castanotto *et al*, 2002).

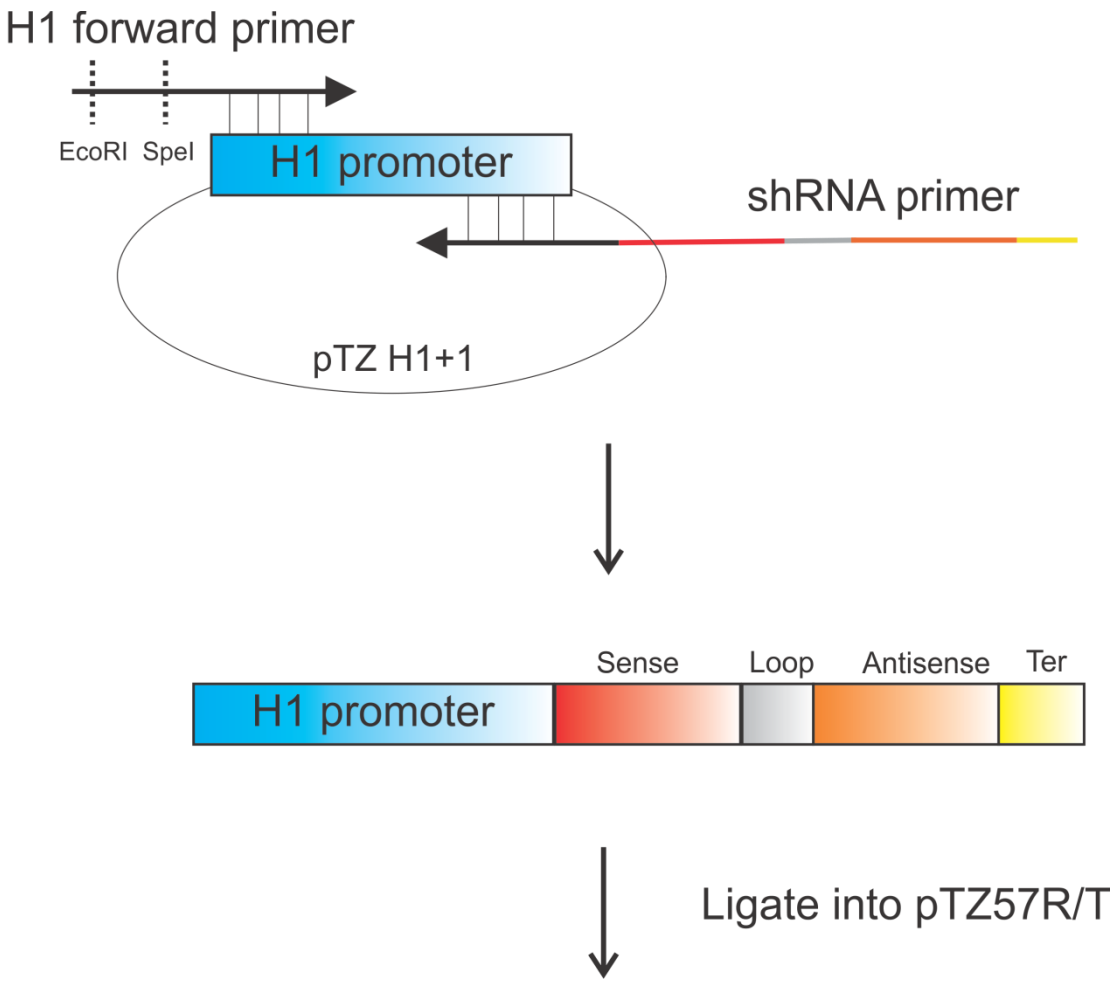


Figure 2.1: One-step PCR approach.

The empty plasmid pTZ H1+1 (H1 mock) served as the template for the H1 forward primer (section 2.3.1) and shRNA reverse primer to generate a shRNA in the PCR product. The PCR product was then ligated into the pTZ57R/T cloning vector.

Table 2.1: Primers used to generate shRNA-expressing constructs.

The primers served as the reverse primer in the one-step PCR. The termination tail is underlined. The tetraloop is underlined in bold. The guide arranged into the sense strand is indicated in bold. The italicised segment is complementary to the H1 promoter.

Primer name	Oligonucleotide reverse primer (5' → 3' sequence)
H1 shG19	AAAAAATAATCTTGTGGGGTGGCTCTTTC**GAGCCACCCCACAAGATTC***GGGTCCGAGTGGTCTCATAC*
H1 shG25	AAAAATAATCTTGTGGGGTGGCTCCTTCTGTTTC**CAGAAGGAGCCACCCCACAAGATTC***GGGTCCGAGTGGTCTCATAC*
H1 shE19	AAAAAAATATAATTCACTTCACCATTTC**TGGTGAAGTGAATTATATC***GGGTCCGAGTGGTCTCATAC*
H1 shE25	AAAAAATATAATTCACTTCACCAATTGTCTTTC**GACAATTGGTGAAGTGAATTATATC***GGGTCCGAGTGGTCTCATAC*
H1 shL19	AAAAAATTGAGGCTTAAGCAGTGGTTTC**CCACTGCTTAAGCCTCAAC***GGGTCCGAGTGGTCTCATAC*
H1 shL25	AAAAAATTGAGGCTTAAGCAGTGGGTTCCCTTTC**GGGAACCCACTGCTTAAGCCTCAAC***GGGTCCGAGTGGTCTCATAC*

The reaction was prepared with a final volume of 50 µl and consisting of 15 µM H1 forward primer, 15 µM shRNA oligonucleotide (reverse primer), 1 µg pTZ H1+1 (vector plasmid with the H1 promoter) template DNA, 10 µM dNTP mix (Thermo Scientific, USA), High Fidelity *Taq* polymerase, 5 u/µl (Thermo Scientific, USA), 1x High Fidelity PCR Buffer (Thermo Scientific, USA) with 15 mM $MgCl_2$ and 10 µl betaine/DMSO PCR enhancer solution to restrict secondary structure formation. The PCR cycle was carried out within the following parameters: initial denaturation at 94°C for 3 minutes, 40 cycles of denaturation at 94°C for 30 seconds, annealing at 60°C for 30 seconds, extension at 72°C for 30 seconds and a final extension step at 72°C for 15 minutes. The annealing temperature varied according to the PCR gradient (Bio-Rad, USA). The bands were resolved and visualised on a 1% agarose (Lonza, Switzerland) gel using the G:BOX gel doc system (Syngene, UK) and the image was documented using Gel Logic 2000 (Kodak, USA). The bands of interest were excised from the gel and purified using the MinElute Gel Extraction Kit (Qiagen, Germany) (Appendix A.1). The shRNA PCR products (amplicons) were separately ligated into the cloning vector pTZ57R/T from the InsTAclone™ PCR Cloning kit (Thermo Scientific, USA). The process of generating the shRNA constructs relied on T/A cloning. The shRNA amplicons each had adenosine residue 3' overhangs due to *Taq* polymerase activity during the PCR step. These overhangs allow the PCR product to ligate to the thymidine residue overhangs of the multiple cloning site of pTZ57R/T. The ligation reactions had a final volume of 30 µl with the following: T4 DNA Ligase (5 U/µl) [U= units], 1x Ligation buffer, vector pTZ57R/T (0.17 pmol ends), shRNA PCR product (0.52 pmol ends) (Weiss *et al*, 1968).The reaction was incubated at room temperature for an hour or 4°C overnight. Ten microlitres of the ligation reaction was used to transform competent *Escherichia coli* (*E.coli*) DH5-α bacterial cells (Appendix A.2). Ampicillin (1x, Roche, Germany) Luria-Bertani (LB) agar plates were coated with X-gal (Sigma, USA)/IPTG (Roche, Germany) and incubated at 37°C for 20 minutes with the plate lids removed (Appendix A.3). The transformed cells were spread on the X-gal/IPTG ampicillin LB agar plates and incubated overnight at 37°C. Colony forming units (CFUs) transformed with pTZ-shRNA plasmids were identified via blue/white screening (Appendix A.3). White CFUs were picked from the agar plate, inoculated in 6 ml LB and incubated overnight at

37°C in a shaking incubator. The shRNA plasmid DNA was purified following the instructions of the High Pure Plasmid Isolation Kit (Roche, Germany) (Appendix A.4).

The white colonies were screened using a *SacI*/*BamHI* (Thermo Scientific, USA) restriction digest reaction (Supplementary Figure B.2). The test digest reaction had a final volume of 50 µl: 1 U *SacI*, 1 U *BamHI* and *BamHI* buffer, respectively (Thermo Scientific, USA), deionised water and 1.5 µg pTZ-shRNA plasmid DNA. The restriction digest reactions were incubated overnight at 37°C. The DNA fragments of the restriction digest reactions were run on a 3% agarose (Lonza, Switzerland) gel. The plasmid DNA was purified via phenol/chloroform (Merck, Germany) extraction (Appendix A.5). The phenol/chloroform-purified shRNA plasmid DNA was sent to Inqaba (Pretoria, RSA) for automated cycle sequencing to verify whether they had the correct sequence using universal M13 forward (5'-GTA AAA CGA CGGCCA G-3') and reverse (5'-CAG GAA ACA GCT ATG AC-3') primers. The sequence files were analysed using FinchTV (Geospiza Inc., USA).

2.2.2 Generation of target reporter plasmids

To assess the silencing efficacy of the shRNAs, vectors containing their respective target sequences were generated. The target sequences were inserted into the 3' untranslated region (UTR) of the *Renilla* luciferase reporter gene in the psiCHECK 2.2 reporter plasmid. The plasmid was designed by Prof M S Weinberg of our laboratory; psiCHECK2 (Promega, USA) was altered with the inclusion of an oligonucleotide bearing restriction sites. The target sequences are complementary to that of the respective shRNA guide strand. A pair of single-stranded oligonucleotides was synthesised by Integrated DNA Technologies (IDT, Germany) for each target (Table 2.3). An additional set of target sequences were generated for the passenger strand of each shRNA (Table 2.4).

Table 2.2: Guide strand target sequences.

The *EcoRV* restriction sites are underlined. The *XhoI* overhangs are in bold and the *NotI* overhangs are italicised.

Primer name	Single-stranded oligonucleotides (5'→ 3' sequence)
Target Gag	
Gag F	**TCGAGA**TATCCAGAAGGAGCCACCCCACAAGATTAGC
Gag R	*GGCCGC*TAATCTTGTGGGGTGGCTCCTTCTGGATATC
Target Env	
Env F	**TCGAGA**TATCGACAATTGGTGAAGTGAATTATATTG
Env R	*GGCCGC*AATATAATTCACTTCACCAATTGTCGATATC
Target LTR	
LTR F	**TCGAGA**TATCGGGAACCCACTGCTTAAGCCTCAATGC
LTR R	*GGCCGC*ATTGAGGCTTAAGCAGTGGGTTCCCGATATC

Table 2.3: Target sequences of the passenger strand of each hairpin.

Primer name	Single-stranded oligonucleotides (5'→ 3' sequence)
Target Gag passenger	
Gag F	**TCGAGA**TATCTAATCTTGTGGGGTGGCTCCTTCTGGC
Gag R	*GGCCGC*CAGAAGGAGCCACCCCACAAGATTAGATATC
Target Env passenger	
Env F	**TCGAGA**TATCAATATAATTCACTTCACCAATTGTCGC
Env R	*GGCCGC*GACAATTGGTGAAGTGAATTATATTGATATC
Target LTR passenger	
LTR F	**TCGAGA**TATCATTGAGGCTTAAGCAGTGGGTTCCCGC
LTR R	*GGCCGC*GGGAACCCACTGCTTAAGCCTCAATGATATC

In order to insert the target sequence into the reporter plasmid, the psiCHECK 2.2 plasmid was first linearised using restriction digest enzymes. Two micrograms (2 µg) of psi-CHECK 2.2 was linearised in a reaction including the following: 3 µl 1x Buffer O, 2 U *XhoI*, 10 U *NotI* and deionised water to make up a final volume of 30 µl (Thermo Scientific, USA). The reaction was mixed and incubated at 37°C for 2 hours.

Before the double-stranded target sequence could be inserted into the linearised psiCHECK 2.2 vector, the pairs of single oligonucleotides were annealed to one another to form double-stranded sequences. The single oligonucleotides were first each phosphorylated in separate 20 µl 10 µM reactions: 2 µl of 100 M stock single-stranded oligonucleotide, 2 µl 10x PNK buffer, 2 µl 10 mM ATP, 0.5 µl T4 PNK and 13.5 µl water (Thermo Scientific, USA). The reactions were incubated for 1 hour at 37°C. Ten microlitres of each complementary phosphorylated oligonucleotide was added together (20 µl total volume) and incubated for ten minutes at 75°C. This step serves to inactivate the enzyme. The oligonucleotides annealed while the heating block was left to cool for 30 minutes. The final concentration of the dsDNA oligonucleotide is 5 µM. The double-stranded oligonucleotide mixture was diluted to a working concentration of 200 nM (4 ng/µl). Five microlitres of the double-stranded oligonucleotide was ligated with 50 ng of the linearised (*XhoI*/*NotI*-digested) psiCHECK 2.2 vector plasmid (Figure 2.4). The ligation mix was transformed into DH5-α *E.coli* cells (Appendix A.2). Bacteria transformed with target plasmids were selected using blue/white screening and picked to inoculate in 6 ml LB (Appendix A.3). The bacterial culture was incubated overnight at 37°C in a shaking incubator. The target plasmid DNA was isolated using the High Pure Plasmid Isolation kit (Roche, Germany) (Appendix A.4). To verify successful ligation of linearised psiCHECK 2.2 and double-stranded target oligonucleotide, the target plasmids were screened using an *EcoRV* restriction digest reaction (Thermo Scientific, USA). The psiCHECK 2.2 vector has a single *EcoRV* restriction site but vectors with the target insert have an additional *EcoRV* site (seen in Tables 2.3 and 2.4). The digest reaction: 1 U *Eco321* (*EcoRV)*, 1X buffer R, 10 U RNaseA enzyme, 2 µg shRNA plasmid DNA and nuclease-free water up to a final volume of 50 µl (Thermo Scientific,

USA). The restriction digest reactions were incubated overnight at 37°C. The DNA fragments of the restriction digest reactions were resolved on a 3% agarose (Lonza, Switzerland) gel. The target plasmid DNA of each clone was sequenced by Inqaba (Pretoria, RSA). The following primers were used: psiCHECK forward (5'-GAC GCT CCA GAT GAA ATG GG-3') and reverse (5'-GTG CCC GTG GCC ACC AAG AC-3') primers (Inqaba, RSA). The sequence files were analysed using FinchTV (Geospiza Inc., USA). A greater and more concentrated volume of each sequence-confirmed PTZ-H1shRNA (described in section 2.4.1) and target plasmid was prepared using the Qiagen Plasmid Midi kit, following the included instructions (Appendix A.6).

2.3 Mammalian tissue culture

The shRNA constructs were tested in mammalian cells (Castanotto *et al*, 2002). Human embryonic kidney 293 (HEK293) and human hepatoma (Huh7) cells were the cell lines used in this study. The HEK293 cells were maintained in DMEM growth medium (Gibco, UK) supplemented with 10% Biochrom fetal calf serum (FCS, Merck, Germany) and 1X penicillin/streptomycin (Gibco, UK) in a humidified incubator at 37°C and 5% CO_2. Once the cells reached 80% confluency (covering 80% of the culture dish surface), the media was removed and the cells washed with 37°C saline (confluency calculation depicted in Appendix A.7). The saline was removed and the cells were incubated with 1 ml of 1× TrypLE Express trypsin (Life Technologies, USA) at 37°C for 3 minutes. The cells were dislodged from the surface by gently tapping the culture dish. The trypsin was inactivated by the addition of 3 ml 37°C DMEM (10% FCS and 1× penicillin/streptomycin). The cells were transferred to a sterile 75 cm^2 tissue culture flask. Sixteen millilitres of DMEM was added and the flask was incubated at 37°C and 5% CO_2 until the cells needed to be passaged again. The reagents used are described in Appendix A.8.

For transfections, HEK293 cells were grown to 80-100% confluency (Appendix A.7). The media was removed and the cells washed with 37°C saline. The saline was removed and the cells were incubated with 1 ml of 1× trypsin at 37°C for 3 minutes. The cells were dislodged from the surface

by gently tapping the culture dish. The trypsin was inactivated by the addition of 4 ml 37°C antibiotic-free DMEM supplemented with 10% FCS. The culture dish (24-well plate, 6-well plate or 10 cm^2) was seeded at 70-80% confluency in antibiotic-free DMEM (10% FCS) and the cells were left to grow overnight at 37°C and 5% CO_2. A 1µg DNA:1µl: Lipofectmine2000™ (Invitrogen, USA) ratio was used per transfection. Twenty four hours post transfection, the media was replaced with DMEM supplemented with 10% FCS and antibiotics.

2.4 Dual-luciferase assay

To assess the target knockdown efficacy of the shRNAs, their respective target sequences were inserted into the multiple cloning site of a reporter plasmid (described section 2.3.4). The selected plasmid was psiCHECK 2.2. The Dual-Luciferase® Reporter Assay System was used (Promega, USA). After removing the supernatant from the cells, 100 µl of 1X Passive Lysis Buffer was added per well. The tissue culture plate was slowly agitated for 20 minutes to help lyse the cells. Twelve microlitres of each lysate was transferred to a well in a 96-well luminometer plate. A master mix of Stop & Glo was prepared to ensure that each well in the 96-well plate received 50 µl of the reagent. A 50 µl per well master mix of luciferase activity agent II (LAR II) was also made. In an automated system, LAR II is first added to the lysate to activate firefly luciferase luminescence. The Stop & Glo reagent is added to stop firefly luminescence and activate *Renilla* luciferase. The luciferase activity of each well was quantified by the Veritas dual-injection luminometer (Turner Biosystems, USA).

2.4.1 Dual-luciferase knockdown assay

To determine the silencing efficacy of each of the shRNA constructs, a luciferase knockdown assay was carried out. HEK293 cells were seeded in 24-well plates at 35-40% confluency (Appendix A.7). On the following day, the cells were co-transfected in triplicate (as described in Section 2.5) with 750 ng shRNA-expressing vector, 150 ng cognate target plasmid and 100 ng pCI-eGFP. Each target plasmid was paired with either a 19mer shRNA expression plasmid, 25mer shRNA; H1 mock plasmid or an anti-HBV plasmid (negative control). Inhibition of the target plasmid expression was determined 48hrs post-transfection using the Dual-Luciferase Reporter Assay System (Promega, USA) and a Veritas dual-injection luminometer (Turner Biosystems, USA).

2.4.2 Dose response assay

To determine whether the silencing efficacy of the pTZ-shRNAs was dose-dependent, dose response assays were conducted. Twenty-four well plates were seeded with Huh7 cells at 35-40% confluency (Appendix A.7). Twenty-four hours later, the cells were transfected in triplicate (as described in Section 2.5) with 0.5 µg of plasmid DNA per well. A fixed concentration of target plasmid and reporter plasmid was co-transfected with varying concentrations of pTZ-shRNA and the pTZ57R stuffer vector (Table 2.5). Forty-eight hours post transfection, a dual-luciferase assay was carried out. To determine the effective dose, the concentration of the effectors was converted to a $\log_{10}$ scale. The EC_{50} values were calculated from the downward-sloping sigmoid graph using GraphPad Prism 4 (GraphPad Software Inc., USA). The equation used was as follows: Y= Bottom + (Top-Bottom)/(1+10^((LogEC_{50}-X))). In this sigmoidal-dose response equation X is the logarithm of concentration and Y is the response (Y starts from the Bottom and ascends to the Top) (GraphPad Software Inc., USA).

Table 2.4: Layout of the dose response assay.

The assay was conducted with a decreasing concentration of shRNA and proportional increasing concentration of stuffer plasmid (pTZ57R).

Target to shRNA ratio	psiCHECK-target (ng)	pTZ-shRNA (ng)	pCI-eGFP (ng)	pTZ57R (ng)
1 to 10	40	400	60	-
1 to 0.1	40	4	60	396
1 to 0.05	40	2	60	398
1 to 0.01	40	0.4	60	399.6
1 to 0.0025	40	0.1	60	399.9
Mock	40	-	60	400

2.5 Interfering with the RNAi pathway

2.5.1 Interferon response assay

HEK293 cells were seeded in a 6-well plate at 35-40% confluency (Appendix A.7). On the following day, the cells were co-transfected in triplicate (as described in Section 2.5) with 4 µg shRNA construct and 1 µg pCI-eGFP. Four micrograms of the dsDNA analogue poly I:C positive control was co-transfected with 1 µg pCI-eGFP in triplicate. The DMEM media was removed from the cells 48 hours post-transfection. To extract whole RNA from the transfected cells, 500 µl of TRI-reagent (Sigma, USA) was added to the HEK293 cells. The cells were lysed via resuspension in sterile centrifuge tubes. The lysates were incubated at room temperature for five minutes. One hundred microlitres of chloroform (Merck, Germany) was added to each lysate. The tubes were closed tightly and vortexed for 15 seconds then left to incubate at room temperature for ten minutes. The tubes were centrifuged at 12, 000 x g (5415 R centrifuge; F45-24-11 rotor) for 15 minutes at 4°C (Eppendorf, Germany). The top aqueous phase was transferred to a new tube. Isopropanol (250 µl, Merck, Germany) was added to the tubes. The tubes were briefly vortexed then stored at -80°C overnight. The tubes were centrifuged at 12000 x g for 30 minutes at 4°C. The pellet was washed with 500 µl 75% ethanol (Merck, Germany) then vortexed briefly. The tubes were centrifuged at 12 000 x g for 5 minutes at 4°C. The pellet was air-dried for 5 minutes then resuspended in 50 µl RNase-free water by frequent pipetting at 55-60 °C for 10 minutes. If the partially dissolved RNA had an A260/280 reading (using the Thermo Scientific Nanodrop) between 1.8 and 2.1, it was stored as 30 µg aliquots at -80°C.

The QuantiTect Reverse Transcription kit was used (Qiagen, Germany). One microgram of whole RNA extract was incubated with 1X gDNA wipeout buffer and RNase-free water up to a final volume of 7 µl at 42°C for 5 minutes. Half a unit (0.5 U) of QuantiTect reverse transcriptase, 1X QuantiTect reverse transcription (RT) buffer and 0.5 U of RT primer mix were added. The mixture was

incubated at 42°C for 30 minutes then 95°C for 3 minutes to deactivate the QuantiTect reverse transcriptase.

Separate real-time quantitative PCR mixes were prepared for the respective interferon-β (*IFN-β*) and glyceraldehyde-3-phosphate dehydrogenase (*GAPDH*) primers (listed in Table 2.6) using the SensiMix Capillary kit (Bioline, UK). Two microlitres of template cDNA from the RT reaction was mixed with 10 µM forward primer, 10 µM of reverse primer, 4 µl SensiMix lite, 0.4 µl 50X SYBR green, 1.5 U enzyme mix and RNase-free water to make up a final volume of 20 µl. The following cycling parameters were carried out in the Light Cycler 2.0 (Roche, Germany): 95°C hot-start for 10 minutes to activate polymerase; 40 cycles of 95°C for 15 seconds, 55-60°C for 15 seconds and 72°C 15 seconds.

Table 2.5: The primers used for the qRT-PCR to assess the induction of an interferon response.

Primer name	Primer sequence (5' → 3')
***IFN*-β forward**	TCC AAA TTG CTC TCC TGT TGT GCT
***IFN*-β reverse**	CCA CAG GAG CTT CTG ACA CTG AAA A
***GAPDH* forward**	AGG GGT CAT TGA TGG CAA CAA TAT CCA
***GAPDH* reverse**	TTT ACC AGA GTT AAA AGC AGC CCT GGT G

2.5.2 MTT assay

HEK293 cells were seeded at ~30% confluency (Appendix A.7) in 125 µl media per well in a 96-well plate. Eight wells were left empty to serve as blank controls. The cells were transfected in triplicate (as described in Section 2.5) with 128 ng shRNA and 32 ng pCI-eGFP per well. The addition of the growth inhibitor 5-azacytidine (5-azaC, Sigma, USA) served as a positive control. A final concentration of 1 µM 5-azaC was added to each positive control well. At 48 hours post-transfection, 20 µl of thiazolyl blue tetrazolium bromide (MTT, Sigma, USA) solution was added to each well. The solution was gently mixed in for 5 minutes and the cell cultures were incubated at 37°C and 5% CO_2 for 5 hours to allow the MTT to be metabolised into formazan. The supernatant was removed and 200 µl dimethyl sulfoxide (DMSO, Sigma, USA) added to dissolve the blue formazan precipitate. The light absorbance per well was measured at 570 nm and 655 nm respectively. The values from the background 655 nm readings were subtracted from the

corresponding 570 nm values. The 655 nm readings served as a reference to account for the effects of cell debris.

2.5.3 Saturation assay

Huh7 cells were seeded in 24-well plates at ~40% confluency (Appendix A.7). Twenty-four hours later, the cells were transfected in triplicate (as described in Section 2.5) with 0.8 µg of plasmid DNA per well. The cells were transfected with a fixed concentration of pCI-eGFP (100 ng) and a fixed concentration (100 ng) of HBV target plasmid psiCHECK-8T-Fw (Ely *et al*, 2008). Three sets of controls were included to determine repressive effects: 1) the non-repression control, 2) the repression control and 3) the derepression control. The non-repression controls consisted of 100 ng pCI-eGFP, 100 ng anti-HBV miR-31/8 (Ely *et al*, 2008), 100 ng or 10 ng H1 mock and pTZ57R to make up a final concentration of 0.8 µg. The repression controls consisted of 100 ng pCI-eGFP, 100 ng HBV target (psiCHECK-8T-Fw), 100 ng anti-HBV miRNA (miR-31/8), 100 ng or 10 ng H1 mock and pTZ57R to make up a final concentration of 0.8 µg. The derepression controls included the following: 100 ng or 10 ng shLTR (Saayman *et al*, 2010), 100 ng pCI-eGFP, 100 ng HBV target (psiCHECK-8T-Fw), 100 ng anti-HBV miRNA (miR-31/8) and pTZ57R to make up a final concentration of 0.8 µg. The hairpin experiments comprised of the following per well: 100 ng pCI-eGFP, 100 ng HBV target (psiCHECK-8T-Fw), 100 ng anti-HBV miRNA (miR-31/8) and 100 ng or 10 ng pTZ-shRNA. The stuffer plasmid pTZ57R made up the deficit to a final concentration of 0.8 µg. Forty-eight hours after the transfection, the dual-luciferase reporter assay was conducted.

2.6 Processing of the shRNA constructs

2.6.1 RNA extraction for northern blot analysis

HEK293 cells were seeded in 10 cm tissue culture dishes 35-40% confluency (Appendix A.7). Twenty-four hours later, the cells were co-transfected (as described in Section 2.5) with 20 µg shRNA-expressing vector and 1 µg pCI-eGFP. Whole RNA was extracted 48hrs post-transfection as described in section 2.7.1 with the following changes: 1ml TRI-reagent (Sigma, USA), 100 µl chloroform (Merck, Germany), 500 µl Isopropanol (Merck, Germany),1 ml 75% ethanol (Merck, Germany) and the pellet was resuspended in 40 µl 0.5% sodium dodecyl sulphate (SDS, Sigma, USA). If the partially dissolved RNA had an A260/280 reading (using the Thermo Scientific Nanodrop) between 1.8 and 2.1, it was stored as 30 µg aliquots with an equal volume of 2X loading dye (Thermo Scientific, USA) at -80°C.

2.6.2 Radio-labelling Decade marker

The following were mixed in an RNase-free tube using reagents from the Ambion Decade™ Marker System (Life Technologies, USA): 100 ng Decade Marker RNA, 1X kinase reaction buffer, 1 µl [Y-^{32}P]ATP radioactivity (PerkinElmer, USA), 1 U T4 polynucleotide kinase and nuclease-free water up to a final volume of 10 µl. The mixture was left to incubate at 37°C for 1 hour. Ten times (10X) cleavage reagent (Life Technologies, USA) and nuclease-free water up to a final volume of 10 µl were added. After a five minute incubation period at room temperature, 20 µl of gel loading buffer II was added. The labelled Decade Marker was split into 10 µl aliquots to minimize freeze-thaw cycles.

2.6.3 Radio-labelling the probes

Two microlitres of 10 µM probe stock, 1X of polynucleotide kinase (PNK) buffer A (Thermo Scientific, USA), 10 U PNK (Thermo Scientific, USA), radioactivity and deionised water (made up to

final volume of 20 µl) were added to a micro centrifuge tube. One microliter of [Y-^{32}P]ATP (PerkinElmer, USA) radioactivity was added last.

The probes (Table 2.6) were incubated at 37°C for 1 hour. G-25 Sephadex (Sigma, USA) columns (Appendix A.10) were prepared during the incubation period. A centimetre of compact filter fiber was stuffed into the bottom of a 1 ml syringe (plunger removed). One millilitre of G-25 Sephadex was added to the syringe which was spun at 2000 x g (5810 R centrifuge; A-4-81 rotor) for 2 minutes in a 15 ml centrifuge tube (Eppendorf, Germany). This step was repeated until the Sephadex column filled the syringe. The column was transferred to a fresh sterile 15 ml centrifuge tube.

After the hour incubation period, 30 µl of water was added to the labelled probes. The probe was purified by spinning it through the prepared Sephadex column at 2000 x g for two minutes and collected in the 15 ml centrifuge tube.

2.6.4 Northern blot analysis to visualise processed shRNA products

The RNA, with an equal volume of 2X loading dye (Appendix A.9) added (Thermo Scientific, USA), was denatured at 95°C for 3 minutes and the decade marker denatured at 95°C for 5 minutes before being loaded. The RNA samples and decade marker were resolved on a 15% polyacrylamide gel (Appendix A.9) at 150 V for 90 minutes, 200 V for 30 minutes and 250 V until the bromophenol blue dye front was approximately 2 cm above the end of the gel. The gel was removed from the glass plates stained with 10 mg/ml ethidium bromide (Sigma, USA) in 100 ml TBE for 5 minutes (agitating). The stained gel was visualised under UV light using the G:BOX gel doc system (Syngene, UK) and the image was documented using Gel Logic 2000 (Kodak, USA).

Six pieces of thick filter paper were cut to match the dimensions of the gel and one similarly cut piece of hybond positively charged nylon membrane (Amersham, USA). A sandwich of 3 filter papers, membrane, the gel and 3 filter papers was placed in a semi-dry blotter. The excess liquid was pressed out. The gel was transferred to the membrane at 0.4 A for 1 hour.

The membrane was briefly cross-linked then baked at 80°C for 1 hour. During this period, 10 ml of Amersham Rapid-hyb buffer (GE Healthcare, USA) was heated to 42°C in hybridisation bottle (one bottle per probe). After the baking step, the membrane was placed in the hybridisation bottle to pre-hybridise for 20 minutes at 42°C. The labelled probe was denatured at 95°C for 5 minutes then added to the Rapid-hyb Buffer. The membrane was left to hybridise with the probe, rotating overnight at 42°C.

The Rapid-hyb Buffer was decanted. The membrane was washed with 50 ml of 5× SSC (Appendix A.9) and 0.1% SDS at room temperature for 10 minutes. This wash was repeated once more. The membrane was placed on a sheet of (polyvinyl chloride) PVC and exposed to an x-ray film for 13 days (Fujifilm, Japan). The blot was developed using the FLA-7000 phosphor imager (Fujifilm, Japan) and the data was analysed using MultiGauge version 2.0 software (Fujifilm, Japan).

Table 2.6: A list of the probe sequences used to detect RNA in the Northern blots.

Probe name	Oligonucleotide sequence (5' → 3')
5' probe GAG	GAGCCACCCCACAAGATTC
5' probe ENV	TGGTGAAGTGAATTATATC
5' probe LTR	CCACTGCTTAAGCCTCAAC
5' LNA probe GAG	GAG+CCAC+CCCAC+AAGATTC
5' LNA probe ENV	TGG+TG+AAG+TGAAT+TA+TATC
5' LNA probe LTR	C+C+A+CTGCTTAAGCCTC+A+AC

'+' indicates the LNA modifications

Chapter 3: Results

3.1 Hairpin sequence selection

RNA interference (RNAi)-based gene therapy has the potential to treat viral diseases including Human Immunodeficiency Virus type 1 (HIV-1). Due to the highly mutable nature of the HIV-1 genetic sequence, a successful RNAi-based therapy needs to mimic the multiple inhibitor approach of currently used highly active antiretroviral therapy (HAART) to minimise the occurrence of viral escape (Ter Brake *et al*, 2006). In RNAi-based HIV-1 therapy, the most suitable RNAi triggers to utilise are short hairpin RNAs (shRNAs) (McIntyre *et al*, 2009). Prior to hairpin construction, anti-HIV-1 shRNA sequences had to be identified from the previous literature. To maximise the therapeutic potential of the shRNAs, the following selection criteria was considered: the anti-HIV-1 sequence had to be potent, the HIV-1 target sequence had to be highly conserved and different regions of the HIV-1 genome had to be targeted (Knoepfel *et al*, 2012). Three sets of potent anti-HIV-1 sequences were selected from the McIntyre *et al* (2009) study where 96 shRNAs targeting conserved regions of NL4-3 HIV-1 were screened. Ten hairpins were shortlisted according to lack of off-targeting effects, silencing efficacy and the level of conservation of the target sequence (McIntyre *et al*, 2009). We selected the LTR 510-21, Gag 532-31 and Env 1428-21 target sequences (Table 3.1) (McIntyre *et al*, 2009). RNAi has great potential in antiviral gene therapy, particularly targeting HIV-1 with an array of potent shRNAs. We successfully identified three highly conserved HIV-1 target sequences that were incorporated into the shRNA design.

Table 3.1: The HIV-1 target sequences used in this study.

Sequence name	Sequence	Non-specific activity (100 minus increased activity)	Conservation (%) LANL and Virco; LANL clade B	Knockdown (% of fluorescence)
Gag 532-21	GGAGCCACCCCACAAGATT	60	70; 80	59.3
LTR 510-21	CCCACTGCTTAAGCCTCAA	70	70; 100	81.3
Env 1428-21	GAGAAGTGAATTATATAAA	60	73: 81	92.7

3.2 Design of shRNAs

A traditional shRNA consists of a sense strand that folds back on itself to a complementary antisense strand with the strands linked by a loop (top panel of Figure 3.1). The antisense (guide) strand is incorporated into the RNAi-induced silencing complex (RISC) to guide the multi-protein complex to target complementary mRNA. To prevent sense strand off-targeting, shRNAs are usually designed to favour the guide strand (Schwarz *et al*, 2003; Khvorova *et al*, 2003). An ideal shRNA design would guarantee guide strand incorporation into RISC with zero risk of inadvertent sense strand off-targeting. ShRNAs (with a 3'-arm guide strand) with stems shorter than 19 bp are not Dicer substrates and generally exhibit gene silencing levels weaker than their Dicer-dependent (stem length > 19bp) equivalents (Siolas *et al*, 2005). ShRNAs are typically designed with the guide strand within the 3'-arm (downstream of the loop) which can leave it vulnerable to inconsistent Dicer cleavage if the stem is ≥19bp long (Macrae *et al*, 2006; Gu *et al*, 2012). This trend in shRNA design is prevalent despite previous literature showing that shRNAs with stem lengths shorter than or equal to 19 bp with a 5'-arm guide strand can be more potent than their 3'-arm guide strand equivalents (McManus *et al*, 2002; Harborth *et al*, 2003; Ge *et al*, 2010). Mimicking the unusual structure of the Dicer-independent mature miR-451 is a potential solution for shRNA sense strand off-targeting (Section 1.4).

For the purpose of this study, each shRNA was constructed with a 5'-arm guide strand, tetra loop (4 nt) and 3'-arm passenger strand (Figure 3.1). All of the shRNAs were assigned the tetra loop "GAAA" (Vlassov *et al*, 2007). Vlassov *et al* (2007) observed that both 19 bp and 25 bp shRNAs exhibited greater silencing efficacy with the GAAA tetra loop compared to a CUCU loop. Each hairpin was assigned a RNA Pol III promoter-terminating tail of 6 thymidine residues (Brummelkamp *et al*, 2002; Paddison *et al*, 2002). Both the 19mer and 25mer constructs were driven by the RNA polymerase III H1 promoter (Figure 3.2).

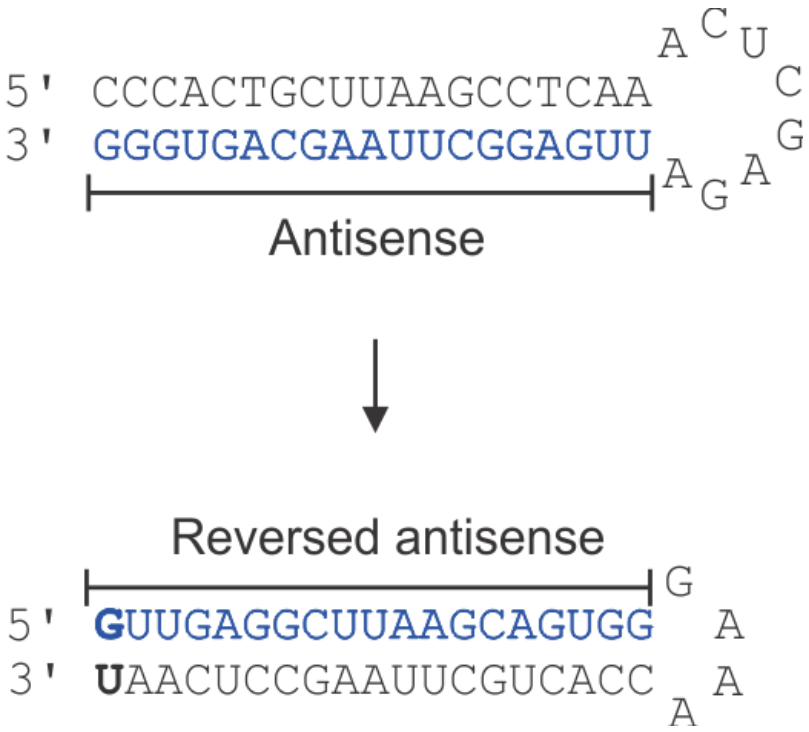


Figure 3.1: Relocation of the antisense strand to the 5' arm of the hairpin.

The top panel shows the original configuration of a hairpin targeting LTR 510-21 (McIntyre, 2009). The bottom panel is an example of how the hairpins were designed. The antisense strand (blue) has been manipulated into the 5' arm. All of the hairpins were given the tetra loop GAAA. The intended guide strand has a leading G or A residue for optimal H1 promoter-driven expression at the first position (bold, blue) at the 5' end.

To ensure that the 5'-arm (intended guide strand) would be loaded into RISC, an adenosine or guanidine (which is preferred by the H1 promoter for optimal hairpin expression) residue was inserted at nucleotide **position 1** (indicated in blue and bold in Figure 3.1) (Li *et al*, 2007). With the A or G residue at this position, the 5'-arm strand was less thermodynamically stable (compared to the 3'-arm) and given a greater chance of being recognised as the guide strand (Khvorova *et al*, 2003). A terminal 5' mismatch of either the sense or antisense strand confers asymmetry strand bias but this rule only applies in shRNAs with a >19 nt stem (Ding *et al*, 2008) therefore the mismatch was inserted in the 5' arm of both the 19mers and 25mers. Pairs of shRNAs were

designed to target the same HIV-1 gene. One hairpin had a 19 bp-long stem and the other, a 25 bp-long stem (Figure 3.2). The hypothetically Dicer-independent 19mers were designed to mimic miR-451. The 25mers were designed to serve as canonical shRNAs.

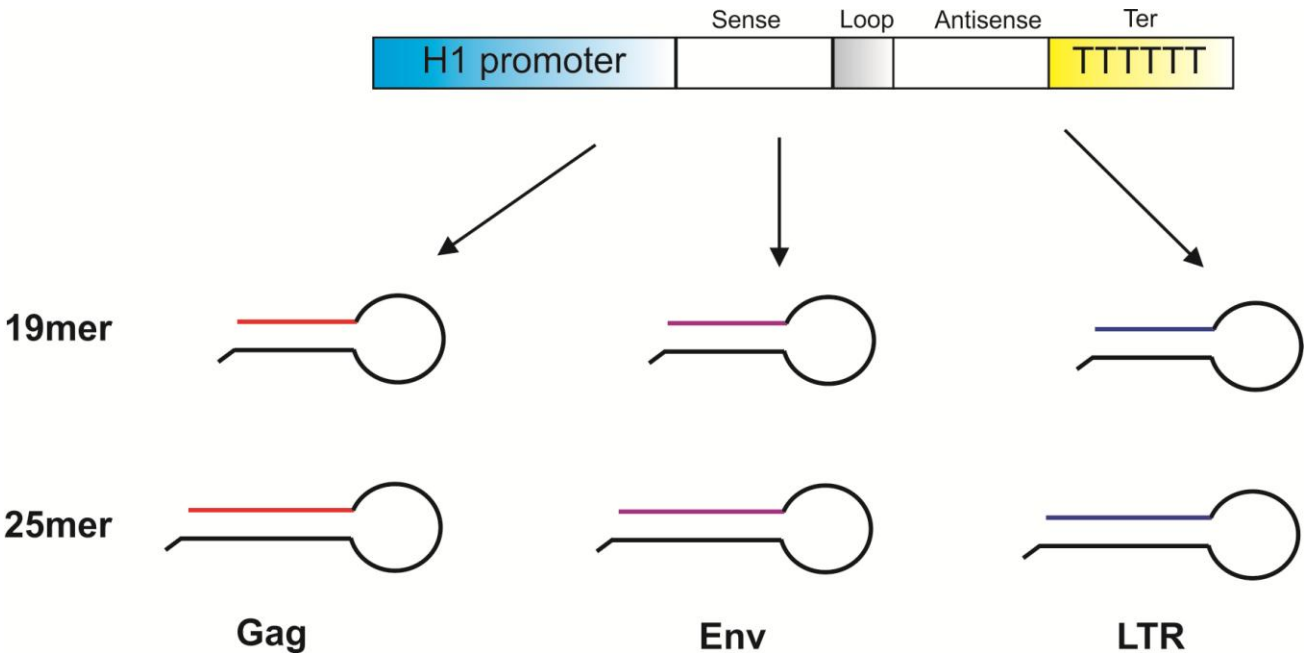


Figure 3.2: Design of the PTZ-H1shRNA cassettes.

The transcription of each shRNA is driven by an H1 promoter. Three sets of hairpins (a 19mer and 25mer) were generated to target Gag (red), Env (purple) and LTR (blue). The terminating tail of thymidines (Ter) is at the 3' end of each shRNA.

3.3 Molecular cloning of the H1-driven shRNAs

The designed shRNAs were encoded into DNA expression vectors (Figure 3.2). shRNA expression cassette construction can be difficult due to the high presence of PCR mutations that negatively affect sequence verification (McIntyre and Fanning, 2006). In this study, we utilised the one-step PCR technique that was devised by Castanotto *et al* (2002) for the rapid synthesis of RNAi effector constructs. The use of a single oligonucleotide reduces the chance of PCR mutations occurring (Castanotto *et al*, 2002; McIntyre and Fanning, 2006). The H1-driven shRNA expression cassettes were generated using the following steps: 1) one-step gradient PCR to produce amplicons that each contain an shRNA downstream of an H1 promoter (depicted in Figure 2.2 in Section 2.2); 2) ligation of the shRNA amplicon into the vector plasmid pTZ57R/T and 3) screening of the produced clones. The band strength weakened as the annealing temperature was incrementally increased from 55.5°C up to 63.5°C. Increasing the annealing temperature reduced non-specific binding resulting in a more defined amplified PCR product without the ±500 bp bands and larger amplicons in lanes 3 and 4 of Figure 3.3. The annealing temperature selected for amplifying the shRNAs was 60.8°C. The ±100 bp bands indicate primer dimers. The PTZ-H1shRNA PCR products were cloned into the pTZ57R/T vector plasmid (Thermo Scientific, USA) as described in Section 2.4.1. The resultant pTZ-H1shRNAs clones were designated into the following categories according to target sequence and stem length: shGag19, shGag25, shEnv19, shEnv25, shLTR19 and shLTR25. The pTZ-H1shRNA clones were screened using a *SacI*/*BamHI* double digest (Supplementary Figure B.1).

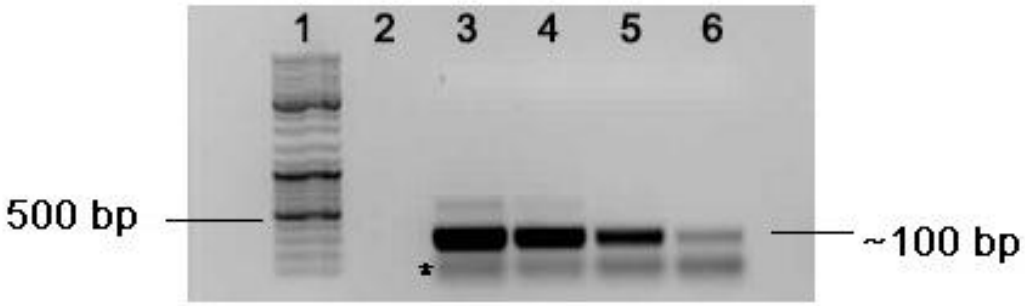


Figure 3.3: An example of a PCR gradient conducted for an shLTR25 amplicon.

The O'GeneRuler™ DNA ladder (Thermo Scientific) served as the molecular weight ladder (lane 1). The shLTR25 amplicons in lanes 3-6 are the result of the same PCR protocol with varying annealing temperature (Ta) values used. The Ta values in lanes 3-6 are 55.5˚C, 58.1˚C, 60.8˚C and 63.5˚C respectively. No PCR reaction or ladder was loaded into lane 2. The asterisk (*) indicates the presence of primer dimers.

Using a single oligonucleotide and *Taq* polymerase to generate each pTZ-H1shRNA was problematic due to the amplification of false positive products with various mutations. The false positives were a result of strong secondary structure formation within the primer (McIntyre and Fanning, 2006). The strong secondary structure of some of the pTZ-H1shRNAs also caused the premature termination of sequencing reactions (Guo *et al*, 2005). In these cases, the pTZ-H1shRNAs had to be sequenced using both forward and reverse primers and the processed chromatograms overlapped at the loop sequence. The chromatograms of the successfully cloned PTZ-H1shRNAs were viewed using the FinchTV application (Figure 3.4). The sequence-confirmed were shG19, shG25, shE19, shE25, shL19 and shL25.

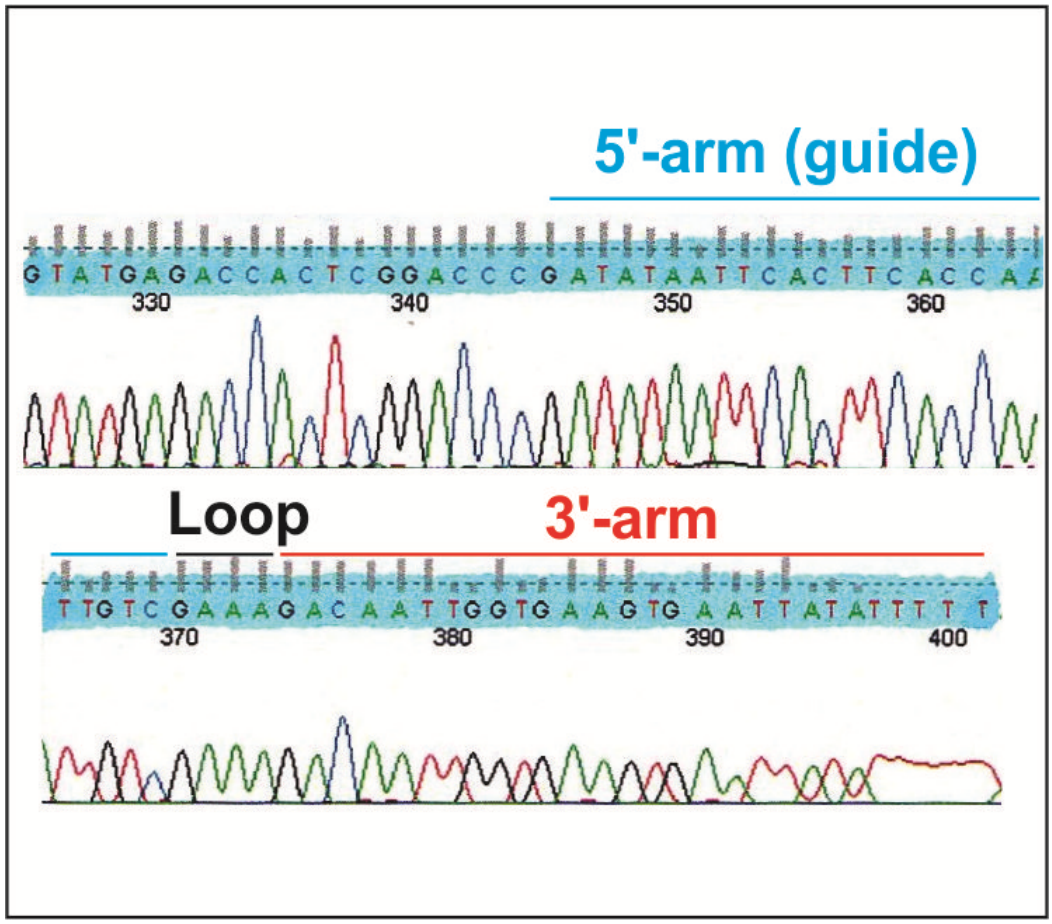


Figure 3.4: Chromatogram of the sequenced positive shE25 clone.

The sequenced clone is a 25mer shRNA targeted against *Env*; the hairpin is known as shE25. Blue: guide strand. Black: loop. Red: passenger strand. The chromatogram was viewed using FinchTV software.

3.4 Generation of reporter plasmids with target sequence inserts

To determine the silencing efficacy of the PTZ-H1shRNAs, their ability to silence complementary target sequences had to be assessed. The interaction between the shRNA guide/passenger strand and its complementary target mRNA was reconstructed in a cell-based assay. The respective cognate target sequences were inserted into the 3' UTR of the psiCHECK2.2 reporter plasmid. psiCHECK2.2 expresses two luciferases: *Renilla* and Firefly. This reporter plasmid when combined with a rapid dual-luciferase assay (described in Section 3.7), allows one to measure the degree at which the PTZ-H1shRNAs knockdown their respective target sequences.

The target sequences LTR 510-21, Gag 532-31 and Env 1428-21 (McIntyre et al, 2009) were generated using single-stranded oligonucleotides that were arranged into their respective pairs to form DNA duplexes with sticky ends that are complementary to *XhoI* and *NotI* processed sites. The double-stranded target sequences were each inserted into a linearised vector (psiCHECK2.2) with ends that were digested by the restriction enzymes *XhoI* and *NotI*. The psi-target plasmids were cloned as described in Section 2.4.2 into psiCHECK2.2. A previously sequence-verified psi-target plasmid served as the positive control (lane 1, Figure 3.5). The *EcoRV* insert is approximately 500 bp which is indicated by the positive control plasmid in lane 2 (Figure 3.5). The plasmid in lane 3 was cut by in the large backbone, an approximately 600 bp band and a smaller insert that is not visible (< 400 bp). All of the *EcoRV*-screened positive clones (example in lane 9, Figure 3.5) were sequenced by Inqaba Biotech (Pretoria, RSA). The target sequences were viewed using FinchTV software (Figure 3.6). The target plasmids were: psi-Gag-AS, psi-Gag-SS, psi-Env-AS, psi-Env-SS, psi-LTR-AS and psi-LTR-SS (AS= antisense/guide strand target; SS= sense/passenger strand target).



Figure 3.5: Example of EcoRV-screening of the psi-target clones.

The O'GeneRuler™ DNA ladder in lane 1 served as the molecular weight ladder. A positive psi-LTR-AS clone with the correct insert size was identified in lane 9. The clone in lane 3 is a negative clone due to incorrect insert size.

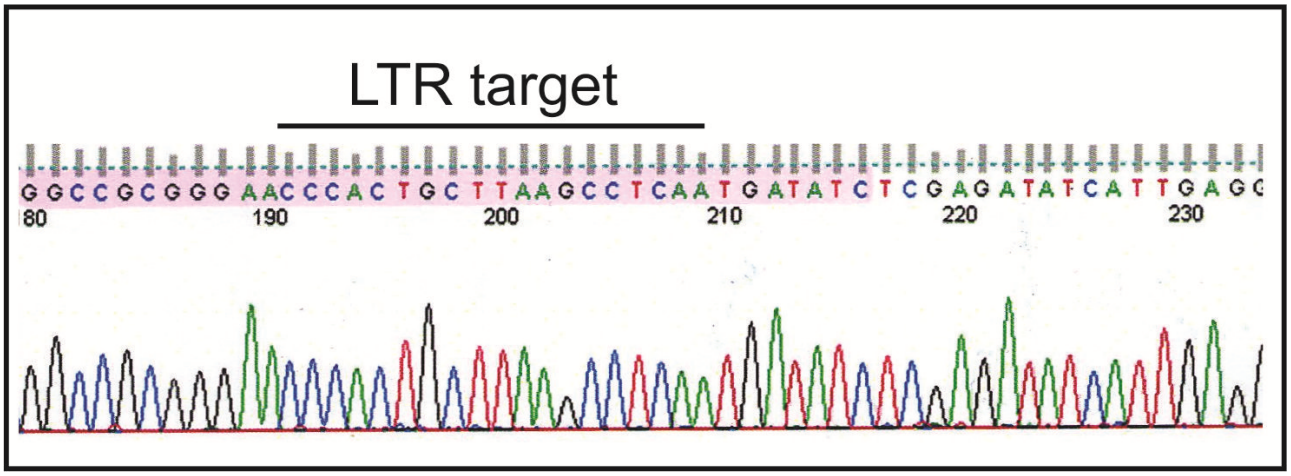


Figure 3.6: Chromatogram of sequence-verified LTR target plasmid, psi-LTR-AS.

The LTR 510-21 (McIntyre *et al*, 2009) is highlighted beneath the black bar. Chromatogram viewed using FinchTV.

3.5 The 19mer shRNA RNAi products are larger than that of the 25mers

One of most important ways to characterise the hairpins was to determine whether the 19mers and 25mers were processed differently by the RNAi pathway. The most definitive technique available to both determine the size and expression level of RNA molecules was the combination of polyacrylamide gels and northern blotting (Calin *et al*, 2002; Lagos-Quintana *et al*, 2001). Additionally, this method is more sensitive than microarray analysis and more specific than RT-PCR (Taniguchi *et al*, 2001; Streit *et al*, 2009). This technique allows one to detect the RNA expression of genes of interest in a given sample (Alwine *et al*, 1977). Whole RNA was extracted from HEK293 cells that were transfected with either pTZ-H1shRNAs or H1 Mock plasmid and a northern blot was used for analysis. The H1-driven mock vector (referred to as H1 Mock) served as a mock control in the dual-luciferase assays (Section 2.6.1). Radio-labelled DNA probes (Table 2.6) complementary to the sequences of interest were used to detect guide sequences. A U6 small nuclear RNA (snRNA) oligonucleotide probe was included to assess equal loading of the RNA samples.

When processed, shG25 and shL25 each yielded a canonical ~22 nt product (Figure 3.7). The *Env* probe did not detect the 19mer or the 25mer. The H1 Mock samples had no signal that could be detected by any of the DNA probes. The evident U6 snRNA confirms that H1 Mock RNA was loaded into the polyacrylamide gel. The radio-labelled DNA oligonucleotide LTR probe detected a ~30 nt product shL19 product. None of the other processed 19mers were detectable. The detection levels of the LTR-targeting PTZ-H1shRNA pair was as follows: shL19= 5.3% and shL25= 4.7% (Figure 3.7); the PSL value of the PTZ-H1shRNAs were normalised to their respective U6 snRNA PSL values.

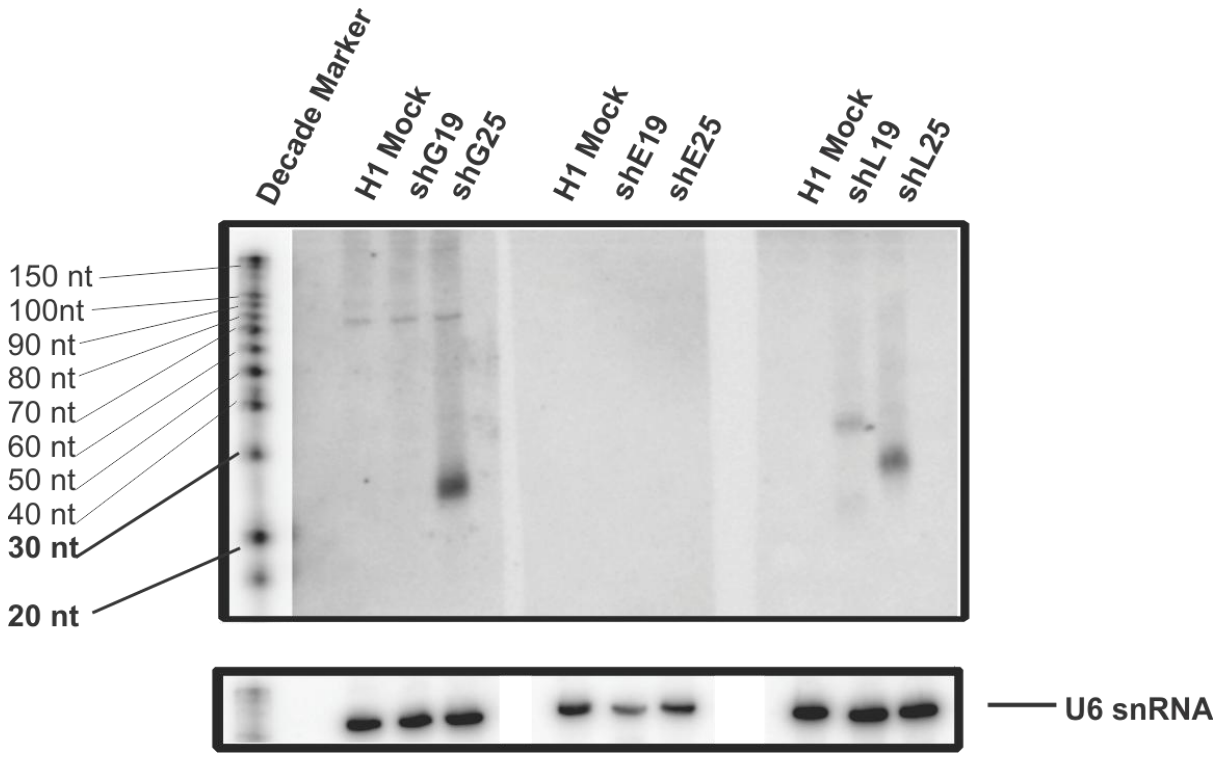


Figure 3.7: Processing of the shRNAs detected by northern blot analysis.

Radio-labelled probes were used. U6 snRNA-probing served as a loading control.

Evidently, there is a difference between the canonical processing of the 25mers (shG25 and shL25) versus that of shL19 (Figure 3.7). To determine whether this phenomenon applied to other 19mers or was sequence-dependent and thus limited to sh19 (in this case), the sensitivity of the northern blot had to be enhanced. The GC content of the *Env* DNA oligonucleotide probe is lower than that of the *Gag* and LTR probes and therefore its melting temperature (T_m) is ~10°C lower (T_m values: *Gag*= 55.9°C; Env= 43.8°C and LTR= 53.6°C). An oligonucleotide probe with a lower T_m value exhibits comparably poorer thermal stability (than probes with higher T_m) during the hybridisation step in northern blotting (Válóczi *et al*, 2004). This is an additional factor to account for the poor detection of shE19 and shE25 RNA expression.

To detect a stronger signal from the processed products, a separate northern blot was hybridised with the more sensitive locked nucleic acid (LNA)-modified oligonucleotide probes (Válóczi *et al*, 2004) that are listed in Table 2.6 (Section 2.8.2). LNAs are bicyclic, high-affinity RNA analogoues (Válóczi *et al*, 2004; Várállyay *et al*, 2007). These monomers have a chemical alteration in the sugar-phosphate backbone that locks the furanose ring in an N-type (C3'-endo) conformation due to the insertion of a 2'-O,4'-C methylene bridge (Válóczi *et al*, 2004). DNA oligonucleotides modified to insert an LNA at every third nucleotide have been shown to exhibit significantly increased mismatch discrimination and sensitivity in detecting small RNAs in northern blot studies (Várállyay *et al*, 2007). The LNA-modified oligonucleotide probes used in this study were designed by Prof Marco Weinberg and synthesised by Exiqon (Denmark).

Band patterns similar to those in the blot probed with DNA oligonucleotides (Figure 3.5) were detected by the radio-labelled LNA probes but in more of the RNA samples (Figure 3.6). The increased thermal stability (compared to traditional DNA oligonucleotide probes) of the LNA oligonucleotide probes allows for a higher temperature during the hybridisation and wash steps with the exception of the *Env* probe. The stringency and protocol of the SSC washes for the LTR and *Gag* probes was altered to follow that conducted by Várállyay *et al* (2007).

All three 25mer RNAi products were visualised; ~22 nt bands were detected by the LNA-modified DNA oligonucleotides for shG25, shE25 and shL25 (Figure 3.8). The band signal of the shE25 product was only 2.6% of the total RNA according to the U6 PSL (photo-stimulated luminescence) value. The poor detection of the shE19 product (~6.2% of its U6 PSL value) may be due to inaccessible target mRNA. A strong and stable (target mRNA) secondary structure would be difficult to probe or perhaps the hybridisation step may have altered the target mRNA secondary structure thus obstructing LNA probe:target binding. An alternative and more likely explanation for the fore-mentioned observation is that the shE19 RNA is significantly degraded compared to the other

hairpins (indicated by the faint U6-probed band in Figure 3.8). The altered SSC detergent stringency resulted in non-specific binding of the probes (large bands in Figure 3.8). Non-canonical processing of the 19mer hairpins was observed resulting in faint shL19, and shG19 (possibly shE19) ~ 30 nt products (Figure 3.8). The PSL values of the 19mer bands normalised to their corresponding U6 snRNA PSL values were as follows: shG19= 14.7%; shE19= 6.2% and shL19= 4.6% (Figure 3.8). The bands larger than 30 nt (Figure 3.8) are a result of non-specific binding between the radio-labelled LNA oligonucleotides and non-target nucleic acids (Várallyay *et al*, 2007). These non-target nucleic acids may be precursors of the pTZ-H1shRNAs. The shRNAs may be highly expressed but poorly processed by the RNAi machinery resulting in a build-up of shRNA precursors instead of mature shRNA product (Boudreau *et al*, 2009). The presence of these non-specific bands is influenced by factors including the hybridisation temperature and the stringency of the washes (Várallyay *et al*, 2007). The lower the hybridisation temperature and stringency of the washes, the less specific the detection of small RNAs. The non-specific bands in the *Env*-probed membrane (Figure 3.8) are present due to low stringency hybridisation and washing conditions (Válóczi *et al*, 2004). The non-specific background in the Gag- and LTR-probed membranes is likely the result of the low stringency wash steps (Válóczi *et al*, 2004).

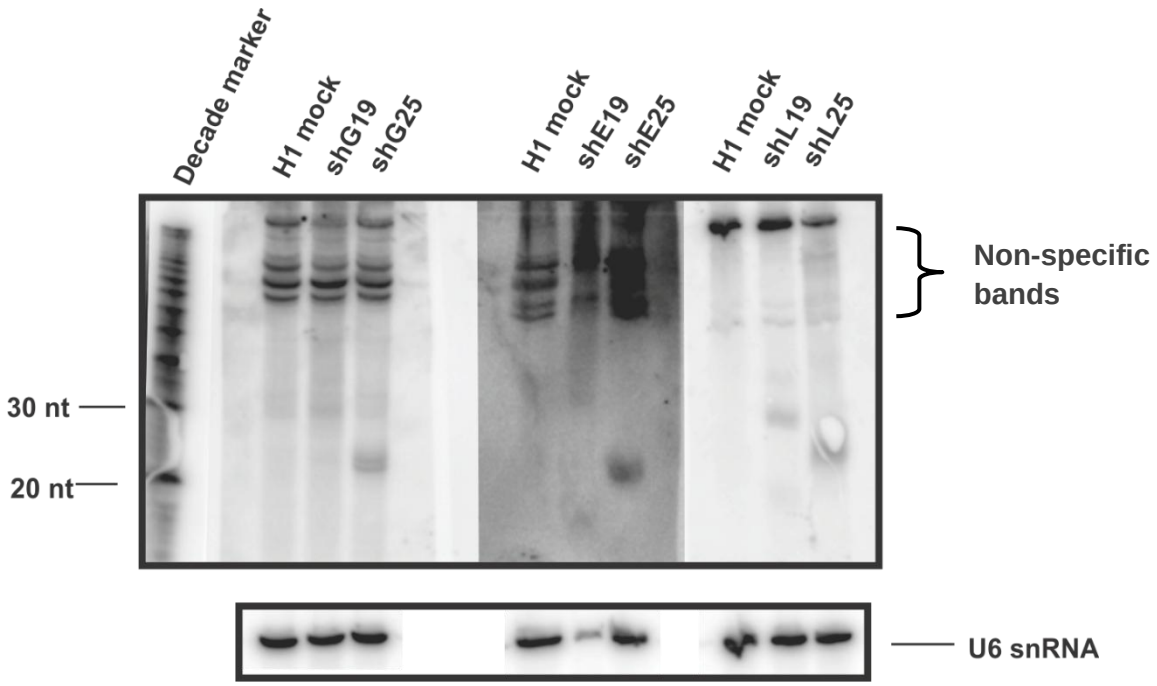


Figure 3.8: Northern blot analysis with radio-labelled LNA-modified oligonucleotide probes.

The 25mers were all successfully processed by the endogenous RNAi pathway. The presence of the large ~30 nt RNA product in both the shG19 and shL19 samples (Figure 3.8) is evidence that the 19mers may have most likely been processed by an enzyme other than Dicer (Cheloufi *et al*, 2010; Cifuentes *et al*, 2010).

3.6 Knockdown comparison of the 5' and 3' arms

The sequence of each PTZ-H1shRNA was selected from previous literature that had identified potent RNAi effectors (McIntyre *et al*, 2009). There are differences in the design of the shRNAs generated for this study and the McIntyre *et al* (2009) hairpins; the McIntyre *et al* (2009) shRNAs had varying 8 nt loops and the targeting sequence in the antisense strand (3'-arm). The shRNAs in this study all have the same 4 nt loop sequence and the antisense strand sequence repositioned to the 5'-arm of the hairpin.

The Promega Dual-Luciferase Reporter Assay System offers rapid and sensitive quantitation of relative gene expression (Figure 3.9) (Elbashir *et al*, 2001a). The reporter plasmid psiCHECK 2.2 has both Renilla (with a SV40 promoter) and Firefly (with a HSK TV promoter) luciferase. The target sequence was cloned into the 3' UTR of the *Renilla* luciferase gene. If the shRNA guide strand binds to its complementary sequence, the target mRNA is degraded and *Renilla* expression reduced. *Renilla* luciferase expression was knocked down by the respective hairpin thus diminishing its luminescence (Figure 3.9). In the absence of a silencing hairpin, the *Renilla* luciferase luminescence is unaffected. The firefly luciferase reporter gene is constitutively expressed and serves as an internal control to which the expression experimental *Renilla* luciferase reporter gene is normalised. Changes in luciferase activity are indicative of changes in shRNA activity. The degree of target knockdown is determined by calculating the ratio between *Renilla* and Firefly luciferase luminescence. Forty-eight hours post transfection, the reporter assay was carried out using the Promega Dual-Luciferase Reporter Assay System following instructions.

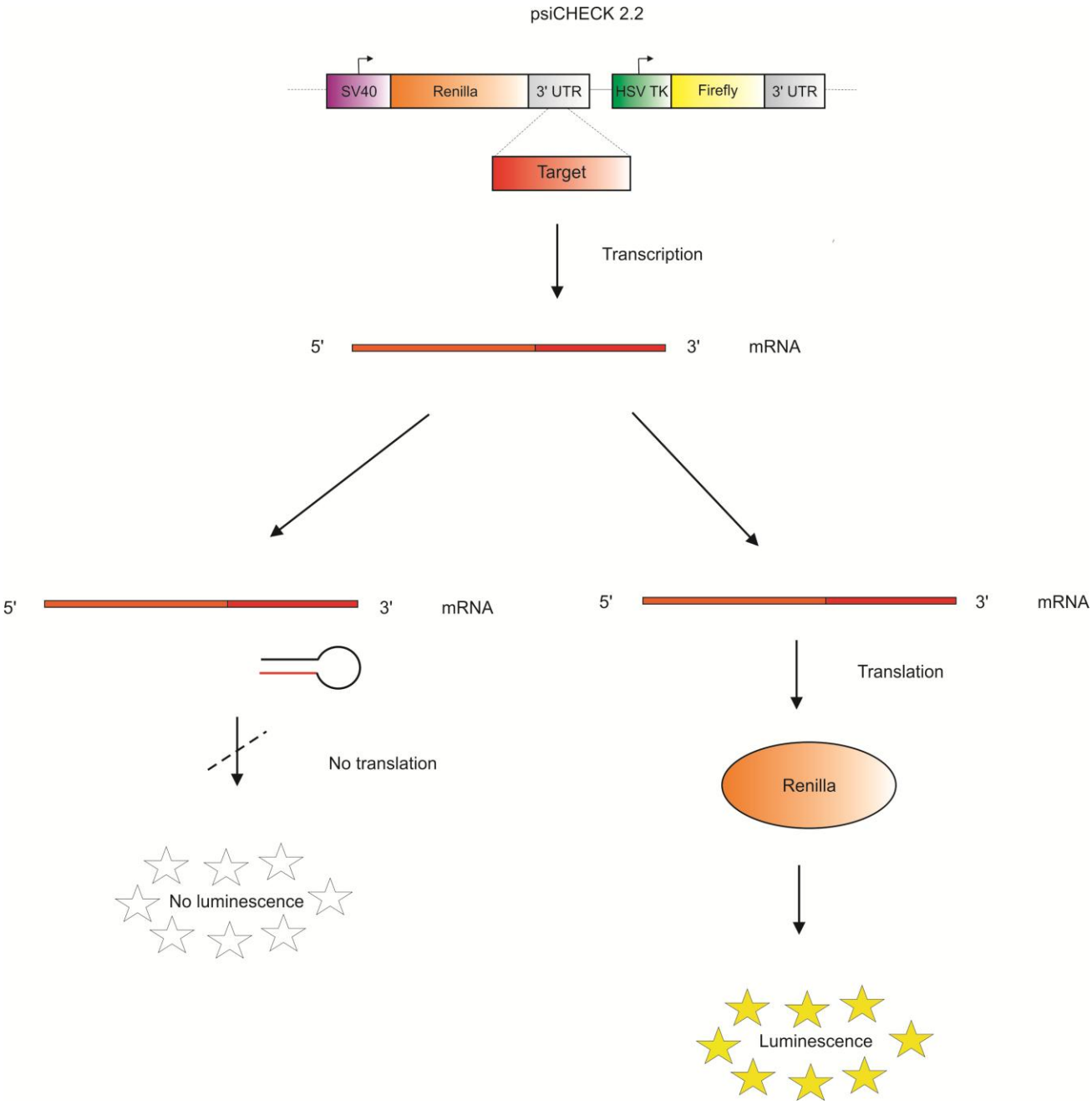


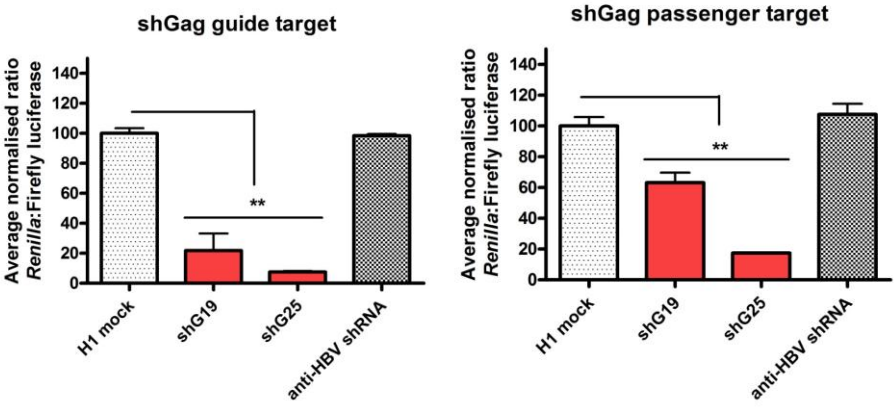
Figure 3.9: Dual-luciferase reporter assay.

The reporter plasmid psiCHECK 2.2 expresses both Renilla and Firefly luciferase. The target sequence is inserted in the 3' UTR of Renilla. In the presence of a silencing shRNA, Renilla gene expression is negatively affected, resulting in diminished luminescence. The ratio between Renilla and Firefly luciferase activity reveals the silencing efficacy of the shRNAs.

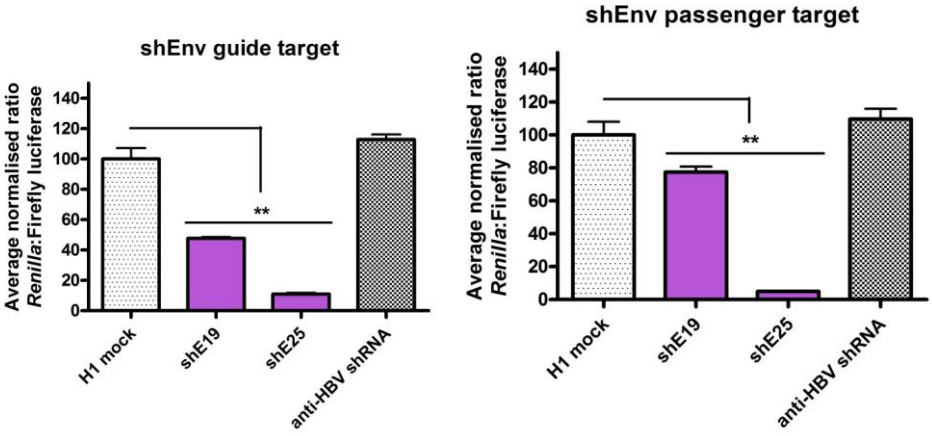
To evaluate the silencing efficacy of the expressed PTZ-H1shRNA cassettes, they were each co-transfected with a cognate target. Each anti-HIV-1 hairpin, a mock plasmid (H1 Mock) and a non-HIV-1 targeting plasmid (negative control) were transfected in HEK293 cells in triplicate. An anti-HBV shRNA (donated by Tristan Scott) served as the non-targeting plasmid. All of the values were normalised to the mock plasmid (H1 Mock). A rapid dual-luciferase assay was conducted 48 hrs post-transfection to quantitate target knockdown.

The shG19 guide strand exhibited ~80% knockdown of its target but the passenger strand exhibited only 40% knockdown (Figure 3.10 A). Both guide and passenger strands of shG25 were potent, exhibiting ~90% and 80% knockdown respectively (Figure 3.10 A). The shE19 guide and passenger strands were both weaker than shE25 guide and passenger strands. The shE19 hairpin is active but its RNA is degraded (Figure 3.8) compared to its 25mer counterpart. The shE19 guide strand reduced its target expression down to ~50% and the shE19 passenger strand exhibiting ~25% target knockdown (Figure 3.10 B). The Env-targeting 25mer guide strand exhibited ~90% knockdown and the passenger strand, ~95% knockdown (Figure 3.10 B). The guide strand of the 19mer LTR-targeting hairpin (shL19) exhibited greater silencing ability compared to its 25mer counterpart (shL19: ~90% knockdown; shL25: ~75% knockdown) (Figure 3.10 C). Poor activity was observed of the shL19 passenger strand with only 20% knockdown compared to the shL25 passenger strand that exhibited ~80% target knockdown (Figure 3.10 C). The guide strand of the 25mer shRNAs targeting *Gag* and *Env* respectively are stronger gene silencers than the shorter 19mers (shE19 and shG19) (Figure 3.10 A and B).

A


shGag guide target
Average normalised ratio Renilla:Firefly luciferase
140
120
100
80
60
40
20
0
**
H1 mock
shG19
shG25
anti-HBV shRNA
shGag passenger target
Average normalised ratio Renilla:Firefly luciferase
140
120
100
80
60
40
20
0
**
H1 mock
shG19
shG25
anti-HBV shRNA

B


shEnv guide target
Average normalised ratio Renilla:Firefly luciferase
140
120
100
80
60
40
20
0
**
H1 mock
shE19
shE25
anti-HBV shRNA
shEnv passenger target
Average normalised ratio Renilla:Firefly luciferase
140
120
100
80
60
40
20
0
**
H1 mock
shE19
shE25
anti-HBV shRNA

C

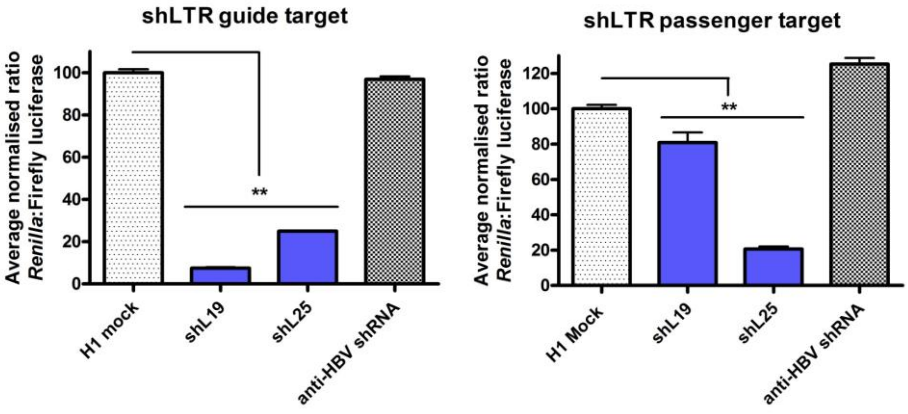

shLTR guide target
Average normalised ratio Renilla:Firefly luciferase
100
80
60
40
20
0
**
H1 mock
shL19
shL25
anti-HBV shRNA
shLTR passenger target
Average normalised ratio Renilla:Firefly luciferase
120
100
80
60
40
20
0
**
H1 Mock
shL19
shL25
anti-HBV shRNA

Figure 3.10: Knockdown efficacy of the guide (Gag/Env/LTR target) and passenger strands respectively.

The 19mer guide strands exhibited silencing efficacy. Both the guide and passenger of the 25mers were capable of significantly silencing their respective target sequences. All of the values were normalised to the H1 mock control (100 %). A) Red = Gag. B) Purple = Env. C) Blue = LTR. Student's t-test (n = 3, ** = $p < 0.05$).

The 25mers were promiscuous silencers with both the 5'-arm and 3'-arm exhibiting ≥ 70% knockdown (Figure 3.10). The 19mers were able to silence the 5'-arm targets (Figure 3.10). These results combined with the non-canonical large ~30 nt 19mer RNA products observed in the northern blots (Figures 3.7 and 3.8) suggest that the 19mer passenger strand is inactive or degraded due to circumventing Dicer-processing similar to mature miR-451 (Cheloufi *et al*, 2010; Cifuentes *et al*, 2010; Liu *et al*, 2013) (Figure 1.3 of Section 1.4). All of the 25mer guide and passenger strands were active but only the 19mer guide strands exhibited effective target knockdown.

3.7 The H1-driven shRNA expression cassettes inhibit expressed targets in a dose-dependent manner

The sequences incorporated into the shRNA design have been previously shown to be potent RNAi effectors (McIntyre *et al*, 2009) but does the efficacy remain at low doses? To determine the effective concentration (EC) of each expressed shRNA, a dose inhibition response assay was conducted. To assess the efficacy of the generated shRNAs, each H1 hairpin cassette was transfected in triplicate into Huh7 cells in decreasing doses. A fixed concentration of psiCHECK2.2 vector containing the target sequence and pCI-eGFP were included in each transfection. A breakdown of the dosages is described in Table 2.5 (Section 2.6.2). The degree of expression by pCI-eGFP was visualised by fluorescence microscopy and served as an indicator of transfection efficacy. A dual-luciferase assay was carried out 48 hours post transfection.

Each expressed shRNA silenced its cognate target in a dose-dependent manner. At the highest dose of pTZ-shRNA (10 to 1; 400 ng pTZ-shRNA and 40 ng psiCHECK-target), shG19, shG25 (Figure 3.11 A), shE25 (Figure 3.12 A) and shL19 (Figure 3.13 A) exhibited more than 80% knockdown of their respective targets. As in the Vlassov *et al* (2007) study, the majority of the 25mer shRNAs exhibited a stronger inhibition. The LTR-targeting 19mer (shL19) was a consistently more effective silencer than its 25mer counterpart (Figure 3.13 A).

According to the EC_{50} values, the shE19 and shL25 plasmids were the least potent of the set with comparably higher EC_{50} values of 56.6 ng and 45.2 ng respectively. The most effective hairpins were shG19 and shL19 with low EC_{50} values of 3.2 ng and 2.2 ng respectively. The most potent 25mer was shG25 with an EC_{50} dosage of 4.7 ng.

In order for a short shRNA to have therapeutic potential, it needs to be potent and remain effective at low dosages. shE19 and shL25 exhibited poor RNAi efficacy at low concentrations. Potent PTZ-H1shRNAs were identified: shG19, shG25, shE25 and shL19. These results suggest that shG19 and shL19 are potential candidates for clinical testing.

A **B**

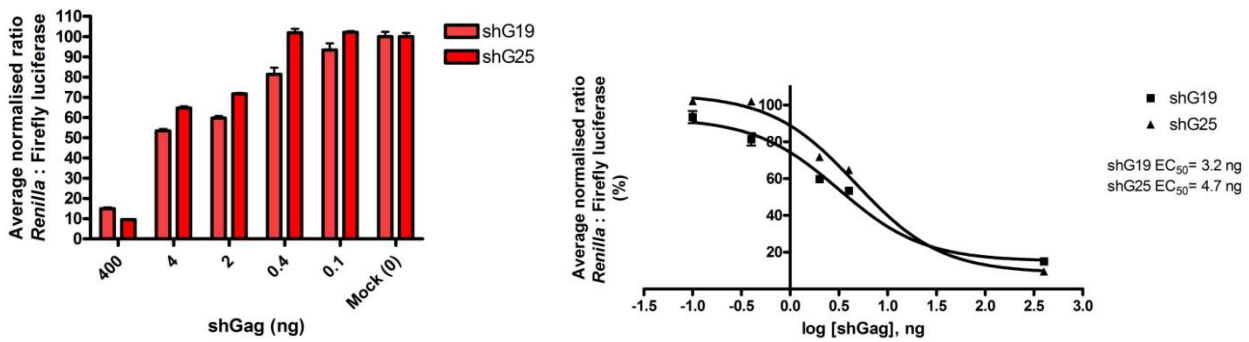


Figure 3.11: *Gag* dose response assay.

A) Huh7 cells were transfected with varying concentrations of the hairpins. Dose-dependent knockdown of the Gag target was determined from a dual-luciferase assay 48 hrs post transfection. The mock (0 ng shGag) value was set at 100% and the other dose values were relativised to the mock. One-way ANOVA (n = 3, ±SEM). ** ($p > 0.05$). B) Inhibition dose response curve. The EC_{50} values for shG19 (solid squares) and shG25 (solid triangle) were 0.08 to 1 (3.2 ng) and 0.012 to 1 (4.7 ng) respectively. Log10 x-axis values.

A **B**

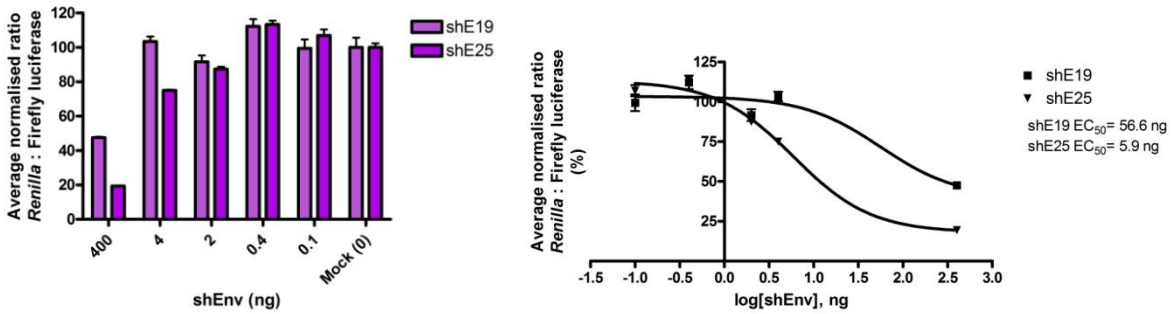


Figure 3.12: *Env* dose response.

A) The silencing efficacy of the expressed anti-Env shRNAs in varying concentrations. Huh7 cells were transfected and a dual-luciferase assay was conducted 48 hrs post transfection. All of the dose values were relativised to the mock (0 ng shEnv) values (set to 100%). (n = 3, ±SEM). B) Inhibition dose response curve. The EC_{50} values for shE19 (solid squares) and shE25 (solid inverted triangle) were 1.42 to 1 (56.6 ng) and 0.15 to 1 (5.9 ng) respectively. X-axis values in log10 scale.

A **B**

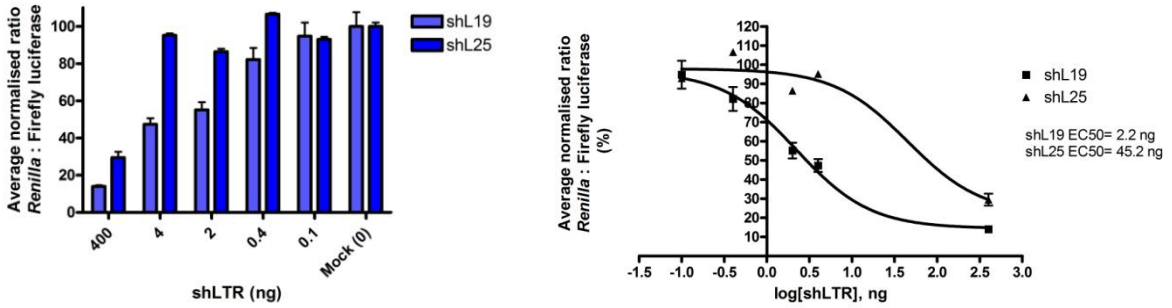


Figure 3. 13: Dose response of LTR target.

A) Each hairpin pair was transfected into Huh7 cells in decreasing concentrations. A dual-luciferase assay was conducted 48 hrs post transfection. Values relativised to the mock (0 ng shLTR). (n = 3,

±SEM). B) Inhibition dose response curve constructed with log10 x-axis values. The EC_{50} values for shL19 and shL25 were 0.06 to 1 (2.2 ng) and 1.13 to 1 (45.2 ng) respectively.

3.8 The PTZ-H1shRNAs do not compete with other exogenous RNAi effectors

A series of assays was conducted to determine whether the endogenous RNAi pathway is negatively affected by the hairpins (Sections 3.10 and 3.11) or whether the generated hairpins can potentially affect other exogenous RNAi effectors (Section 3.9). A common concern about RNAi therapy is disrupting and over-saturating the endogenous miRNA biogenesis pathway (Grimm *et al*, 2006; Boudreau *et al*, 2009). Exogenously expressed RNAi effectors can compete with one another for the endogenous miRNA machinery including the nucleus-exporting protein Exportin-5 and Dicer (Grimm *et al*, 2006; Boudreau *et al*, 2008). Several factors contribute to the saturation effect of an exogenously introduced RNAi effector including the concentration of the RNAi effector. Saturation is less likely if lower concentrations are used (Ely *et al*, 2008; Castanotto *et al*, 2007).

A sensitive *in vitro* saturation assay was used to demonstrate the interaction between the shRNAs and an anti-HBV pri-miRNA and its cognate target. If the shRNA disrupted the function of the exogenously introduced miRNA, it would indicate a potential to saturate the endogenous RNAi machinery. The shLTR plasmid was generated by Saayman *et al* (2010). The plasmid is driven by a U6 promoter and targets the long terminal repeat (LTR) promoter of HIV-1. shLTR served as the highly disruptive derepression control in the saturation assay. The exogenously introduced RNAi effector used in the same saturation assay was HBV-targeting miR-31/8 and its cognate target psiCHECK-8T-Fw (Ely *et al*, 2008). Three sets of controls were used to demonstrate possible effects the pTZ-shRNAs could have on the system. The non-repression control served as a mock to which the experimental values were normalised. The repression control (pri-miRNA and its target) exhibited normal target knockdown, serving as the positive control. The shLTR plasmid was expected to interfere with miR31/8 inhibition of its target psiCHECK-8T-Fw when transfected at high (100 ng) concentration thus serving as a negative control indicative of oversaturation of the endogenous miRNA pathway (Saayman *et al*, 2010). Figure 3.14 depicts how the assay functions..

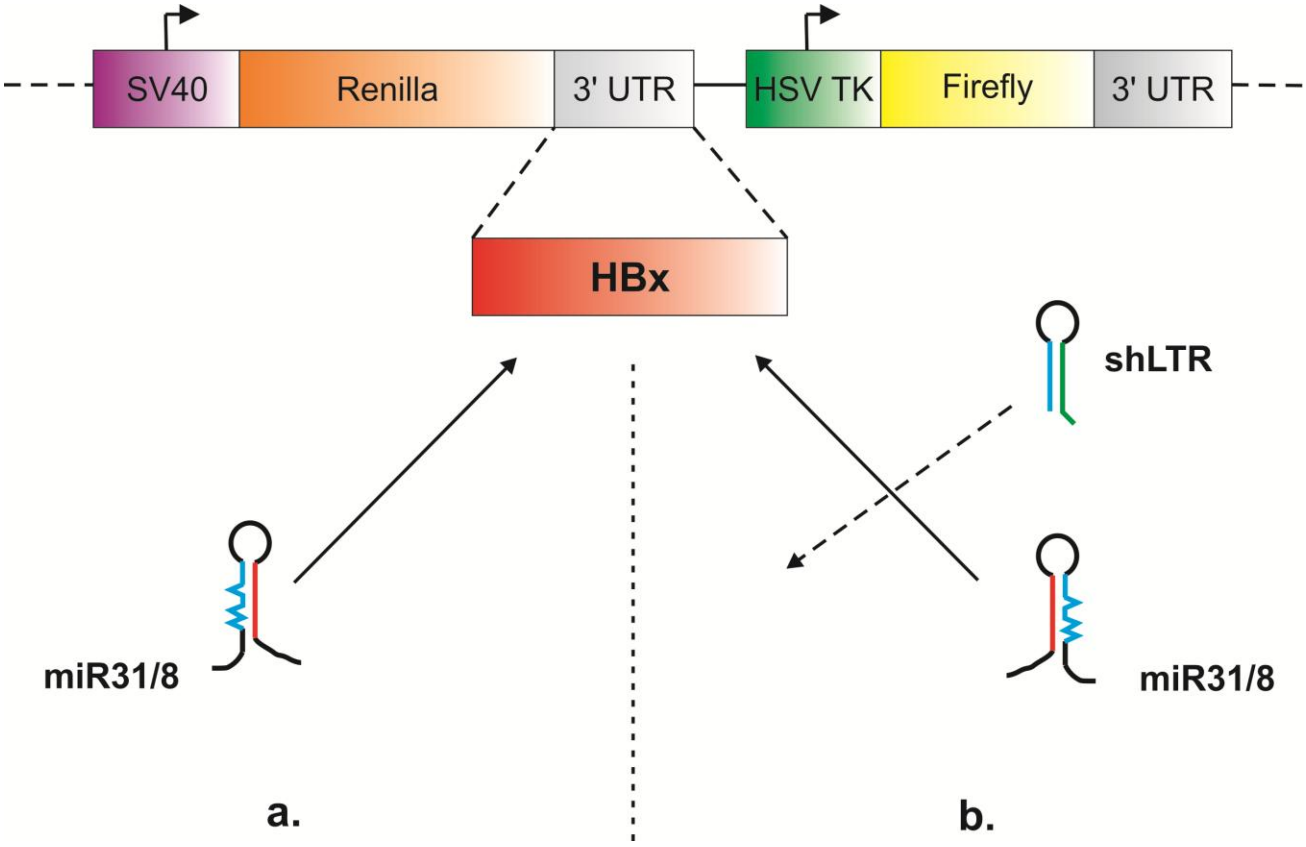


Figure 3.14: Explanation of the saturation assay.

a. Non-repression occurs when the exogenous miRNA (miR31/8) knocks down complementary target expression as per normal (normal target knockdown). b. shLTR represses miRNA activity, the miRNA silencing efficacy is negatively affected.

The saturating effect of the shRNAs was assessed by co-transfecting each control plasmid or pTZ-shRNA in varying concentrations (100 ng or 10 ng) in triplicate into Huh7 cells with a fixed concentration of an anti-HBV miRNA shuttle and its cognate target. A dual-luciferase assay was conducted 48 hours post-transfection to determine the repressive effects of each plasmid.

The controls were as follows: the non-repression control, the repression control and the derepression control. The non-repression controls consisted of 100 ng pCI-eGFP, 100 ng anti-HBV

miRNA (miR-31/8), 100 ng or 10 ng H1 mock and pTZ57R to make up a final concentration of 0.8 µg. The repression controls consisted of 100 ng pCI-eGFP, 100 ng HBV target (psiCHECK-8T-Fw), 100 ng anti-HBV miRNA (miR-31/8), 100 ng or 10 ng H1 mock and pTZ57R to make up a final concentration of 0.8 µg. The derepression controls included the following: 100 ng or 10 ng shLTR, 100 ng pCI-eGFP, 100 ng HBV target (psiCHECK-8T-Fw), 100 ng anti-HBV miRNA (miR-31/8) and pTZ57R to make up a final concentration of 0.8 µg. In both concentration sets, the pTZ-shRNA values were not significantly different ($p > 0.05$) from the repression control (Figure 3.15). These data suggest that the pTZ-shRNAs did not compete with the expression of the anti-HBV shuttle hence did not saturate the system. The validity of the system is called into question due to the unexpected poor repressive effect of shLTR (Figure 3.15).

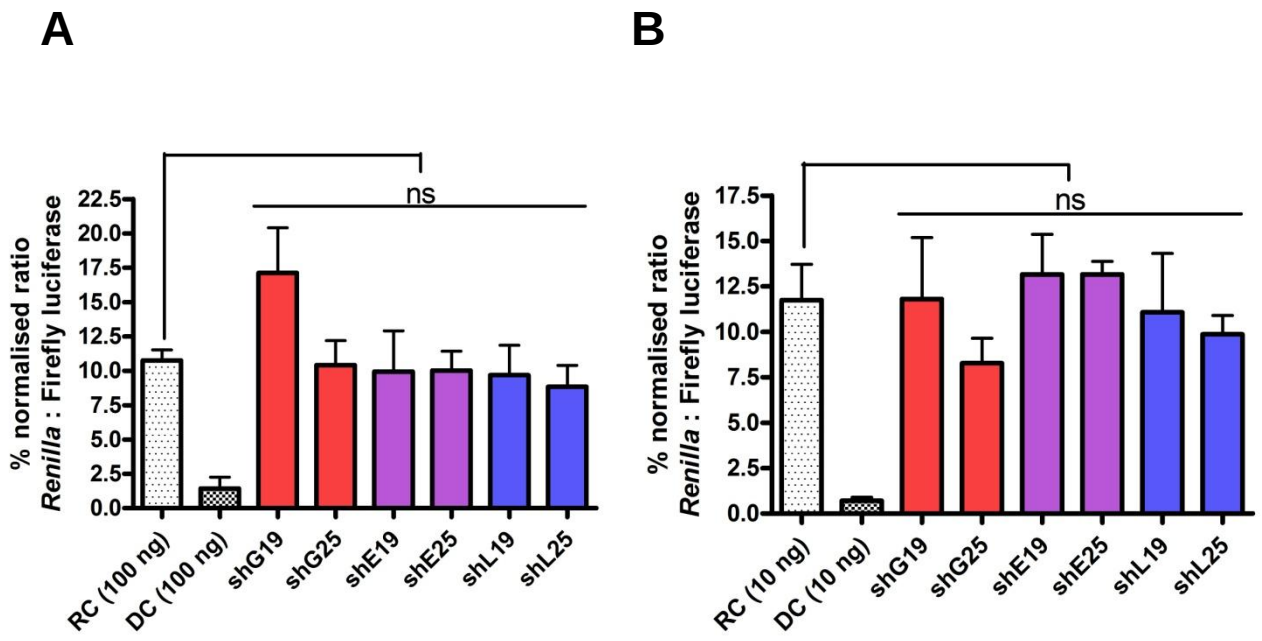


Figure 3.15: Assessment of the repressing effect of shRNAs on an exogenous HBV-expressing cassette.

Huh7 cells were transfected with 100 ng or 10 ng of plasmid with a fixed concentration of an anti-HBV cassette and its target. Values were normalised to the mock values. RC= repression (positive) control. DC= de-repression control. ns, $p > 0.05$. (n = 3, ±SEM). Red = Gag. Purple = Env. Blue = LTR.

3.9 The 19mers and 25mers induce a negligible interferon response compared to poly I:C

When shRNAs are transfected into mammalian cells, they are processed into short interfering RNAs (siRNAs). Depending on the length of the siRNA, an interferon response can be induced (Bridge *et al*, 2003; Reynolds *et al*, 2006). Both the 25mers and 19mers should be too short to elicit significant interferon expression (Reynolds *et al*, 2006) but do the 25mers induce a greater interferon response compared to their shorter 19mer counterparts? To answer this question, an interferon response assay was conducted. The transfection of foreign RNAi effectors into cultured cells can activate an innate immune response. Long RNA duplexes (> 27 bp) are at risk of triggering off-target gene silencing and are generally considered to be potent inducers of an interferon response in HEK293 and HeLa cells (Reynolds et al, 2006). To determine whether the 19mers elicit an interferon response at a significantly lesser degree compared to the longer 25mers, the interferon-β and *GAPDH* mRNA levels in PTZ-H1shRNA-transfected HEK cells were quantified via real-time PCR. The dsRNA analogue poly I: C served as the positive control and the mock plasmid pTZ-H1 +1 served as the negative control. The greater the *IFN-β*: *GAPDH* ratio, the greater induction of an interferon response. The interferon-β induction triggered by the PTZ-H1shRNAs does not differ significantly between the short shRNAs (19mers) and 25mers (Figure 3.16). The LTR-targeting shRNA cassettes and shG25 elicited a negligible interferon-β response compared to the mock plasmid (Figure 3.16). The shG19, shE19 and shE25 plasmids induce a statistically greater interferon response ($p < 0.05$) than the mock plasmid. The interferon induction of all of the plasmids is significantly lower than that poly I:C ($p < 0.05$). The shG25, shL25 and shL19 hairpins induced a negligible interferon response compared to the H1 mock positive control plasmid (Figure 3.16). The *IFN-β:GAPDH* values (y-axis of Figure 3.16) were converted to a $\log_{10}$ scale to discern between the hairpins targeting against Gag, Env and LTR (supplementary Figure B.4).

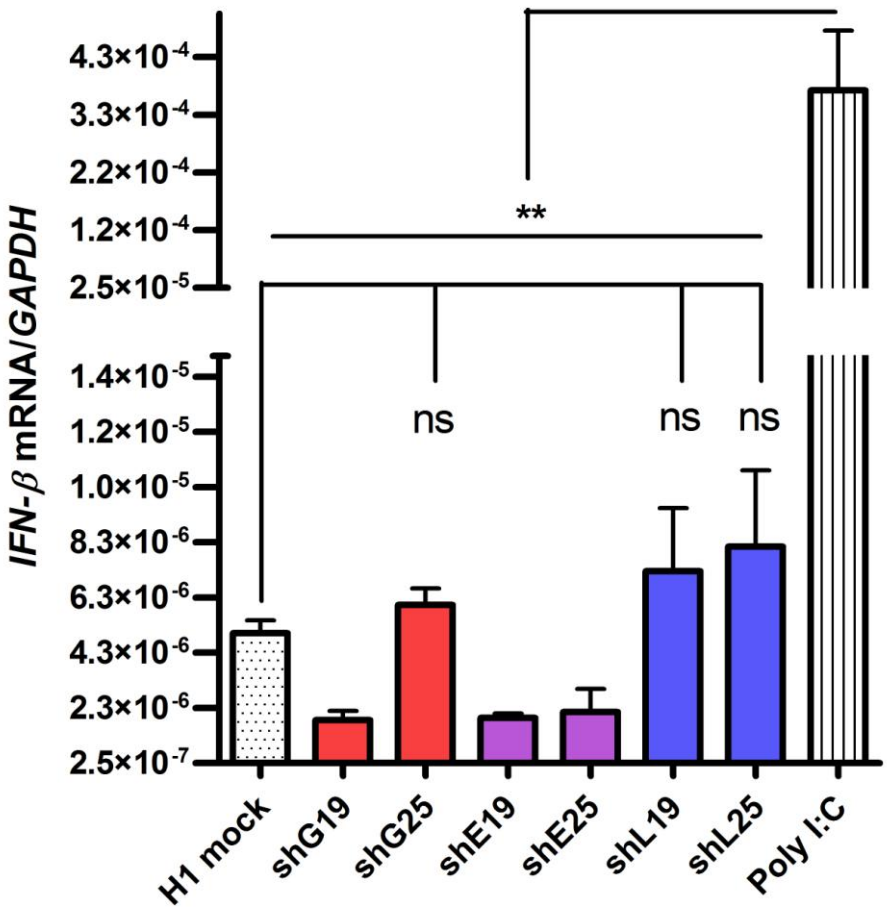


Figure 3.16: The induction of the interferon response in shRNA-transfected cells measured by real-time RT-qPCR.

HEK293 cells were transfected with the shRNAs. Interferon-β induction was determined by measuring the IFN-β mRNA concentration in whole RNA extracted from cells transfected with the respective shRNAs, H1 mock (negative control) or the Poly I: C positive control. Quantitative RT-PCR was conducted to measure the concentration of IFN-β mRNA and normalised to the GAPDH values. (±SEM, n=3). The y-axis has been split to clearly indicate the scale of the shRNA and H1 mock interferon response.

3.10 The shRNAs do not negatively affect cell viability

RNAi triggers cannot be utilised if they have cytotoxic effects. The thiazolyl blue tetrazolium bromide (MTT) assay is a measure of metabolic dysfunction and cytotoxicity in transfected cells. This assay was used to determine whether transfecting the shRNAs into mammalian cells affected normal cell function. Treatment with the DNA methyltransferase inhibitor 5-azacytidine (5-azaC) served as a positive control for cytotoxicity. Visual confirmation of cell viability was determined via light microscopy.

An optical density reading is directly correlated with cell density (Mosmann, 1983). The optical density readings of all the shRNA-transfected cells do not significantly deviate ($p > 0.05$) from that of the untransfected control (Figure 3.17). The OD readings of the PTZ-H1shRNAs were as follows: shG19= 1.25; shG25= 1.16; shE19= 1.24; shE25= 1.19; shL19= 1.02 and shL25= 1.42 (Figure 3.17). The OD reading of the 5-azaC-treated cells (0.553) was significantly lower ($p < 0.01$) than that of the untransfected cells that served as the negative control with an OD reading of ~1.5 in all three PTZ-H1shRNA pairs (Figure 3.17).

These data confirm that the metabolic activity of the 19mer and 25mer-transfected cells is similar to that of the untransfected cells therefore the hairpins do not have any cytotoxic effects. The optical density reading of shL19 compared to that of the untransfected (Figure 3.17 C) may call the prior statement into question but the Dunnet's post-hoc test is highly stringent and thus reliable.

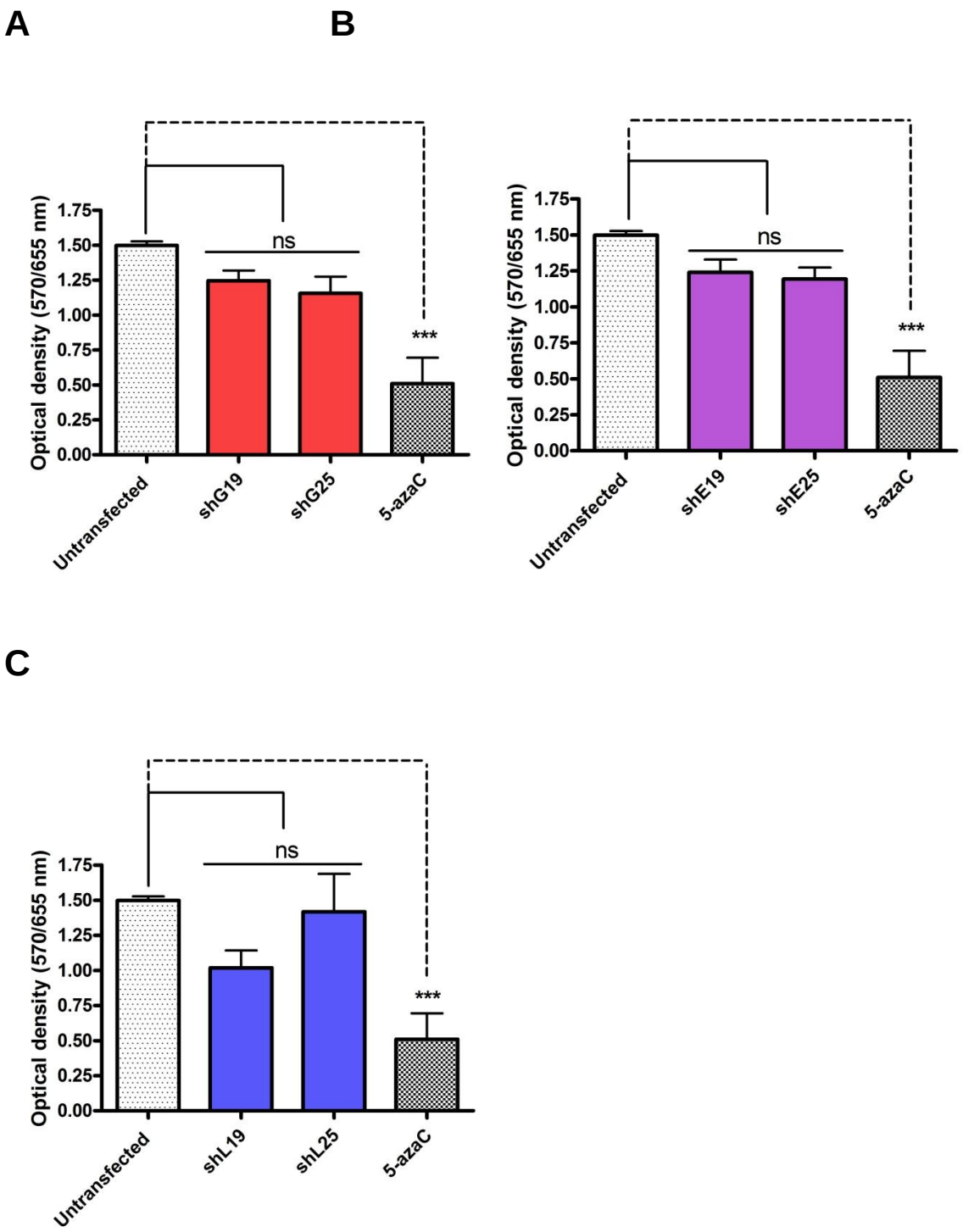


Figure 3.17: Cytotoxicity assessment.

HEK293 cells were transfected with an expressed shRNA ,treated with 5-azacytidine (5-azaC) or not transfected. One-way ANOVA of the untransfected control versus the hairpin-expressing cassette (solid line) or the5-azaC control (dotted line) with Dunnet's post-hoc test. (n = 3, SEM). Red = Gag. Purple = Env. Blue = LTR. Ns= $p > 0.05$. ***= $p < 0.01$.

Chapter 4: Discussion

Potent shRNAs have great therapeutic potential but pose safety concerns. shRNA can be considered for clinical testing if potent even at low dosages, its off-target effects are minimal, doesn't negatively affect the endogenous RNAi pathway or normal cell function. The silencing efficacy of an RNAi effector is influenced by hairpin structure and sequence. This study focused on the effects of stem length on shRNA RNAi efficacy. Three sets of anti-HIV-1 vector-expressed shRNAs were designed for this study. In each set, a theoretically Dicer-independent 19 bp stem shRNA (19mer) and a Dicer-substrate 25 bp stem shRNA (25mer) was generated (Figure 3.2). All of the shRNAs had a small 4 nt loop, six thymidine termination tail and a H1 promoter to drive transcription. The RNAi processing, target knockdown efficacy, shRNA potency and adverse effects were determined and compared between the 19mers and 25mers.

4.1 shRNA potency and stem length

There are contradictory publications about the link between stem length and shRNA efficacy (Siolas et al, 2005; Vlassov et al, 2007; Ge *et al*, 2010). For years, the general consensus about shRNA potency was that there is a direct correlation between shRNA stem length and silencing efficacy; the longer the hairpin (≥ 27 bp stem), the more potent it can be (Kim and Rossi, 2004; Siolas *et al*, 2005; Kim and Rossi, 2005). Siolas *et al* (2005) reinforced this rule in rational shRNA design by stating that Dicer-substrate shRNAs are more potent RNAi triggers. The study determined that expressed shRNAs with a stem length too short (< ~22 bp) to be recognised by Dicer, may still be incorporated into the RNA-induced silencing complex (RISC) but cannot be potent (Siolas *et al,* 2005).

An increasing number of reports observed the contrary, where 19 bp stem shRNAs with 4-10 nt loops proved to be potent RNAi effectors (Li *et al*, 2007; Vlassov *et al*, 2007; Ge *et al*, 2010). Ge *et*

al (2010) determined that 19 bp shRNAs are Dicer-independent. The study identified potent 5'-arm antisense hairpins with 19 bp-long stems and minimal loops but Ge *et al* (2010) were unable to determine how these non-Dicer substrates are processed by the RNAi machinery.

A non-canonical Dicer-independent RNAi pathway was simultaneously discovered by Cifuentes *et al* (2010) and Cheloufi *et al* (2010) after identifying the small RNA miR-451 in zebra fish and mammals respectively. The two groups observed that miR-451 processing was Drosha-dependent but Dicer-independent with the Drosha product being loaded directly into Ago2 (Cifuentes *et al*, 2010; Cheloufi *et al*, 2010). The distinct 17 bp stem and 4 nt loop of miR-451 allowed it to enter the non-canonical processing route (Cifuentes *et al*, 2010; Cheloufi *et al*, 2010; Yang *et al*, 2010).

In this study, three sets of shRNAs were designed and generated to determine whether or not Dicer processing affects silencing efficacy. A pair of shRNAs was produced for each target sequence: 1) a 25mer due to previous literature dictating that shRNAs with stems longer than 22 bp are recognised and processed by the ribonuclease Dicer, 2) a 19mer to mimic miR-451 which is processed by RNAi machinery other than Dicer (Ge *et al*, 2010; Cifuentes *et al*, 2010; Cheloufi *et al*, 2010). The guide strands of all of PTZ-H1shRNAs produced for this study exhibited significant knockdown of their respective target sequences therefore all of the hairpins were effective silencing effectors. Short shRNAs were identified that remain potent at low doses. Northern blot analysis revealed that the RNAi machinery yields a large RNA fragment when processing 19mers (excluding shE19).

4.2 The 19mers have guaranteed strand bias with a single RNA strand

In the canonical RNAi signalling pathway, dsRNA is processed by the endonuclease Dicer resulting in two active ~22 nt siRNA strands. One of the siRNA strands is incorporated into RISC where the sense strand guides sequence-specific knockdown of the target mRNA. The silencing efficacy of the 5'-arm (guide strand) and the 3'-arm (passenger strand) of each expressed shRNA was compared via dual-luciferase activity. Target knockdown was expected from both the 5'-arm and 3'-arm of the shRNAs.

Contrary to Siolas *et al* (2005), this study has successfully identified a 19mer (shL19) which is comparably more potent than its 25mer counterpart. Both arms of the 19mers and 25mers exhibited target knockdown but the 3'-arm of the 19mers is comparably weaker than the 3'-arm of the 25mers. The passenger strand (3'-arm) of shG19 was the most potent of the 19mers with ~40% knockdown of the target sequence but an shRNA needs to exhibit a minimum of 50% knockdown to be categorised as an active suppressor (McIntyre *et al*, 2009). We speculated that the observed strand bias towards the 5'-arm in the 19mers was due to an inactive or non-existent 3'-arm as observed in mature miR-541 (Cheloufi *et al*, 2010; Cifuentes *et al*, 2010). This consistent 5'-arm bias in the target knockdown data is a novel demonstration of expressed 19mers being processed differently (compared to the 25mers) by the RNAi machinery.

In a study that was conducted concurrently with our own, a group of shRNAs with varying stem lengths and loop sizes and sequences were tested, similar results were observed (Liu *et al*, 2013). The 5'-arm of 19mers with 3-8 nt loops was highly suppressive of their cognate target sequence and the 3' arm exhibited poor activity (Liu *et al*, 2013).

The detection of the large ~30 nt mature RNA products in the northern blots (Figures 3.8 and 3.9) suggests that shG19 and shL19 were successfully processed in a manner similar to mature miR-451 (Cifuentes *et al*, 2010; Cheloufi *et al*, 2010). We've dubbed our 19mers "guide shRNAs" because the single, long mature RNA fragment most likely guides RISC to target complementary mRNA. This data (combined with the dual-luciferase knockdown observations) illustrates that our novel guide shRNAs offer a streamlined shRNA design with guaranteed strand bias to the 5'-arm. Most siRNA design tools focus on RNAi efficacy instead of specificity (Boudreau *et al*, 2011). This guide shRNA design circumvents the need for predictive algorithms to determine factors required for shRNA strand bias therefore simplifying the screening for highly effective shRNA sequences.

Liu *et al* (2013) conducted an Ago2 co-immunoprecipitation assay (to assess the interaction activity between AGO2 and the shRNAs) and revealed that Ago2 processes a 19 bp shRNA with a 5 nt loop into a ~33 nt RNA fragment. This observation supports the theory that my guide shRNAs were processed like mature miR-451; in a Dicer-independent and Ago-dependent manner. Ago2 cleaved the 3'-arm of the 19mer resulting in: 1) a long RNA product consisting of the 19 nt 5'-arm, the minimal loop and ~6 nt of the 5' end of the 3'-arm and 2) the degraded 3' end of the 3'-arm (Liu *et al*, 2013).

The notable poor signal of the RNA products, particularly the 19mers, may be due to poor processing efficiency. shRNAs are generally poorly processed and thus yield an abundance of precursors (Boudreau *et al*, 2009). No unprocessed shRNA precursors were visible in the northern blot hybridised with DNA oligonucleotide probes and yet the RNA product bands were bold (strong signal). The poor signal detection may be due to the selection of a weaker RNA polymerase III promoter (H1) (Brummelkamp *et al*, 2002). Another factor to consider in the case of the 19mers is that circumventing Dicer-processing also bypasses interaction with the TAR RNA binding protein (TRBP); Dicer-TRBP binding is considered essential for RNAi function (Daniels *et al*, 2009). The potency of shL19 either contradicts the importance of Dicer-TRBP binding or is influenced by other

unidentified factors. To establish a greater understanding of the 19mers, testing in a Dicer-null environment is required. Additionally, *in vivo* testing will help further characterise this 19mer and help determine whether these minimal length guide shRNAs with small terminal loops have a future in clinical testing.

RNAi activity in short shRNAs is sequence-dependent which may explain the poor silencing efficacy exhibited by shE19. A larger number of potent short shRNAs need to be identified in order to determine what characteristics generate potent minimal-length shRNAs. Ge *et al* (2010) speculated that the presence of an exposed 5'-phosphate in shRNAs with a 5'-arm-positioned guide strand enhances Ago2-binding. As interest in guide shRNA increases, the possible over-saturation of Ago2 should be investigated. This alternative RNAi processing route has removed Dicer as a saturation bottleneck, leaving Ago2 (Grimm *et al*, 2006; Grimm *et al*, 2010; Börner *et al*, 2013).

4.3 The guide shRNAs reduce off-targeting and maximise potency

Potent shRNAs run the risk of inducing negative side-effects such as off-target silencing via miRNA-like partial complementarity, saturating the endogenous RNAi pathway and inducing an interferon response (Saxena *et al*, 2003; Grimm *et al*, 2007; Rao *et al*, 2009). The saturation effects of highly expressed shRNAs are dose dependent and highly potent siRNA sequences can minimise off-targeting if low doses prove to be effective. To minimise the negative side effects associated with shRNAs, one must increase the potency of shRNAs in order to reduce the required dose (Bridge *et al*, 2003; Aagaard and Rossi, 2007). Both shG19 and shL19 were shown to be effective target suppressors at low dose values.

Off-target RNAi activity is unpredictable and best to be avoided. Off-targeting can have cytotoxic effects (Fedorov *et al*, 2006). Off-target effects can result from as little as a 6 – 7 nucleotide match

between the seed region and target mRNA (Jackson *et al*, 2006; Birmingham *et al*, 2006). Off-target effects may be caused by inadvertent sense (passenger strand) strand incorporation into RISC resulting in incorrect target recognition (Schwarz *et al*, 2003; Khvorova *et al*, 2003; Wei *et al*, 2009). Alterations to siRNAs and shRNAs including the insertion of sequence and chemical modifications change the internal stability of the duplex in favour of ensuring that only the intended (guide/antisense) strand is taken up by RISC (Khvorova *et al*, 2003; Schwarz *et al*, 2003; Rao *et al*, 2009). These modifications of siRNAs to potently reduce off-target effects include the use of asymmetric terminal overhangs, guide strands must be AU-rich at the 5'-end and GC-rich at the 3'-end, a 3' blunt end on the passenger strand combined with a dinucleotide overhang on the guide strand and nucleotide mismatches (Rose *et al*, 2005; Sano *et al*, 2008; Engels, 2013). Functional strand asymmetry in shRNAs can be achieved by ensuring that the sense strand only has 8 to 12 C/G nucleotides, inserting a terminal 5' mismatch pair, limiting the number of C/G sequences in tandem to five, inserting miRNA-like bulges (e.g. a G:U wobble in the seed region) or mismatches in the sense strand to inactivate the sense strand (McIntyre and Fanning, 2006; Ui-Tei *et al*, 2008a; Ding *et al*, 2008). Software can be used to determine the thermodynamic profiles of shRNAs to assess the stability of the intended guide strand (Ding *et al*, 2004; Gonzalez-Alegre *et al*, 2005). The choice of promoter and controlling shRNA dosage both significantly influence the saturation risk of shRNAs (Boden et al, 2003a; Rao *et al*, 2009).

One of the main advantages of using synthetic RNAi triggers is that one can engineer the RNAs with minimal off-target effects; particularly sense strand off-target effects. The use of synthetic siRNAs to secure strand bias is an option that is not afforded in expressed RNA systems. The single RNA strand of our processed guide shRNAs has great potential to serve as an ideal alternative without the limitations novel synthetic RNAi activators face; such as high synthesis cost, increased cytotoxicity or sense strand off-target effects (Sibley *et al*, 2010). The northern blot and target knockdown data indicate that mature guide shRNAs do not have a passenger strand. This absence nullifies the risk of sense strand-related off-target effects and simplifies shRNA design. The

revolutionary design of the guide shRNAs can potentially improve the specificity of previously characterised potent traditional (canonically processed by the RNAi pathway) shRNAs.

4.4 Insignificant interferon response

The innate response system is an evolutionarily-derived trait for mammalian cells to combat viral invasion through stunted protein synthesis and/or cell death (Aagaard and Rossi, 2007). The introduction of double-stranded RNA in mammalian cells can activate an innate immune response. Bridge *et al* (2003) observed that the commonly used Pol III-driven shRNA expression system does is capable of inducing an interferon response.

The protein kinase PKR is activated in response to the presence of dsRNAs resulting in the upregulation of IFN-β mRNA via the interferon signalling pathway (Sledz *et al*, 2003). It is unlikely that the shRNAs generated in this study activated PKR because dsRNAs need stem lengths ≥ 30 bp to be recognised (Kim and Rossi, 2007).

Toll-like receptors that are expressed from the endosomes (internal vesicles) can recognise both single-stranded (ss) and dsRNAs (Kim and Rossi, 2007). Both Toll-like receptor 3 (TLR3) and the RNA helicases RIG-I and Mda-5 recognise and are activated by dsRNAs leading to the induction of type I interferon transcription (Kim and Rossi, 2007). The signalling pathways of TLR3, RIG-I and Mda-5 converge downstream in the induction of inflammatory cytokines and type I interferons including IFN-β (Sen & Sarkar, 2007). Real-time quantitative RT-PCR was used to determine the level of IFN-β upregulation induced by the shRNAs relative to the housekeeping gene *GAPDH*.

Liu *et al* (2013) speculated that Ago-dependent shRNAs may activate a comparably lesser interferon response than Dicer-processed shRNAs and thus be safer to use in therapeutic applications. None of the PTZ-H1shRNAs elicited an interferon response comparable to the dsRNA analogue, poly I:C. The LTR-targeting shRNAs (shL19 and shL25) and shG25 each induced a negligible interferon response relative to the mock plasmid. The other shRNAs did elicit an interferon response greater than the mock plasmid but significantly less than poly I:C.

Assessing the *in vitro* induction of interferon stimulated genes is not a completely definitive measure of immunostimulation or cytokine dynamics as the results can vary between cell lines but the assay serves as an initial guide. One of the most critical factors to consider with in vitro assessment of an immune response is the time period after which the supernatants are collected. Twenty-four hours was given in these assays due to IFN-β mRNA reaching its maximal induction at this time point.

4.5 Negligible interference of the endogenous RNAi pathway

Conventional shRNAs are substrates for the cellular transporter, Exportin-5 (Aagaard and Rossi, 2007). Exportin-5 mediates the transport and stabilisation of both endogenous and ectopic pre-miRNAs and shRNAs from the nucleus to the cytoplasm (Yi *et al*, 2003; Grimm *et al*, 2006). High expression of shRNA cassettes can result in oversaturation of the RNAi machinery (Exportin-5, Dicer, Ago2 incorporation into RISC) leading to cellular toxicity (Castanotto *et al*, 2007; Grimm *et al*, 2007; Grimm *et al*, 2006). The link between cytotoxicity and Exportin-5 saturation was determined in a study where the negative saturation effects of shRNAs outcompeting miRNAs was reversed by the over-expression of Exportin-5 (Yi *et al*, 2005). Additionally, Grimm *et al* (2006) observed fatalities in mice that were treated with liver-specific shRNAs; liver toxicity/damage was shown to be the cause. Due to essential liver-specific miRNAs being out-competed by the highly expressed shRNAs, the endogenous RNAi system could not facilitate normal liver function (Grimm *et al*, 2006). The ectopic shRNAs and endogenous miRNAs each competed to be shuttled from the nucleus to

the cytoplasm by the transport factor Exportin-5; this lead to saturation of Exportin-5 (Grimm *et al*, 2006). There is no significant metabolic difference between the 19mer and 25mer-transfected cells (Figure 3.13 in Section 3.8) leading one to speculate that the short shRNA (19mer) constructs may also transported from the nucleus to the cytoplasm by Exportin-5 or that neither the 19mers nor 25mers were shuttled into the cytoplasm by Exportin-5.

Börner *et al* (2013) suggested that saturation of Ago2 (rather than Exportin-5) by exogenous RNAi triggers leads to cytotoxic effects. The presence of Ago2 in the nucleus challenges the idea of the Exportin-5-dependent shuttling of the guide shRNAs from the nucleus to the cytoplasm. Active Ago2 in the nucleus may retain its ability to "slice" therefore shRNA-processing could possibly occur in the nucleus (Gagnon and Corey, 2012). RNAi saturation effects may be due to exogenous RNAi effectors competing to interact with nuclear Ago2. Exportin-5 recognises the dinucleotide 3' overhang characteristic of Drosha-processing, which the shRNAs expressed in this study do not have, removing Exportin-5 as the saturation limiting factor (Kim et al, 2004).

RISC can assemble and function in the nucleus therefore RISC is a potential saturation factor (Robb *et al*, 2005). Expressed shRNAs also compete for downstream factors in the RNAi pathway. RISC saturation may occur as siRNAs, miRNAs and shRNAs alike bind to the Ago2 component of RISC in both the nuclear and cytoplasmic areas of a cell (Grimm *et al*, 2007). If shG19 and shL19 are indeed Dicer-independent and Ago2-dependent, the guide shRNAs did not over-saturate Ago2.

Key determinants that dictate shRNA cytotoxicity are shRNA length, sequence and dose (Grimm *et al*, 2009). Despite possessing different attributes, none of the shRNAs in this study caused significant cytotoxic effects. Promoter selection contributes to both shRNA efficacy and saturation effects (Grimm *et al*, 2009). The saturation assay results suggest that the shRNAs do not out-

compete endogenous RNAi triggers. Using the weaker H1 Pol III promoter instead of a U6 Pol III promoter can help prevent cytotoxic effects (An *et al*, 2006).These data show that selecting the constitutively active RNA polymerase III H1 promoter to drive the transcription of each of the shRNAs contributed to maintaining a balance between silencing activity and saturation.

4.7 Potential antiviral combinatorial therapy

Anti-viral gene therapy usually requires a combinatorial RNAi approach to initially reduce viral escape routes and negatively regulate viral replication (Grimm and Kay, 2007). Different studies have engineered strategies that include using the presence of naturally clustered polycistronic transcripts to coordinate expression of anti-HIV-1 miRNAs that most resemble the natural pre-miRNA structures (Liu *et al.*, 2008), small RNAs multiplexed (arranged in tandem) into shuttles that resemble the natural polycistron with substituted anti-viral guide and complementary sequences (Chung *et al.*, 2006; Boden *et al.*, 2004), under the transcriptional control of a single or multiple promoters and the use of various small RNAs in a single therapeutic attack (DiGuisto *et al.*, 2010).

Highly specific and potent short shRNAs may be applicable for combinatorial RNAi therapy. It may be worth investigating whether guide RNAs can be multiplexed either in miR-451 shuttles or as shRNAs expressed in tandem.

4.8 Future work

To further validate my findings and to dispel any doubt about the validity of my results, I'd recommend that the northern blot analysis (Figure 3.8) be repeated with new RNA samples for each of the tested 19mer and 25mer hairpins. The *in vitro* assay results can be repeated in HIV-infected cells or in cells infected with a non-replicating version of HIV. An *in vivo* study using an appropriate animal model can also be conducted. Humanised mouse non-human primate models exist that mimic different stages of HIV infection (e.g. the humanised Rag2 $^{-/-}{}_{\gamma}c^{-/-}$ mouse model simulates the

progression of HIV replication and decreased CD4 count) (Neff *et al*, 2011; Hatziioannou & Evans, 2012).

Chapter 5: Conclusion

The ideal expressed vector-based shRNA system should be highly efficient with maximal target knockdown and minimal cytotoxic effects and off-targeting. Efficiency is determined by the silencing efficacy of the shRNAs. Although both shG19 and shL19 were shown to be highly effective, the shL19 hairpin was more potent than its 25mer counterpart therefore the guide shRNA design enhanced the RNAi efficacy of the shRNA sequence. shL19 is transcribed by a moderately powerful promoter that may limit potential Ago2 saturation and the 19mer is efficient at a low dose. With the single processed RNA strand, non-specific effects are minimised and specificity is highly ensured with potential sense strand off-target effects abrogated. The shL19 guide shRNA may be a prime candidate for therapeutic application.

This study has generated novel data identifying a shRNA design that yields a single active RNA (guide) strand. Our guide shRNAs have completely altered shRNA design by abolishing sense strand off-target effects thus improving the shRNA safety profile and simultaneously enhancing shRNA specificity; essentially leaping over major hurdles in RNAi-based therapy.

References

Aagaard, L. & Rossi, J.J. (2007). RNAi therapeutics: principles, prospects and challenges. *Adv Drug Deliv Rev* **59**(2-3): 75-86.

Allfrey, V.G., Faulkner, R., and Mirsky, A.E. (1964). Acetylation and methylation of histones and their possible role in the regulation of RNA synthesis. *Proc Natl Acad Sci* **51**: 786-794.

Alwine, J.C., Kemp, D.J., and Stark, G.R. (1977). Method for detection of specific RNAs in agarose gels by transfer to diazobenzyloxymethyl-paper and hybridization with DNA probes. *Proc Natl Acad Sci* **74**(12):5350-5354.

Amarzguioui, M., Rossi, J.J., and Kim. D. (2005). Approaches for chemically synthesized siRNA and vector-mediated RNAi. *FEBS Letters* **579**: 5974-5981.

An, D.S., Qin, F.X., Auyeung, V.C., Mao, S.H., Kung, S.K., Baltimore, D., and Chen, I.S. (2006). Optimization and functional effects of stable short hairpin RNA expression in primary human lymphocytes via lentiviral vectors. *Mol Ther* **14**: 494–504.

Asparuhova, M.B., Barde, I., Trono, D., Shranz, K., and Schumperli D. (2008). Development and characterization of a triple combination gene therapy vector inhibiting HIV-1 multiplication. *J Gene Med* **10**:1059-1070.

Babiarz, J.E., Ruby, J.G., Wang, Y., Bartel, D.P., and Blelloch, R. (2008). Mouse ES cells express endogenous shRNAs, siRNAs, and other Microprocessor-independent, Dicer-dependent small RNAs. *Genes Dev* **22**: 2773.

Bartel, D.P. (2004). MicroRNAs: genomics, biogenesis, mechanism and function. *Cell* **116**: 281-297.

Bartel, D.P. 2009. MicroRNAs: Target recognition and regulatory functions. Cell 136: 215–233.

References

Bernards, R., Brummelkamp, T.R., and Beijersbergen, R.L. (2006). shRNA libraries and their use in cancer genetics. *Nat Methods* **3**:701–706.

Berezikov, E., Chung, W. J., Willis, J., Cuppen, E., Lai, E. C., (2007). Mammalian miRtron genes. *Mol Cell* **28**: 328.

Bernstein, E., Caudy, A.A., Hammond, S.M. and Hannon, G.J. (2001a). Role for a bidentate ribonuclease in the initiation step of RNA interference. *Nature* **409**(6818): 368-366.

Bernstein, E., Denli, A.M., and Hannon, G.J. (2001b). The rest is silence. *RNA* **7**:1509–1521.

Birmingham, A., Anderson, E.M., Reynolds, A., Ilsley-Tyree, D., Leake, D., Fedorov, Y., Baskerville, S. (2006). 3'UTR seed matches, but not overall identity, are associated with RNAi off-targets. *Nat Methods* **3**(3): 199-204.

Boden, D., Pusch, O., Lee, F., Tucker, L., Shank, P.R., and Ramratman, B. (2003a). Promoter choice affects the potency of HIV-1 specific RNA interference. *Nucleic Acids Res* **31**(17): 5033-5038.

Boden, D. Pusch, O., Silbermann, R., Lee, F., Tucker, L., and Ramratman, B. (2004). Enhanced gene silencing of HIV-1 specific siRNA using microRNA designed hairpins. *Nucleic Acids Res* **32**(3): 1154-1158.

Bohnsack, M. T., Czaplinski, K. and Gorlich, D. (2004). Exportin-5 is a RanGTP-dependent dsRNA-binding protein that mediates nuclear export of pre-miRNAs. *RNA* **10**: 185–191.

Börner, K., Niopek, D., Cotugno, G., Kaldenbach, M., Pankert, T., Willemsen, J., Zhang, X., *et al*. (2013). Robust RNAi enhancement via human Argonaute-2 overexpression from plasmids, viral vectors and cell lines. *Nucleic Acids Res* 1-22.

Boudreau, R.L., Monteys, A.M., and Davidson, B.L. (2008). Minimizing variables among hairpin-based RNAi vectors reveals the potency of shRNAs. *RNA* **14**: 1834-1844.

References

Boudreau,R.L., Martins,I.and Davidson,B.L. (2009). Artificial microRNAs as siRNA shuttles: improved safety as compared to shRNAs in vitro and in vivo. *Mol Ther* **17**: 169–175.

Boudreau, R.L., Spengler, R.M., and Davidson, B.L. (2011). Rational design of therapeutic siRNAs: minimizing off-targeting potential to improve the safety of RNAi therapy for Huntington's Disease. *Mol Ther* **19**(12): 2169-2177.

Bridge, A.J., Pebernard, S., Ducraux, A., Nicoulaz, A., and Iggo, R. (2003). Induction of an interferon response by RNAi vectors in mammalian cells. *Nat Genet* **34**(3): 263-264.

Brummelkamp, T.R., Bernards, R., and Agami, R. (2002). A system for stable expression of short interfering RNAs in mammalian cells. *Science* **296**: 550-553.

Cai, X., Hagedorn, C.H., and Cullen, B.R. (2004). Human microRNAs are processed from capped, polyadenylated transcripts that can also function as mRNAs. *RNA* **10**:1957–1966.

Calin, G.A., Dumitru, C.D., Shimizu, M., Bichi, R., Zupo, S., Noch, E., Aldler, H., et al. (2002). Frequent deletions and down-regulation of micro-RNA genes *miR15* and *miR16* at 13q14 in chronic lymphocytic leukemia. *Proc Natl Acad Sci* **99**(24): 15524-15529.

Carmell, M.A. & Hannon, G.J. (2004). RNase III enzymes and the initiation of gene silencing. *Nat Struct Mol Biol* **11**: 214–218.

Castanotto, D., Li, H., and Rossi, J.J. (2002). Functional siRNA expression from transfected PCR products. *RNA* **8**: 1454-1460.

Castanotto, D., Sakurai, K., Lingeman, R., Li, H., Shirely, L., Aagaard, L., Soifer, H., Gatignol, A., Riggs, A and Rossi, J.J. (2007). Combinatorial delivery of small interfering RNAs reduces RNAi efficacy by selective incorporation into RISC. *Nucleic Acids Res* **35**(15): 5154-5164.

Castanotta, D. (2011). Sensor and sensitivity: a screen for elite shRNAs. *Mol Ther* **19**(5): 823-825.

Chan, J.A., Krichevsky, A.M., and Kosik, K.S. (2005). MicroRNA-21 is antiapoptotic factor in human glioblastoma cells. *Cancer research* **65**(14): 6029-6033.

References

Chendrimada, T. P., Gregory, R. I., Kumaraswamy, E., Norman, J., Cooch, N., Nishikura, K., and Shiekhattar, R. (2005). TRBP recruits the Dicer complex to Ago2 for microRNA processing and gene silencing. *Nature* **436**, 740-4.

Cheloufi, S., Dos Santos, C.O., Chong, M.M.W., and Hannon, G.J. (2010). A Dicer-independent miRNA biogenesis pathway that requires Ago catalysis. *Nature* **465**: 584-590.

Chu, C. & Rana, T. M. (2006). Translation repression in human cells by microRNA-induced gene silencing requires RCK/p54. *PLoS Biol* **4**, e210.

Chung, K., Hart, C.C., Al-Bassam, S., Avery, A., Taylor, J., Patel, P.D., Vojtek, A.B., *et al*. (2006). Polycistronic RNA polymeraseII expression vectors for RNA interference based on BIC/miR-155. *Nucleic Acids Res* **34**(7): e53.

Cifuentes, D., Xue, H., Taylor, D.W., Patnode, H., Mishima, Y., Cheloufi, S., Ma, E., *et al*. (2010). A novel miRNA processing pathway independent of Dicer requires Argonaute2 catalytic activity. *Science* **328**: 1694-1698.

Czech, B. & Hannon, G.J. (2011). Small RNA sorting: matchmaking for Argonautes. *Nat Rev* **12**: 19-31.

Daniels, S.M., Melendez-Pena, C.E., Scarborough, R.J., Daher, A., Christensen, H.S., El Far, M., Purcell, D.F.J., et al. (2009). Characterization of the TRBP domain required for Dicer interaction and function in RNA interference. *BMC Mol Biol* **10**: 38.

Dickins, R.A., McJunkin, K., Hernando, E., Premsrirut, P.K., Krizhanovsky, V., Burgess, D.J., Kim, S.Y., Cordon-Cardo, C., Zender, L., Hannon, G.J., and Lowe, S.W. (2007). Tissue-specific and reversible RNA interference in transgenic mice. *Nat Genet* **39**(7): 914-921.

DiGuisto, D.L., Krishnan, A., Li, L., Li, H., Li, S., Rao, A., Mi, S., *et al* (2010). RNA-based gene therapy for HIV-1 with lentiviral vector mediated CD34(+) cells in patients undergoing transplantation for AIDS-related lymphoma. *Sci Transl Med* **2**(36): 36ra43.

References

Ding, Y., Chan, C.Y., and Lawrence, C.E. (2004). Sfold web server for statistical folding and rational design of nucleic acids. *Nucleic Acids Res* **32**: W135-W141.

Ding, H., Liao, G., Wang, H., and Zhou, Y. (2008). Asymmetrically designed siRNAs and shRNAs enhance the strand specificity and efficacy in RNAi. *J RNAi Gene Silencing* **4**(1): 269-280.

Dlakic, M. (2006). DUF283 domain of Dicer proteins has a double-stranded RNA-binding fold. *Bioinformatics* **22**: 2711–2714.

Doench, J.G. & Sharp, P.A. (2004). Specificity of microRNA target selection in translational repression. *Genes Dev* **18**: 504-511.

Dyer, V., Weinberg, M.S., and Arbuthnot, P. (2010). Assessing the efficacy of RNA polymerase II- and RNA polymerase III promoter-driven RNA interference effecter cassettes targeted to HBx. Thesis.

Elbashir, S.M., Harborth, J., Lendeckel, W., Yalcin, A., Weber, K., and Tuschl, T. (2001a). Duplexes of 21-nucleotide RNAs mediate RNA interference in cultured mammalian cells. *Nature* **411**: 494-498.

Ely, A., Naidoo, T., Mufamadi, S., Crowther, C., and Arbuthnot, P. (2008). Expressed anti-HBV primary microRNA shuttles inhibit viral replication efficiently *in vitro* and *in vivo*. *Mol Ther* **16**(6): 1105-1112.

Engels, J.W. (2013). Gene silencing by chemically modified siRNAs. *New Biotech* **30**(3): 302-307.

Fellman, C., Zuber, J., McJunkin, K., Chang, K., Malone, C.D., Dickins, R.A., Xu, Q., *et al*. (2011). Functional identification of optimized RNAi triggers using a massively parallel sensor assay. *Mol Cell* **41**(6): 733-746.

Fedorov, Y., Anderson, E.M., Birmingham, A., Reynolds, A., Karpilow, J., Robinson, K., Leake, D., *et al* (2006). Off-target effects by siRNA can induce toxic phenotype. *RNA* **12**: 1188-1196.

References

Fire, A., Xu, S.Q., Montgomery, M.K., Kostas, S.A., Driver, S.E., and Mello, C.C. (1998). Potent and specific genetic interference by double-stranded RNA in Caenorhabditis elegans. *Nature* **391**:806–811.

Filipowizc, W. (2005). RNAi: the nuts and bolts of the RISC machine. *Cell* **122**: 17-20.

Frank, F., Sonenberg, N., and Nagar, B. (2010). Structural basis for 5′-nucleotide base-specific recognition of guide RNA by human AGO2. *Nature* **465**: 818–822.

Gagnon, K.T. & Corey, D.R. (2012). Argonaute and the nuclear RNAs: new pathways for RNA-mediated control of gene expression. *Nucleic Acid Therapeutics* **22**(1): 3.

Garcia-Sastre, A., & Biron, C.A. (2006). Type 1 interferons and the virus-host relationship: a lesson in détente. *Science* **312**: 879-882.

Ge, Q., Ilves, H., Dallas, A., Kumar, P., Shorenstein, J., Kazakov, S.A., and Johnston, B.H. (2010). Minimal-length short hairpin RNAs: The relationship of structure and RNAi activity. *RNA* **16**: 106-117.

Giering, J.C., Grimm, D., Storm, T.A., and Kay, M.A. (2008). Expression of shRNA from tissue-specific pol II promoter is an effective and safe RNAi therapeutic. *Mol Ther* **16**(9): 1630-1636.

Gonzalez-Alegre, P., Bode, N., Davidson, B.L., and Paulson, H.L. (2005). Silencing dystonia: lentiviral-mediated RNA interference therapyfor DYT1 dystonia. *J Neurosci* **25**: 10502-10509.

Grimm, D., Streetz, K.L., Jopling, C.L., Storm, T.A., Pandey, K., Davis, C.R., Marion, P., *et al*. (2006). Fatality in mice due to oversaturation of cellular microRNA/short hairpin RNA pathways. *Nature* **441**: 537-541.

Grimm, D. And Kay, M. A. (2007). Therapeutic application of RNAi: is mRNA targeting finally ready for prime time? *J Clin Invest* **117**(12): 3633-3641.

References

Grimm, D., Wang, L., Lee, J.S., Schurmann, N., Gu, S., Borner, K., Storm, T.A., et al. (2010). Argonaute proteins are key determinants of RNAi efficacy, toxicity, and persistence in the adult mouse liver. *J Clin Invest* **120**(9): 3106-3119.

Gu, S., Jin, L., Zhang, Y., Huang, Y., Zhang, F., Valdmanis, P.N., and Kay, M.A. (2012). The loop position of shRNAs and pre-miRNAs is critical for the accuracy of Dicer processing in vivo. *Cell* **151**(4): 900-911.

Guo, Y., Liu, J., Li, Y.H., Song, T.B., Wu, J. Zheng, C.X., and Xue, C.F. (2005). Effect of vector-expressed shRNAs on hTERT expression. *World J of Gastroenterol* **11**: 2912-2915.

Hacein-Bey-Abina, S. et al. 2008. Insertional oncogenesis in 4 patients after retrovirus-mediated gene therapy of SCID-X1. J. Clin. Invest. **118**, 3132–3142.

Hammond, S.M., Boettcher, S., Caudy, A.A., Kobayashi, R and Hannon, G.J. (2001). Argonaute2, a link between genetic and biochemical analyses of RNAi. *Science* **293**(5532): 1146-1150.

Han, J., Lee, Y., Yeom, K.H., Nam, J.W., Heo, I., Rhee, J.K., Sohn, S.Y., Cho, Y., Zhang, B.T., and Kim, V.N. (2006). Molecular basis for the recognition of primary microRNAs by the Drosha–DGCR8 complex. *Cell* **125**:887–901.

Harborth, J., Elbashir, S.M., Vandenburgh, K., Manninga, H., Scaringe, S.A., Weber, K., and Tuschl, T. (2003). Sequence, chemical, and structural variation of small interfering RNAs and short hairpin RNAs and the effect on mammalian gene silencing. *Antisense Nucleic Acid Drug Dev* **13**: 83-105.

Hatziioannou, T., and Evans, D.T. (2012). Animal models for HIV/AIDS research. *Nature Reviews Microbiology* **10**: 852-867.

He, L., Thomson, M., Hemann, M.T., Hernando-Monge, E., Mu, D., Goodson, S., Powers, S., Cordon-Cardo, C *et al*. (2005). A microRNA polycistron as a potential human oncogene. *Nature* **435**: 828-833.

References

Heale, B.S.E., Soifer, H.S., Bowers, C., and Rossi, J.J. (2005). siRNA target site secondary structure predictions using local stable substructures. *Nucleic Acids Res* **33**(3): e30.

Heo, I. & Kim, V. N. (2009). Regulating the regulators: posttranslational modifications of RNA silencing factors. *Cell* **139**: 28–31.

Holen, T., Amarzguioui, M., Wiiger, M.T., Babaie, E., and Prydz, H. (2002). Positional effects of short interfering RNAs targeting the human coagulation trigger Tissue Factor. *Nucleic Acids Res* **30**(8): 1757-1766.

Huang, M., Chan, D.A., Jia, F., Xie, X., Li, Z., Hoyt, G., Robbins, R.C., *et al*. (2008). Short hairpin RNA interference therapy for ischemic heart disease. *Circulation* **118**(14 Suppl): S226-S233.

Hutvagner, G. & Simard, M.J. (2008). Argonaute proteins: key players in RNA silencing. *Nat Rev Mol Cell Biol* **9**: 22–32.

Ilves, H., Kaspar, R.L., Wang, Q., Seyhan, A.A., Vlassov, A.V., Contag, C.H., Leake, D., *et al*. (2006). Inhibition of hepatitis C IRESmediated gene expression by small hairpin RNAs in human hepatocytes and mice. *Ann N Y Acad Sci* **1082**:52–55.

Jackson, A.L., Bartz, S.R., Schelter, J., Kobayashi, S.V., Burchard, J., Mao, M, Li, B., *et al*. (2003). Expression profiling reveals off-target gene regulation by RNAi. *Nature Biotech* **21**(6): 635-637.

Jackson, A.L., Burchard, J., Schelter, J., Chau, B.N., Cleary, M., Lim, L., and Linsley, L. (2006b). Widespread siRNA “off-target” transcript silencing mediated by seed region sequence complementarity. *RNA* **12**: 1179-1187.

Jinek, M. & Doudna, J.A. (2009). A three-dimensional view of the molecular machinery of RNA interference. *Nature* **457**: 405-412.

Khvorova, A., Reynolds, A and Jayasena, S. (2003). Functional siRNAs and miRNAs exhibit strand bias. *Cell* **115**: 209-216.

References

Kim, D., Longo, M., Han, Y., Lundberg, P., Cantin, E., and Rossi, J.J. (2004). Interferon induction by siRNAs and ssRNAs synthesized by phage polymerase. *Nat Biotech* **22**: 321-325.

Kim, D., Behlke, M.A., Rose, S.D., Chang, M., Choi, S., and Rossi, J.J. (2005). Synthetic dsRNA Dicer substrates enhance RNAi potency and efficacy. *Nat Biotech* **23**(2): 222-226.

Kim, V.N. and Nam, J.W. (2006). Genomics of microRNA. *Trends Genet* **22**:165–173.

Kim, D.H. & Rossi, J.J. (2007). Strategies for silencing human disease using RNA interference. *Nat Rev Genet* **8**: 173-184.

Kornberg, R.D. & Klug, A. (1981). The nucleosome. *Sci Am* **244**(2): 52-64.

Knoepfel, S.A., Centlivre, M., Liu, Y.P., Boutimah, F., and Berkhout, B. (2012). Selection of RNAi-based inhibitors for anti-HIV-1 gene therapy. *World J Virol* **1**(3): 79-90.

Kutay, U., Lipowsky, G., Izaurralde, E., Bischoff, F.R., Schwarzmaier, P., Hartmann, E., and Gorlich, D. (1998). Identification of a tRNA-specific nuclear export receptor. *Mol Cell* **1**(3): 359-369.

Lagos-Quintana,M., Rauhut,R., Lendeckel,W. and Tuschl,T. (2001). Identification of novel genes coding for small expressed RNAs. *Science* **294**: 853-858.

Lee,Y., Ahn,C., Han,J., Choi,H., Kim,J., Yim,J., Lee,J., Provost,P., Radmark,O., Kim,S.*et al*. (2003). The nuclear RNase III Drosha initiates microRNA processing. *Nature* **425**: 415-419.

Lee, Y.S., Nakahara, K., Pham, J.W., Kim, K., He, Z., Sontheimer, E.J., and Carthew, R.W. (2004). Distinct roles for Drosophila Dicer-1 and Dicer-2 in the siRNA/miRNA silencing pathways. *Cell* **117**(1): 69-81.

Lee,H.Y., Zhou K., Smith A.M., Noland C.L. and Doudna,J.A. (2013). Differential roles of human Dicer-binding proteins TRBP and PACT in small RNA processing. *Nucleic Acids Res*, 1-9.

Lewis, B.P., Shih, I.H., Jones-Rhoades, M.W., Bartel, D.P., and Burge, C.B. (2003). Prediction of mammalian microRNA targets. *Cell* **115**:787–798.

References

Li, M., Kim, J., Li, S., Zaia, J., Yee, J., Anderson, J., Akkina, R., *et al*. (2005). Long-term inhibition of HIV-1 infection in primary hematopoietic cells by lentiviral vector delivery of a triple combination of anti-HIV-1 shRNA, anti-CCR5 ribozyme, and a nucleolar-localizing TAR decoy. *Mol Ther* **12**(5): 900-909.

Li, L., Lin, X., Khvorova, A., Fesik, S.W., and Shen, Y. (2007). Defining the optimal parameters for hairpin-based knockdown constructs. *RNA* **13**: 1765-1774.

Lin, X., Ruan, X., Anderson, M.G., McDowell, J.A., Kroeger, P.E., Fesik, S.W., and Shen, Y. (2005). siRNA-mediated off-target gene silencing triggered by a 7 nt complementation. *Nucleic Acids Res* **33**(14): 4527-4535.

Liu, P.Y., Schopman, N., and Berkhout, B. (2013). Dicer-independent processing of short hairpin RNAs. *Nucleic Acids Res* 1-11.

Macrae, I.J., Zhou, K., Li, F., Repic, A., Brooks, A.N., Cande, W.Z., Adams, P.D., *et al*. (2006). Structural basis for double-stranded RNA processing by Dicer. *Science* **311**(5758): 195-198.

Martinez, J., Patkaniowska, A., Urlaub, H., Luhrmann, R and Tuschl, T. (2002). Single-stranded antisense siRNAs guide target RNA cleavage in RNAi. *Cell* **110**: 563-574.

Matranga, C., Tomari, Y., Shin, C., Bartel, D.P., and Zamore, P.D. (2005). Passenger-strand cleavage facilitates assembly of siRNA into Ago2-containing RNAi enzyme complexes. *Cell* **123**: 607–620.

Matveeva, O., Nechipurenko, Y., Rossi, L., Moore, B., Saetrom, P., Ogurstov, A.Y., Atkins J.F., and Shabalina, S.A. (2007). Comparison of approaches for rational siRNA design leading to new efficient and transparent methods. *Nucleic Acids Res* **35**: e63.

McBride, J.L., Boudreau, R.L., Harper, S.Q., Staber, P.D.,Monteys, A.M., Martins, I., Gilmore, B.L., *et al*. (2008). Artificial miRNAs mitigate shRNA-mediated toxicity in the brain: Implications for the therapeutic development of RNAi. *Proc Natl Acad Sci* **105**: 5868–5873.

References

McIntyre, G.J. & Fanning, G.C. (2006). Design and cloning strategies for constructing shRNA expression vectors. *BMC Biotech* **6**: 1.

McIntyre, G.J., Groneman, J.L., Yu, Y., Jaramillo, A., Shen, S., and Applegate, T.L. (2009). 96 shRNAs designed for maximal coverage of HIV-1 variants. *Retrovirology* **6**: 55-70.

McIntyre, G.J., Yu, Y., Lomas, M., and Fanning, GC. (2011). The effects of stem length and core placement on shRNA activity. *BMC Mol Biol* **12**: 34.

McManus, M.T., Petersen, C.P., Haines, B.B., Chen, J., and Sharp, P.A. (2002). Gene silencing using micro-RNA designed hairpins. *RNA* **8**: 842-850.

Meister, G. & Tuschl, T. (2004). Mechanisms of gene silencing by double-stranded RNA. *Nature* **431**: 343–349.

Morris, K.V., Chan, S.W.-L., Jacobsen, S.E., and Looney, D.J. (2004). Small interfering RNA-induced transcriptional gene silencing in human cells. Science **305**(5688): 1289-1292.

Mosmann, T. (1983). Rapid colorimetric assay for cellular growth and survival: Application to proliferation and cytotoxicity assays. *J Immunol Methods* **65**: 55-63.

Neff, C.P., Zhou, J., Remling, L., Kuruvilla, J., Zhang, J., Haitang, L., Smith, D.D. et al. (2011). An aptamer-siRNA chimera suppreses HIV-1 viral loads and protects from helper CD4+ T cell decline in humanized mice. Science Translational Medicine **3**(66): 66ra6.

Noma, K., Sugiyama, T., Cam, H., Verdel, A., *et al*. (2004). RITS acts in *cis* to promote RNA interference-mediated transcriptional and post-transcriptional silencing. *Nat Genet* **36**(11): 1174-1180.

Paddison, P.J., Caudy, A.A., Bernstein, E., Hannon, G.J. and Conklin, D.S. (2002). Short hairpin RNAs (shRNAs) induce sequence-specific silencing in mammalian cells. Genes *Dev* **16**: 948–95.

References

Paddison, P.J. (2008). RNA interference in mammalian cell systems. In: RNA interference. *Curr Topics Micro Immunol*. Paddison, P.J., Vogt, P.K. (eds.). Springer Press.

Papapetrou, E.P., Korkola, J.E., and Sadelain, M. (2010). A genetic study for single and combinatorial analysis of miRNA function in mammalian hematopoietic stem cells. *Stem Cells* **28**(2): 287-296.

Park, J.E., Heo, I., Tian, Y., Simanshu, D.K., Chang, H., Jee, D., Patel, D.J., and Kim, V.N. (2011). Dicer recognizes the 5′ end of RNA for efficient and accurate processing. *Nature* **475**: 201–205.

Rand, T. A., Petersen, S., Du, F. and Wang, X. 2005. Argonaute2 cleaves the anti-guide strand of siRNA during RISC activation. *Cell* **123**: 621–629.

Rao, D.D., Vorhies, J.S., Senzer, N., and Nemunaitis, J. (2009). siRNA vs shRNA: similarities and differences. *Adv Drug Deliv Rev* **61**: 746-759.

Rea, S., Eisenhaber, F., O' Carroll, D., *et al*. (2000). Regulation of chromatin structure by site-specific histone H3 methyltransferases. *Nature* **406**: 593-599.

Reynolds, A., Leake, D., Boese, Q., Scaringe, S., Marshall, W.S., and Khvorova, A. (2004). Rational siRNA design for RNA interference. *Nat Biotech* **22**(3): 326-330.

Reynolds, A., Anderson, E.M., Vermeulen, A., Federov, Y., Robinson, K., Leake, D., Karpilow, J., *et al*. (2006). Induction of the interferon response by siRNA is cell type- and duplex length dependent. *RNA* **12**: 988-993.

Rose, S.D., Kim, D., Amarzguioui, M., Heidel, J.D., Collingwood, M.A., Davis, M.E., Rossi, J.J., *et al*. (2005). Functional polarity is introduced by Dicer processing of short substrate RNAs. *Nucleic Acids Res* **33**(13): 4140-4156.

References

Saayman, S., Arbuthnot, P., and Weinberg, M.S. (2010). Deriving four functional anti-HIV-1 siRNAs from a single Pol III-generated transcript comprising two adjacent long hairpin RNA precursors. *Nucleic Acids Res*: 1-12.

Sano, M., Haitang, L., Nakanishi, M and Rossi, J.J. (2008). Expression of long anti-HIV-1 hairpin RNAs for the generation of multiple siRNAs: advantages and limitations. *Mol Ther* **16**(1): 170-177.

Saxena, S., Jonsson, Z.O., and Dutta, A. (2003). Small RNAs with imperfect match to endogenous mRNA repress translation. *J Biol Chem* **278**: 44312-44319.

Sen, G.C. & Sarkar, S.N. (2007). The interferon-stimulated genes: targets of direct signalling by interferons, double-stranded RNA, and viruses. *Curr Topics Micro Immunol* **316**: 233-250.

Schwarz, D.S., Hutvágner, G., Haley, B and Zamore, P.D. (2002). Evidence that siRNAs function as guides, not primers, in the *Drosophila* and human RNAi pathways. *Mol Cell* **10**, 537–548.

Schwarz, D.S., Hutvágner, G., Du, T., Xu, Z., Aronin, N and Zamore P.D. (2003). Asymmetry in the assembly of the RNAi enzyme complex. *Cell* **115**(2): 199-208.

Siolas, D., Lerner, C., Burchard, J., Ge, W., Linsley, L., Paddison, P.J., Hannon, G.J., et al. (2005). Synthetic shRNAs as potent RNAi triggers. *Nat Biotech* **23**(2): 227-231.

Sibley, C.R., Seow, Y., and Wood, M. (2010). Novel RNA-based strategies for therapeutic gene silencing. *Mol Ther*.

Silva, J.M., Li, M.Z., Chang, K., Ge, W., Golding, M.C., Rickles, R.J., Siolas, D., Hu, G., *et al*. (2005). Second-generation shRNA libraries covering the mouse and human genomes. *Nat Genet* **37**(11): 1281-1288.

Sledz, C.A., Holko, M., de Veer, M.J., Silverman, R.H., and Williams, B.R. (2003). Activation of the interferon system by short-interfering RNAs. *Nat Cell Biol* **5**(9): 834-839.

References

Song J.J., Liu, J., Tolia, N.H., Schneiderman, J., Smith, S.K., Martienssen, R.A., Hannon, G.J., and Joshua-Tor, L. (2003b). The crystal structure of the Argonaute2 PAZ domain reveals an RNA binding motif in RNAi effector complexes. *Nat Struct Biol* **10**: 1026-1032.

Song, J.J., Smith, S.K., Hannon, G.J., and Joshua-Tar, L. (2004). Crystal structure of Argonaute and its implications for RISC slicer activity. *Science* **305**(5689): 1434-1437.

Stegmeier, F., Hu., G., Rickles, R.J., Hannon, G.J., and Elledge, S. (2005). A lentiviral microRNA-based system for single-copy polymerase II-regulated RNA interference in mammalian cells. *Proc Natl Acad Sci* **102**(37): 13212-13217.

Sui, G., Soohoo, C., Affar, E.B., Gay, F., Shi, Y., Forrester, W.C., and Shi, Y. (2002). A DNA vector-based RNAi technology to suppress gene expression in mammalian cells. *Proc Natl Acad Sci* **99**(8): 5515-5520.

Streit, S., Micahlski, C.W., Erkan, M., Kleeff, J., and Friess, H. Northern blot analysis for detection and quantification of RNA in pancreatic cancer cells and tissues. *Nat Protoc* **4**(1): 37-43.

Taniguchi, M., Miura, K., Iwao, H., and Yamanaka, S. (2001). Quantitative assessment of DNA microarrays: Comparison with Northern blot analyses.*Genomics* **71**: 34–39.

Tan, X., Lu, Z.J., Gao, G., Xu, Q., Hu, L., Fellman, C., Li, M., et al. (2012). Tiling genomes of pathogenic viruses identifies potent antiviral shRNAs and reveals a role for secondary structure in shRNA efficacy. *Proc Natl Acad Sci* **109**(3): 869-874.

ter Brake, O., Konstantinova, P., Mustafa, C., and Berkhout, B. (2006). Silencing of HIV-1 with RNA interference: a multiple shRNA approach. *Mol Ther* **14**(6): 883-892.

ter Brake, O., & Berkhout, B. (2008) Development of an RNAi-based gene therapy against HIV-1. *Therapeutic Oligonucleotides*: 296-311

Terasawa, K., Shimizu, K., and Tsujimoto, G. (2011) Synthetic pre-miRNA-based shRNA as potent RNAi triggers. *J Nuc Acids* **2011**: 1-6.

References

Tolia, N.H. & Joshua-Tor, L. (2007). Slicer and the Argonautes. *Nat Chem Biol* **3**: 36–43.

Ui-Tei, K., Naito, Y., Nishi, K., Juni, A., and Saigo, K. (2008a). Thermodynamic stability and Watson-Crick base pairing in the seed duplex are major determinants of the efficiency of the siRNA-based off-target effect. *Nucleic Acids Res* **36**(22): 7100-7109.

Uprichard, S.L., Boyd, B., Althage, A., and Chisari, F.V. (2005). Clearance of hepatitis B virus from the liver of transgenic mice by short hairpin RNAs. *Proc Natl Acad Sci* **102**: 773-778.

Valencia-Sanchez, M.A., Liu, J., Hannon, G.J., and Parker, R. (2006). Control of translation and mRNA degradation by miRNAs and siRNAs. *Genes Dev* **20**:515–524.

Válóczi, A., Hornyik, C., Varga, N., Burgyan, J., Kauppinen, S., and Havelda, Z. (2004). Sensitive and specific detection of microRNAs by northern blot analysis using LNA-modified oligonucleotide probes. *Nucleic Acids Res* **32**(22): e175.

Várállyay, E., Burgyan, J., and Havelda, Z. (2007). MicroRNA detection by northern blotting using locked nucleic acid probes. *Nat Proto* **3**(2): 190-196.

Verdel, A., Jia, S., Gerber, S., Sugiyama, T., Gygi, S., Grewal, S.I.S., and Moazed, D. (2004). RNAi-mediated targeting of heterochromatin by the RITS complex. *Science* **303**(5658): 672-676.

Vlassov, A.V., Korba, B., Farrar, K., Mukerjee, S., Sayhan, A.A., Ilves, H., Kaspar, R.L., et al. (2007). shRNAs targeting hepatitis C: effects of sequence and structural features, and comparison with siRNA. *Oligs* **17**: 223-236.

Wang, H., Noland, C., Siridecchadilok, B., Taylor, D.W., Ma, E., Felderer, K., Doudna, J.A., *et al*. (2009). Structural insights into RNA processing by the human RISC-loading complex. *Nat Struc Mol Biol* **16**(11): 1148-1153.

Wang, X., Li, Y., Huang, H., Zhang, X., Xie, P., Hu, W., Li, D., *et al*. (2013). A simple and robust vector-based shRNA expression system used for RNA interference. *PLoS ONE* **8**(2): e56110.

References

Wei, J., Yang, J., Sun, J., Jia, L., Zhang, Y., Zhang, H., Li, Z., *et al* (2009). Both strands of siRNA have potential to guide posttranscriptional gene silencing in mammalian cells. *PLoS ONE* **4**(4): e5382.

Welker, N.C., Maity, T.S., Ye, X., Aruscavage, P.J., Krauchuk, A.A., Liu, Q., and Bass, B.L. (2011). Dicer's helicase domain discriminates dsRNA termini to promote an altered reaction mode. *Mol Cell* **41**: 589–599.

Wolffe, A.P. & Matzke, M.A. (1999). Epigenetics: regulation through repression. *Science* **286**(5439): 481-489.

Xiang, S., Fruehauf, J., and Li, C.J. (2006). Short hairpin RNA-expressing bacteria elicit RNA interference in mammals. *Nat Biotech* **24**(6): 697-702.

Yang, J., Maurin, T., Robine, N., Rasmussen, K.D., Jeffrey, K.L., Chandwani, R., Papapetrou, E.P., *et al*. (2010). Conserved vertebrate miR-451 provides a platform for Dicer-independent, Ago2-mediated microRNA biogenesis. *Proc Natl Acad Sci* **107**(34): 15163-15168.

Yi, R., Qin, Y., Macara, I. G., and Cullen, B. R. (2003). Exportin-5 mediates the nuclear export of pre-microRNAs and short hairpin RNAs. *Genes Dev* **17**: 3011–3016.

Yi, R., Doehle, B.P., Qin, Y., Macara, I.G., and Cullen, B.R. (2005). Overexpression of Exportin 5 enhances RNA interference mediated by short hairpin RNAs and microRNAs. *RNA* **11**: 220-226.

Yiu, S.M., Wong, P.W.H., Lam, T., Mui, Y., Kung, H.F., Lin, M., and Cheun, Y.T. (2005). Filtering of ineffective siRNAs and improved siRNA design tool. *Bioinformatics* **21**(2), 144-151.

Zeng, Y., Wagner, E.J., and Cullen, B.R. (2002). Both natural and designed micro RNAs can inhibit the expression of cognate mRNAs when expressed in human cells. *Mol Cell* **9**: 1327-1333.

Zeng, Y. & Cullen, B.R. (2005). Efficient processing of primary microRNA hairpins by Drosha requires flanking non-structured RNA sequences. *J Biol Chem* **280**: 27595–27603.

References

Zhang, J., & Rossi, J.J. (2010). Strategies in designing multigene expression units to downregulate HIV-1. *Methods Mol Biol* **623**: 123–136.

Zhou, H. & Zeng, X. (2009). Energy profile and secondary structure impact shRNA efficacy. *BMC Genomics* **10**(Suppl 1): S9.

Appendix A – Experimental protocols

A.1 MinElute Gel extraction

Reagents

Qiagen® MinElute Gel Extraction kit

Protocol

The DNA fragment was excised from the agarose (Lonza, Switzerland) gel and weighed in a micro centrifuge tube. Three volumes of Buffer QG were added to 1 volume of gel (100 mg ~ 100 µl). The tube was incubated at 50°C for 10 minutes; the tube was vortexed every 2 to 3 minutes to mix. Once the gel slice was completely dissolved, one volume of isopropanol was added and the sample mixed. A column was inserted into a 2 ml collection tube. The sample was applied to the column and the DNA bound to the membrane of the column. The tube assembly was centrifuged for 1 minute at maximum speed in a standard tabletop micro centrifuge (Mini spin centrifuge; F-45-12-11 rotor)(Eppendorf, Germany). The flow-through was discarded and the column re-inserted into the collection tube. To wash the DNA, 750 µl of Buffer PE was added to the column. The tube was centrifuged for 1 minute. The flow-through was discarded and the tube assembly spun for an additional minute. The column was transferred to a sterile 1.7 ml micro centrifuge tube. The DNA was eluted out of the column membrane and into the tube by adding 50 µl of Buffer EB to the centre of the membrane.

A.2 Chemically competent *E.coli* cells

Reagents

Transformation buffer

Transformation buffer constitutes the following: 100 nM $CaCl_2$, 10 nM PIPES-HCl (Sigma, USA) and 15% Glycerol (Merck, Germany). Using NaOH, the buffer pH was changed to 7.0. The buffer was autoclaved at 121°C and 1 kg/cm^2 for 30 minutes then stored at -20°C.

Luria Bertani medium

Ten grams of tryptone (Oxoid, UK), ten grams of sodium chloride (Merck, Germany) and five grams of yeast (Oxoid, UK) were mixed together in a one litre Schott bottle. Distilled water was added, making up the total volume to one litre The LB medium was autoclaved at 121°C and 1 kg/cm^2 for 30 minutes.

Protocol

Two hundred millilitres of Luria Bertani medium was inoculated with 100 µl of DH5-α *E. coli*. The broth was left to incubate overnight at 37°C in a shaking incubator. Five millilitres of the inoculated broth was added to 45 millilitres of fresh LB medium; the culture was left to incubate at 37°C until its absorbance at 600 nm was 0.3 – 0.5. The cells were centrifuged at 3000 x g (5810 R centrifuge; A-4-81 rotor) for 15 minutes and the pellet resuspended in 5 ml transformation buffer (Eppendorf, Germany). This was followed by 20 minute incubation on ice. The cells were centrifuged at 1000 x g for ten minutes and the pellet resuspended in 2 ml transformation buffer. Aliquots of 100 µl were prepared in sterile micro centrifuge tubes and stored at -70°C.

A.3 Blue/white screening

Reagents

X-gal

One hundred milligrams of X-gal (Sigma, USA) was dissolved in 5 ml dimethyl formanide (Sigma, USA).

IPTG

One hundred milligrams of IPTG (Roche, Germany) was dissolved in 1 ml of water and filter sterilised

1000× Ampicillin

Five grams of ampicillin was dissolved 50 ml of 50% ethanol.

Ampicillin-positive Luria Bertani agar plates

Ten grams of tryptone, ten grams of sodium chloride, and five grams of yeast and six grams of agar were mixed together in a one litre Schott bottle. Distilled water was added, making up the total volume to one litre. The LB medium was autoclaved at 121°C and 1 kg/cm^2 for 30 minutes. In the case of LB-ampicillin media, 1 ml of 1000× ampicillin was added once the solution had cooled down. The medium was poured into Petri dishes and left to solidify at room temperature.

Protocol

One hundred nanograms of DNA was added to 100 µl of competent *E. coli* cells. The mixture was left on ice for 28 minutes. Forty microlitres of X-gal (Sigma, USA) and 8 µl of IPTG (Roche, Germany) were spread on the LB-ampicillin plates for the blue/white screening of the pTZ57R/T plasmids. The plates were left to incubate for 20 minutes at 37°C with the lids removed. Once the 28 minutes were up, the cells were heat-shocked at 42°C for 90 seconds. The cells were left on ice for five minutes then spread onto the X-gal/IPTG LB-ampicillin plates using a glass spreader. The plates were sealed and left to incubate upside down (to avoid condensation on the cells) at 37°C overnight.

A.4 Small scale plasmid isolation (mini prep)

Reagents

Roche High Pure Plasmid Isolation Kit

Ampicillin-positive Luria Bertani medium

Protocol

A single bacterial colony from a transformed ampicillin-positive LB plate was used to inoculate 4 ml of ampicillin-positive LB medium. The bacteria were left to culture overnight in a shaking incubator at 37°C. The bacterial cells were centrifuged at 4000 × g (5810 R centrifuge; A-4-81 rotor) for 10 minutes (Eppendorf, Germany). The supernatant was decanted and the pellet resuspended in 250 µl of suspension buffer (with RNase) and gently mixed by inverting the micro centrifuge tube 3 to 6 times. Two-hundred and fifty microletres of lysis buffer was added to the mixture. After a five minute incubation period at room temperature, 350 µl of chilled binding buffer was added. After gently inverting the tube 3 to 6 times, the mixture was incubated on ice for 5 minutes. The tube was centrifuged for 10 minutes at maximum speed (5415 R centrifuge; F45-24-11 rotor) at 4°C (Eppendorf, Germany).

A High Pure Filter Tube was placed in a collection tube (provided by the kit). The supernatant from centrifugation was transferred to the upper buffer reservoir of the filter tube. The tube was centrifuged for one minute at full speed (Mini spin centrifuge; F-45-12-11 rotor) in a standard tabletop micro centrifuge (Eppendorf, Germany). The filter tube was removed from the collection tube, the flow-through liquid discarded and the filter tube re-inserted into the collection tube. The cells were washed with 700 µl wash buffer II and centrifuged for 1 minute at full speed. The flow-through was discarded. To remove any excess ethanol from the wash buffer, the High Pure tube was centrifuged for an additional minute. The collection tube was discarded and the filter tube placed in a sterile 1.7 ml micro centrifuge tube. One hundred microlitres of elution buffer was added to the upper reservoir of the filter tube. The entire tube assembly was centrifuged for 1 minute at full speed to elute the plasmid from the filter.

A.5 Phenol chloroform extraction

Reagents

Phenol:choloroform

Protocol

Phenol and chloroform are organic solvents that denature proteins and dissolve hydrophobic molecules. One tenth (of the initial volume) of 3 M sodium acetate (pH = 7) was added to the prepared plasmid DNA in a micro centrifuge tube. An equal volume of 50/50 phenol: chloroform (Merck, Germany) was then added. The tube(s) was briefly vortexed then spun at the maximum speed for 60 seconds at 4°C (Eppendorf 5415 R centrifuge; F45-24-11). The upper aqueous phase containing DNA was extracted and transferred to a fresh eppendorf tube. The organic phase and interphase containing cellular proteins and membrane was discarded. An equal volume of chloroform was added to the tube which was then vortexed and spun for 60 seconds at the maximum speed at 4°C. This step was repeated. After the third spin, 2.5 times the volume (of the aqueous phase) of isopropanol was added. The prep was left at -70°C for 30 minutes. The prep was then spun at the maximum speed for 30 minutes at 4°C. The supernatant was decanted and the pellet washed with 100 µl of 70% ethanol. It was then spun for five minutes at the maximum speed at 4°C. The supernatant was decanted and the residual ethanol removed by inverting the tubes on paper towel for 5 to 10 minutes. The pellet was resuspended in half the initial volume's worth of deionised water.

A.6 Medium scale plasmid (midi-prep) preparation

Reagents

Qiagen® Plasmid Midi Kit

Ampicillin-positive Luria Bertani medium

Protocol

A single bacterial colony (from an ampicillin-positive LB plate that was transformed with sequence-confirmed plasmid) was used to inoculate 25 ml of ampicillin-positive LB medium. The bacteria were left to culture overnight in a shaking incubator at 37°C. The bacterial cells were centrifuged at 4000 × g (5810 R centrifuge; A-4-81 rotor) for 15 minutes at 4°C (Eppendorf, Germany). The

supernatant was decanted and the pellet resuspended in 4 ml of Buffer P1 (50 mM Tris-HCl, pH 8.0 and 10 mM EDTA) with 100 µg/ml RNase. Four millilitres of Buffer P2 (200 mM NaOH and 1% SDS) was added to the mixture and vigorously mixed by inverting the 15 ml tube 4 to 6 times. After a five minute incubation period at room temperature, 4 ml of chilled Buffer P3 (3 M KAc, pH 5.5) was added. After vigorously inverting the tube 4 to 6 times, the mixture was incubated on ice for 20 minutes. The tube was centrifuged for 45 minutes at 4000 × g (5415 R centrifuge; F45-24-11 rotor) at 4°C (Eppendorf, Germany). The supernatant was transferred to a sterile 15 ml tube and centrifuged for 30 minutes at 4000 × g at 4°C.

A QIAGEN-tip 100 was equilibrated by applying 4 ml of Buffer QBT (750 mM NaCl; 50 mM MOPS, pH 7.0; 15% isopropanol and 0.15% Triton® X-100) and leaving the column to empty by gravity flow. The supernatant from the prior centrifugation step was transferred to the QIAGEN-tip 100 column and left to drain out by gravity flow. The column was washed twice with 10 ml of Buffer QC (1 M NaCl; 50 mM MOPS, pH 7.0 and 15% isopropanol). The DNA was eluted out of the QIAGEN-tip 100 column and into a 15 ml tube with 5 ml of Buffer QF (1.25 M NaCl; 50 nM Tris-Cl, pH 8.0 and 15% isopropanol). The DNA was precipitated with 3.5 ml of room temperature Isopropanol, mixed and centrifuged at 4000 × g for 45 minutes at 4°C. The pellet was washed with 2 ml of room temperature 70% ethanol and centrifuged at 4000 × g for 20 minutes at 4°C. The pellet was air-dried for 10 minutes and the DNA resuspended in 150 µl of TE buffer (10 mM Tris-Cl, pH 8.0 and 0.1 mM EDTA).

A.7 Cell seeding calculation

When seeding the cells for *in vitro* work, the following formula was used to achieve the desired confluency:

$$\text{Dilution factor to dilute cells in} = \frac{\text{Current surface area x current confluency (\%)}}{\text{Desired surface area x desired confluency (\%)}}$$

A.8 Mammalian tissue culture

Reagents

Dulbecco's Modified Eagle Medium (DMEM)

Ten grams of powdered DMEM (Life Technologies, USA) and 3.7 g of sodium hydrogen carbonate were diluted in 1 L of room temperature distilled water with gentle stirring. The pH was adjusted to 6.8 using NaOH. The medium was then filter sterilised.

1000× Penicillin/Streptomycin

One gram of streptomycin (Gibco, UK) and 0.61 g of penicillin (Gibco, UK) was dissolved in deionised water then filter sterilised.

A.9 Northern blot hybridisation

Reagents

2 x RNA loading dye

95% formamide, 0.025% SDS, 0.025% bromophenol blue, 0.025% xylene cyanol FF, 0.025% ethidium bromide and 0.5 mM EDTA (Thermo Scientific, USA).

10 × Tris Borate EDTA (TBE) buffer

Fifty grams of Boric acid powder (Merck, Germany), 40 ml of 0.5 M EDTA (pH 8.0, Associated Chemical Enterprises, RSA) and 100 g of Tris (Sigma, USA) were dissolved in 1 L of deionised water. The buffer was autoclaved at 121 °C and 1 kg/cm^2 for 30 minutes.

15% polyacrylamide gel (1:19 bis-acrylamide: acrylamide)

Thirty grams of 8 M urea (Merck, Germany), 0.45 g *bis*-acrylamide (Merck, Germany) and 8.55 g of acrylamide (Merck, Germany) were added together in a 100 ml beaker. Six

millilitres of 10× TBE buffer was added and the final volume made up to 60 ml with water. Thirty microlitres of TEMED (Sigma, USA) and 300 µl 1% Ammonium persulphate (Merck, Germany) were added before pouring the gel.

20 × SSC

Eighty eight grams of 0.3 M Tris-sodium citrate dihydrate ($NA.3C_6H_50_7.2H_20$) (Merck, Germany), 175 g of 3 M sodium chloride (Merck, Germany) were dissolved in deionised water (made up to a final volume of 1 L). The pH was adjusted to 7.0 using HCl.

A.10 Radioactive labelling of the probes

Reagents

TE buffer

10 ml of 0.5 M Tris-HCl (pH 8.0, Sigma, USA) and 1 ml 0.5 M EDTA (pH 8.0, Associated Chemical Enterprises, RSA) were added to a 500 ml Schott bottle. The volume was made up to 500 ml with deionised water.

G-25 Sephadex

5 g of G-25 Sephadex (Sigma, USA) was added to 50 ml TE buffer and left to rotate overnight at room temperature. The dissolved Sephadex was spun at 4000 x g (5810 R centrifuge; A-4-81 rotor) for two minutes, the TE buffer decanted and replaced by 50 ml of fresh TE buffer (Eppendorf, Germany). This step was repeated two more times.

Appendix B - Supplementary Data

The 19mers were identified by the presence of a 324 bp band and the 25mers, a 338 bp band (Figure B.1). PsiCheck 2.2 served as the positive control for both groups of PTZ-H1shRNA clones because it yielded the exact fragment sizes expected after restriction enzyme digest: (i) the 19mer positive control was digested with *NotI* and *NruI* and (ii) the 25mer positive control was digested with *PvuII* (Thermo Scientific, USA)(Figure B.1).

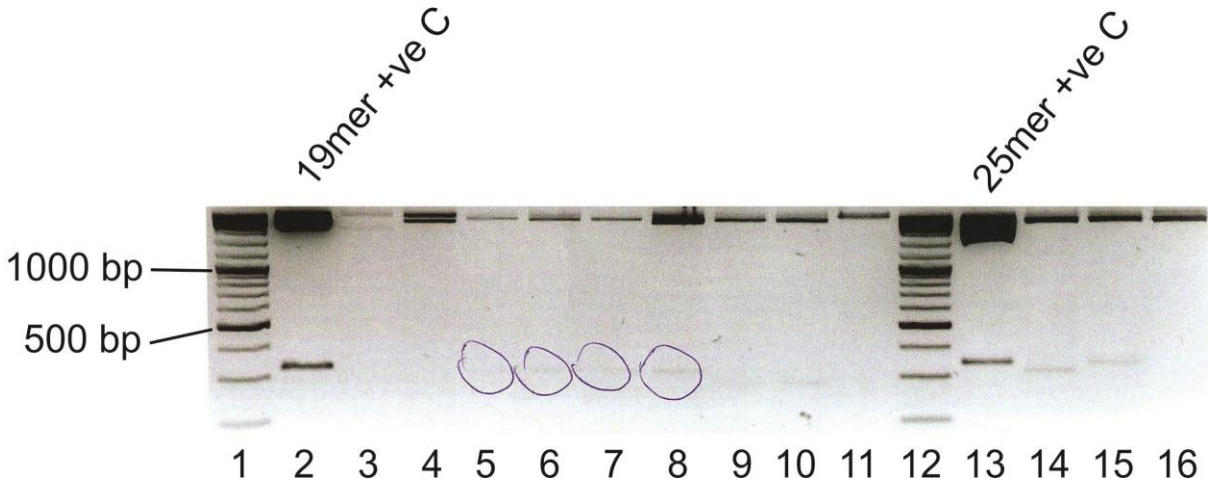


Figure B.1: An example of the shRNA clone screening process.

Lanes 1 and 12: O'GeneRuler DNA molecular weight ladder. Lane 2: *NotI*/*NruI*-digested PsiCheck 2.2 served as the positive control for 19mer screening. Lanes 5-8: identified positive 19mer clones. Lane 13: PsiCheck 2.2 was digested with *PvuII* to yield the band pattern expected of positive 25mer clones. Lane 15: 25mer clone with the correct band size.

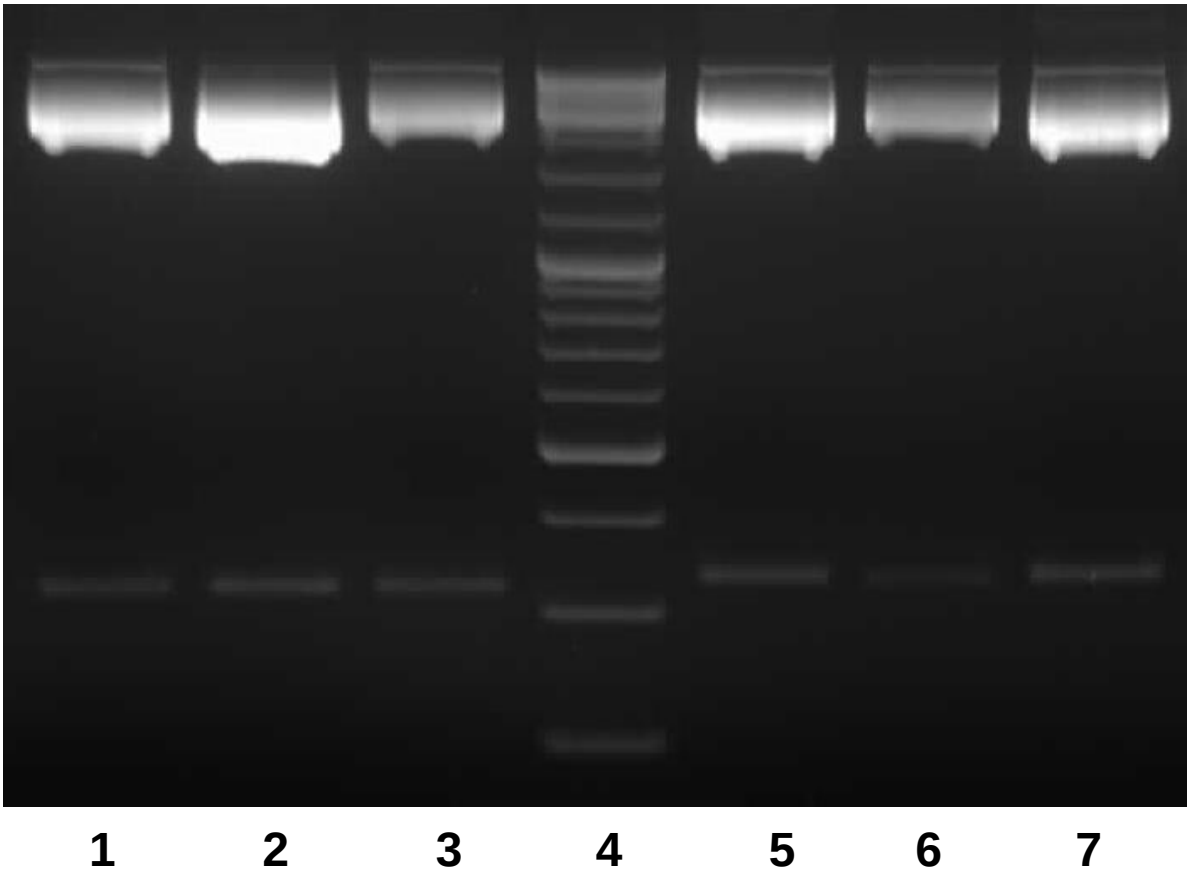


Figure B.2: *SacI* and *BamHI* digest of confirmed positive pTZ-shRNA clones.

The digested clones were loaded onto an ethidium bromide-stained agarose gel, electrophoresed and visualised under UV light. The products in lanes 1-3 are 2857 bp and 327 bp in size. The plasmids in lanes 1-3 were shG19, shE19 and shL19, respectively. The molecular weight marker used in lane 4 was O'GeneRuler™ DNA ladder (Thermo Scientific). Lanes 5-7 are the digested GAG-, ENV- and LTR-targeting 25mers, respectively. The double-digest products in lanes 5-7 are 2857 bp and 338 bp. The shift in product size between lanes 1-3 and lanes 5-7 is notable.

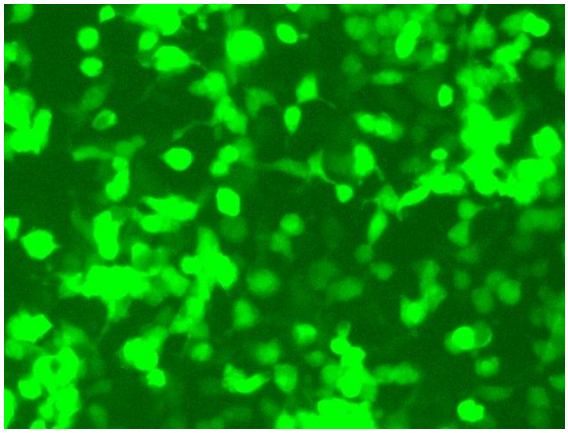


Figure B.3: Example of GFP expression.

HEK293 cells were transfected with 9 µg of shE25 and 1 µg of pCI-eGFP. Forty eight hours post-transfection, the cells were view under a fluorescence microscope.

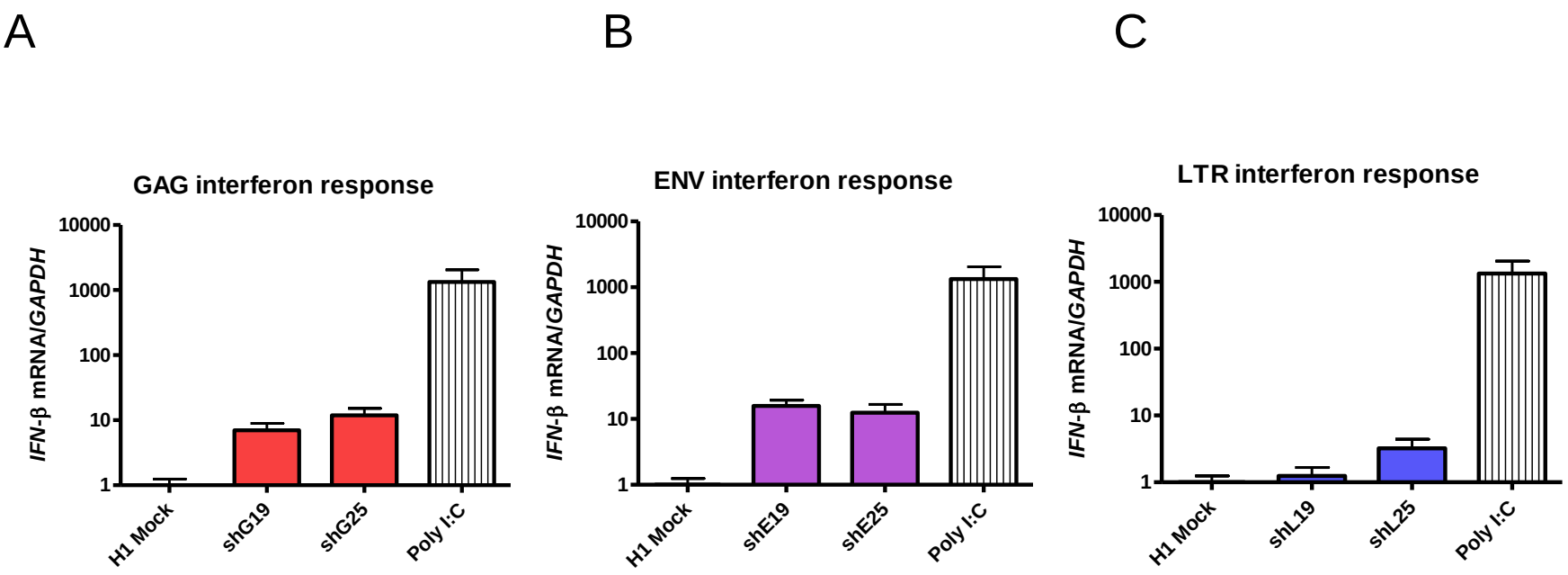


Figure B.4: The induction of the interferon response in shRNA-transfected cells measured by real-time qPCR.

HEK293 cells were transfected with a 19mer and 25mer pair targeting A) Gag, B) Env and C) LTR. (±SEM, n=3). The y-axis is in a log10 scale.

Red = Gag. Purple = Env. Blue = LTR.